Establishing Energetic Cost of Acute Exposure to Select Anthropogenic-Caused Environmental Conditions in the North Gulf of Mexico Derived Eastern Oyster (*Crassostrea virginica*)

by

Kayla Taylor Boyd

A dissertation submitted to the Graduate Faculty of
Auburn University
in partial fulfillment of the
requirements for the Degree of
Doctor of Philosophy

Auburn, Alabama
May 4, 2024

Keywords: Oyster, climate change, PFAS,
thermal stress, salinity stress, physiology

Approved by

James A. Stoeckel, Chair, Auburn University, Associate Professor, School of Fisheries, Aquaculture and Aquatic Sciences
Tham Hoang, Auburn University, Associate Professor, School of Fisheries, Aquaculture and Aquatic Sciences
Moises Bernal de Leon, Auburn University, Assistant Professor, Biological Sciences
Andrea M. Tarnecki, Auburn University, Assistant Extension Professor, School of Fisheries, Aquaculture and Aquatic Sciences
William Walton, Virginia Institute of Marine Science, Acuff Professor, Marine Science and Shellfish Aquaculture Program Coordinator

Abstract

Oyster aquaculture is an important industry in the Gulf of Mexico and has seen a significant increase in interest over the last 20 years. Because oyster farming takes place in ambient waters, farmed oysters are subjected to uncontrollable environmental conditions such as PFAS pollution from industrial discharge, extreme temperature swings, and rapid salinity shifts. Farmers have been reporting massive mortalities in their oyster crops across the United States coastline with no direct cause. Many commercially available oyster lines are locally adapted and, while there are studies addressing some of the suspected primary causes in the northeastern United States, there is significantly smaller body of work that focuses on oysters the Gulf of Mexico. As a result, there is a clear need to study the energetic cost that environmental conditions have on oysters when ambient conditions become unfavorable in the Gulf of Mexico. To address some of these knowledge gaps, two studies were conducted to determine the impact of PFAS bioaccumulation and depuration on energetic cost. Longer-chained PFAS compounds bioaccumulated more rapidly than shorter chained compounds but, regardless of chain length, PFAS concentrations were at undetectable levels within 24 hours after being placed in clean water. Respirometry identified that the act of rapidly depurating PFAS was not energetically expensive in adult oysters. When under combined stressors (PFAS exposure and elevated temperature (33°C)), oysters under thermal stress exhibited a higher metabolic rate but there was no compounded energetic cost to PFAS exposure, suggesting that, at temperatures above what is considered optimal for GOM oysters, PFAS is likely not contributing to mortalities in farmed and wild oyster populations. To address concerns related to environmental stress on polyploidy oysters, two studies were conducted on diploid and triploid oysters to identify which conditions

increased susceptibility of triploids to acute stressors commonly associated with Mobile Bay. Acute thermal ramps revealed that diploid and triploids did not have a significant difference in the temperature at which metabolic, behavioral, and lethal temperatures occurred. It was observed that triploid metabolic rates were lower than diploid oysters, possibly due to inefficient gas exchange across characteristically larger triploid oyster cells. When acute thermal stress was conducted under hyposaline conditions, triploid oysters showed an increased susceptibility by having significantly increased closure frequency and lower respiration rate compared to diploid oysters. Regardless of ploidy, hyposaline events coinciding with high temperature resulted in increased closure frequency and a significant decrease in the temperature at which metabolic peak occurred, demonstrating that metabolic stress during these coinciding stressors likely play a role in oyster mortality.

Acknowledgments

When I began my graduate degree, I didn't fully know what to expect. I knew that it was going to be difficult, and I was right. There were many nights spent sleeping under my desk, which was covered in a mountain of coffee cups, but those days were surrounded by exciting moments in science and comradery. Over the last four years, I found myself in scenarios that not many people will ever do or see: digging for crayfish in the local streams around Auburn, sloshing through hip-deep mud in the Mobile-Tensaw River Delta, dodging angry bees on Dauphin Island, tossing shrimp in Gulf Shores, eating fried worms with world-renowned marine scientists, sword fighting in the Czech Republic, and sharing drinks with other scientists that have just as much passion about oysters as I do to name a few. While I did not know in the beginning what graduate school would entail, I now know that being here was the best decision I could have made.

It takes a village to raise a good scientist so I would like to thank the colorful group of people that gave me support including my family and my found family: To my UW-Stout professors- thank you for your support throughout my undergraduate degree and continued support throughout my PhD. To the professors I worked with at Auburn University both within and outside the School of Fisheries - thank you for taking me under your wing to broaden my scope of aquaculture and wildlife in the state of Alabama. To my committee members- thank you for guiding me in research and encouraging me to think deeper about my work. To my AUSL family- thank you for making every day a treasure that I will cherish forever. To my cohort of graduate students- thank you for the countless memories. To my Stoeckel lab mates- thank you for letting me share in your research and for your never-ending support. To Heather King- thank you for being my roommate and my best friend. To Dr. Kaelyn Fogelman- thank you for being

an inspiration, a protector, and a friend. To my family- I can't say enough about how much your love, support, and interest in my work kept me moving forward. To the many wonderful oyster growers and working professionals I've met over the years- thank you for bringing me into your community and supporting me through every conference and workshop I attended. To my advisor Dr. Jim Stoeckel- thank you for taking a chance on a girl from Wisconsin and giving me the adventure of a lifetime. I hope I made you all proud.

I would like to dedicate this body of work to the lands and waters of Alabama- Thank you for being kind to me and providing me with a place that I can call my home.

Table of Contents

List of Tables

List of Figures

CHAPTER 1

CHAPTER 2

CHAPTER 3

List of Abbreviations

PFAS	Per- and polyfluorinated compounds
SSW	Synthetic seawater
RMR	Resting metabolic rate
MO_2	Oxygen consumption rates
MXR	Multixenobiotic Resistance System
nGOM	North Gulf of Mexico; Texas, Louisiana, Mississippi, Alabama, and West Florida
GBOP	Grand Bay Oyster Park
AUSL	Auburn University Shellfish Laboratory
PPD	Presumed physiological death
CTM	Critical thermal maximum
qPCR	Quantitative polymerase chain reactions
WWW	Whole wet weight (wet tissue including shell)
WTW	Wet tissue weight
DTW	Dry tissue weight
SH	Shell height from umbo to outer shell margin
RODI	Reverse osmosis deionized water
PPT	Salinity in parts per thousand
DO	Dissolved oxygen

CHAPTER 1
INTRODUCTION

1.1 Overview

To understand oyster mortality, there is a need for an interdisciplinary view of the conditions in which oysters live, how variations in those conditions occur naturally, how oysters have adapted to overcome those natural fluctuations, and how humans have fundamentally changed those conditions. Especially in estuarine systems, changes in salinity, temperature, and dissolved oxygen can occur daily, but environmental parameters also shift seasonally with changes in tidal strength, freshwater input from tributaries, groundwater, and rainfall. It takes a good foundation of background knowledge to identify when conditions are abnormal for the tidal cycle and season. Historical reefs have existed throughout the Alabama coastline from the upper Mobile Bay to the Mississippi Sound so, to fully describe and understand mortalities in farmed and wild oysters, we need to look at the system as a whole. Oysters are an important aquaculture crop and so it is important to consider the economic impact oyster mortalities incur on those who depend on them as revenue. This introduction is designed to give an overview on the lifecycle and physiology of oysters, the environmental conditions in Mobile Bay, and detail the human development which has changed the water quality of coastal Alabama. Specific impacts of PFAS, temperature, and salinity on oyster energetics will be discussed more thoroughly in each research chapter.

1.2 The oyster

Crassostrea virginica (also known as the eastern oyster, American oyster, Atlantic oyster, Virginia oyster, Gulf oyster, and the American cupped oyster) is a sessile marine bivalve with great economical, ecological, and cultural importance in coastal communities (Grabowski et al.,

2012; Smith, 2015). Oysters have two asymmetrical valves (a flat right valve and a thicker, cupped left valve) housing the soft tissue. Important organs include two shell-producing mantle skirts, a pair of gills for gas exchange and food manipulation, a pair of labial palps used in food sorting, a large visceral mass that contains vital internal organs, and an adductor muscle that it uses to close its valves in unfavorable conditions (Galtsoff, 1965). Oysters are filter feeders and ingest algae and diatoms from the water column and expel both ingested and rejected suspended particles by biodeposition, contributing to improved water quality in the areas where large oyster populations exist (Bahr & Lanier, 1981).

As broadcast spawners, oysters rely on ocean currents to disperse their gametes and distribute their offspring to ideal locations (Kim et al., 2010). Fertilized oyster eggs will undergo meiosis, producing a polar body to remove excess chromosomes (Masaru et al., 2017). Within a few hours post-fertilization, the fertilized oyster egg will develop into a free-swimming larva that consumes organic material in the water column (Kennedy et al., 1996). Free-swimming larvae proceed to transition through three distinct larval phases over the course of 10-12 days (25-28°C: 2019-2022 AUSL archival hatchery data) post-fertilization: trochophore, veliger, and pediveliger (Kennedy et al., 1996). In the pediveliger stage, larvae possess an eyespot for photoreception and a foot which they use to find suitable consolidated substrate for settlement (Theuerkauf et al., 2015). These can include piers, rocks, and oyster shells. Once an oyster pediveliger “sets”, it loses its velum and foot in exchange for permanently anchoring itself in that location (Kennedy et al., 1996; Masaru et al., 2017). Given their preference for oyster shell, oyster larvae will often settle on dead shell and adult oysters, creating complex reef structures which are a crucial habitat for a wide variety of aquatic species as well as being a vital prey item for fish, birds, and crabs (Ahmed, 1976; Bahr & Lanier, 1981; Galtsoff, 1965; J. G. Stanley & Sellers, 1986). Oyster reefs

also serve as important breakwaters for wave energy entering coastal marshes (Wiberg et al., 2019).

The eastern oyster's impressive range stretches from the Gulf of St. Lawrence in eastern Canada to the furthest southern reaches of the Gulf of Mexico (Fisheries, 2023). While their overall native range is wide, there is a loose population structure in which four distinct population boundaries exist (Rue et al., 2021). These population boundaries have been identified based on nuclear DNA (Anderson et al., 2014; Buroker, 1983; Hare et al., 1996; Hoover & Gaffney, 2005; Karl & Avise, 1992; King et al., 2011) and mitochondrial DNA (Hare & Avise, 1996; Reeb & Avise, 1990; Varney et al., 2009). The large population distribution likely reflects how far oyster larvae can travel via currents before setting, resulting in less population structure than expected of a sedentary animal, but enough geographic separation where both greater and local population boundaries can still form (Rue et al., 2021).

Coastal estuaries along the eastern oyster's range can vary in temperature regime depending on latitude and be widely variable in salinity regimes between close sites depending on the freshwater input flowrate, location, and ocean current patterns (Summers, 2001). Because local adaptations and age can influence thermal and salinity preference, there is a wide range of optimal temperature and salinities reported in the literature for oysters (Bible & Sanford, 2016; La Peyre et al., 2013; Rybovich et al., 2016). In general, oysters can survive temperature ranges between -2°C to 36°C (Shumway, 1977) with the overall optimal temperatures at 20-30°C (Stanley & Sellers, 1986), and the Louisiana oyster population performing optimally within 20-26°C (Lowe et al., 2017). Oysters can tolerate salinities from 5 to 40ppt but their optimal range is between 14-28ppt (Galtsoff, 1965).

1.3 Study location: Mobile Bay and the Mississippi Sound

The Gulf of Mexico (GOM) is a unique and dynamic ecosystem that fosters a wide diversity of aquatic and land-based flora and fauna (Davis, 2018). Most of the GOM coast is considered a beach, consisting of mostly unconsolidated sediment (Britton & Morton, 1989). The tidal fluctuations in the north GOM are so minimal compared to the northeastern coast that there is only one high tide and one low tide each day which has a theoretical mean vertical tide expanse of 0.7 meters (Austin, 1854; Britton & Morton, 1989). Wind intensity and direction has a strong impact on tidal height across the GOM (Britton & Morton, 1989).

1.3.1 Mobile Bay

The Mobile Bay watershed spans almost the entire state of Alabama, covering 65% of the state and portions of Mississippi, Georgia, and Tennessee which accounts for 69,000 square kilometers of land (Austin, 1854; M. Byrnes et al., 2013). Mobile Bay is the fourth largest estuary in the United States with a discharge of over 63,000 cubic feet (1,800 m^2) water per second (Noble et al., 1996). The Mobile-Tensaw River Delta is the terminus of several large river systems (Mobile River, Tombigbee-Black Warrior River, Alabama-Coosa-Tallapoosa River). Additional freshwater inputs to the bay include the Fish River on the eastern side of the bay and Fowl, Dog, and Deer River to the west. Mobile Bay averages 17.7 km from east to west and 49.9 km from north to south with about 1069 square km of open water (M. Byrnes et al., 2013; Isphording et al., 1996) (Fig. 1). The bay itself is relatively shallow given its size, with an average depth of approximately 3 meters (Isphording et al., 1996). The three main areas of water exchange between the GOM and Mobile Bay are through Main Pass Sound (85%), Pass aux

Herons (15%), and through the Mississippi Sound, with exchange rates primarily driven by ocean currents and tidal flow (M. Byrnes et al., 2013).

The waters in Mobile Bay are relatively turbid, especially compared to the clear water of Pensacola and Gulf Shores to the east. Although the Mobile-Tensaw Delta is the largest inland delta complex in the United States, the majority of the river-borne detritus is deposited in Mobile Bay, resulting in cloudy water filled with suspended solids (Isphording et al., 1996). Less than 30% of all sediments deposited from the delta reach the GOM in low to moderate discharge conditions resulting in a high sediment, municipal, and industrial contaminant load deposited in Mobile Bay during drought conditions (Isphording et al., 1996). In high discharge conditions, however, there is a significant amount of riverine-derived sediment that bypasses the estuary completely and flows into the GOM to the south and the Mississippi Sound to the west (Park, Valentine, et al., 2007; Stumpf et al., 1993). Because of the high suspended solid load from the delta, the bay bottom is soft, consisting of approximately 50% clay and 50% silty clay (Hummell & Parker, 1995). Large storms, such as hurricanes, directly hit Mobile Bay every 12-13 years and can significantly change the composition of the bottom bay sediments (M. R. Byrnes et al., 2013). For example, Hurricane Frederic in 1979 resulted in the bay sediment shifting to mostly silty clay (Hummell & Parker, 1995). Despite its rapidly shifting sediment composition, a sediment texture analysis of the estuary has not been completed since 1989.

The salinities in Mobile Bay can be separated into three sections: upper, middle, and lower Bay, the actual boundaries of which are arbitrary and used for general reference only. Salinity regimes in each section of the bay are dependent on tidal cycle, Mobile-Tensaw River Delta flow rates, and wind direction (M. Byrnes et al., 2013). There is a seasonal shift in salinities (lower salinity in the winter/higher salinity in the summer) brought about by wind

direction as well as rainfall regimes in the watershed (McPhearson, Jr, 1970). Generally, the upper bay has low salinity between 0-10ppt, the middle bay has moderate salinity between 10-25ppt, and the lower bay has high salinity between 25-35ppt (NOAA, 2023). In drought conditions, low river flow rates can push salinity in the lower-middle bay to 30ppt (McPhearson, Jr, 1970).

Stratification is present most of the year and is primarily driven by river discharge with vertical salinity differences of 5-10ppt and is most common in the middle and lower bay approximately 1m depth from the surface (Coogan et al., 2020; Noble et al., 1996). When stratification in Mobile Bay occurs, these salinity gradients are not easily broken by wind energy in the summer, but the winter winds are 6–8 times stronger and can cause mixing (Coogan et al., 2020). Stratification results in anoxia in the lower meter of the Mobile Bay and Mississippi Sound water column (Park, Valentine, et al., 2007).

1.3.2 Mississippi Sound

The Mississippi Sound runs parallel to the southern coast of Mississippi and Alabama, beginning to the east of Waveland, MS and ending at the Dauphin Island Bridge, which is approximately 26.1 km wide (McPhearson, Jr, 1970). It is connected to Mobile Bay by Pass aux Herons (also known as Grant's Pass), through which approximately one-fifth of the bays discharge flows (Austin, 1854). The sound is protected from the greater GOM by a string of barrier islands (from west to east): Cat Island, West Ship Island, East Ship Island, Isle of Caprice, Horn Island, West Petit Bois (formerly Sand Island), Petit Bois Island, and Dauphin Island. The majority of these islands are a part of the Gulf Islands National Seashore managed by the National Park Service. The maximum distance between the shoreline and the barrier islands

is approximately 20.7 km, making the overall area of the sound a little over 500 sq km with an average depth of 2.7 meters (McPhearson, Jr, 1970). Tidal scouring occurs around the dips of the islands, resulting in greater depths in those areas (Eleuterius, 1976). Freshwater inputs to the sound include Pascagoula River, Little River, and West Fowl River. The sound is bordered by several bayous and bays. Major land formations within the sound include Point Aux Pins, which separates Grand Bay and Portersville Bay, as well as Marsh Island (located within Grand Bay) and Isle Aux Herbes (located within Portersville Bay). Circulation in the Mississippi Sound is counterclockwise, following classic northern hemisphere estuarine patterns (McPhearson, Jr, 1970).

Water parameters in the east Mississippi Sound are directly influenced by the conditions in Mobile Bay (McPhearson, Jr, 1970). Discharge from freshwater inputs in the sound can result in variations of salinity from 0ppt to 30ppt but there are often regional differences in salinity depending on the location of freshwater streams, distance from shore, and distance to the nearest pass between islands (Eleuterius, 1976; McPhearson, Jr, 1970). In normal conditions, the west Mississippi Sound has an increased salinity compared to the east Mississippi Sound (McPhearson, Jr, 1970). Grand Bay is considered moderate salinity with ranges between 0-10ppt in the winter and 15-20ppt in the summer (HOBO logger data).

1.3.3 Anthropogenic Alterations of Mobile Bay and Mississippi Sound

A major change to Mobile Bay was the creation of the Mobile Ship Channel in 1824 and the continued deepening of the shipping channel, most recently of which was 2023 to the authorized 55’×550’ depth and width respectively (Jacobson, 2018). The dredging of the Mobile Ship Channel and Theodore Ship Channel resulted in the formation of Gaillard Island in 1979 as

a dredge disposal site, which has likely altered the water circulation pattern in the bay. While it's not known what the original water circulation conditions were before the shipping channel was created in the early 1800s, there are general surface currents from before the construction of Gaillard Island (Chermock 1974) (Fig. 2). The establishment of Gaillard Island, dredging of the Mobile Bay and Theodore Ship Channels, and the placement of the dredge spoils along said shipping channels, have altered sediment deposition in the bay, indicating that there has been a change in hydrological patterns from anthropogenic activity (M. Byrnes et al., 2013). Since 1986, dredge materials from projects must be disposed of in open water in the GOM in disposal cells labeled Mobile North Ocean Dredged Material Disposal Sites (ODMDS) except for emergency dredging operations (ARCE, 1999).

Dredging in Mobile Bay for fossilized shell material via suction dredges was common from 1946–1982 (Schroeder et al., 1998). Anoxic zones develop in areas of dredging for materials or placement of materials due the formation of pits and furrows that are over 4m below the natural bay bottom (Schroeder et al., 1998). Some major anoxic zones that have been created during this time include the Brookley Hole near the city of Mobile, created when aggregate was needed for the construction of Brookley Airfield, and the dredging of the Mother Reef near Point Clear, AL (M. Byrnes et al., 2013). While waves and currents did not act upon the sediment strongly enough to fill in the holes within a year, Hurricane Fredric in 1979 and Hurricane Elena in 1985 effectively mobilized the sediments and leveled out the bay bottom according to a survey in 1992 (Schroeder et al., 1998). Although all the holes and furrows were removed from the bay, a depression to the east of Gaillard Island of greater than 4m was still present around 2003. Since 2003, there have been several large hurricanes such as Ivan (2004), Katrina (2005), Sally (2020)

and Zeta (2020), with each one likely impacting the bathymetry and the sediment characteristics of the bay, although the impacts of those storms on bay sediments have not been published.

The Mississippi Sound is a part of the Gulf Intracoastal Waterway and is maintained by the Army Corps of Engineers for mostly barge and towboat traffic. The shipping channel is routinely dredged approximately every 5 years to account for sediment transport within the channel (M. R. Byrnes et al., 2013).

1.3.4 Urbanization around Mobile Bay and Mississippi Sound

The city of Mobile, founded in 1701, is the second largest city in Alabama with a population of over 204,000 residents (U.S. Census Bureau, 2020). Located on the northwest shore of Mobile Bay, Mobile has been an important economic player since its foundation, beginning as a trading center between the French and the native Americans (Davis, 2018). Mobile Bay is home to the Port of Mobile, a major industrial port city, listed as the 12th-largest port in the United States as of 2010 (*Waterborne Commerce of the United States,* 2010). Other major urban areas that have developed around the bay are Spanish Fort (2020 pop'n: 10,049) Daphne (2020 pop'n: 27,462), and Fairhope (2020 pop'n: 22,477) all of which are located in Baldwin county, one of the fastest growing counties in Alabama (Arnold, 2023; U.S. Census Bureau, 2020). Major urban sites along the east Mississippi Sound are the cities of Bayou la Batre, AL and Coden, AL, where boat construction is a major industry. Increasing population with aging infrastructure that was not built to withstand the rapid influx of people into the area is current raising concerns about treated and untreated wastewater discharge into Mobile Bay (Arnold, 2023). Southwest Alabama, particularly the city of Mobile, averages 66 inches of rain per year (US Department of Commerce, 2023). During major rain events, there are often sewer

overflows contaminating the bay with untreated sewage water due to undersized wastewater treatment plants and an exponential increase in population as well as non-point source pollution carried in runoff (Arnold, 2023; Basnyat et al., 1999).

1.4 Oyster population collapse

Oyster populations across the GOM have seen a rapid decline due to overharvesting, freshwater pulses, disease, and predation (Camp et al., 2015; Gledhill et al., 2020; Hintenlang et al., 2023; Jackson et al., 2001; Love et al., 2021; Moore et al., 2020). Mobile Bay was once home to a patchwork of productive reefs from the delta to the southern bay (Fig. 3). Reefs that are open for public harvest are the West and East Cedar Point reef and Heron Bay reef, all of which are located just north of Dauphin Island (Bannon & Hermann, 2020). Portersville Bay reef was also open to harvest in 2023-2024 season, but there were no oysters harvested from that reef over the 75-day season (AMRD, 2024). It is widely believed that the majority of reefs in the bay that still have live oysters are either unproductive due to chronic low dissolved oxygen near the sediment (White House Reef), or moderately productive (Hollinger's Island Reef) (Bannon & Hermann, 2020).

A complete survey of current reefs has not been completed in recent decades, although Alabama Marine Resources Division is scheduled to do a side sonar scan of historical reef areas to identify which areas may still have standing reef structures and identify suitable bottoms for reef enhancement and restoration (Bannon & Hermann, 2020). The timeline for this project and whether or not the data will be publicly available is unknown.

1.5 Traditional oyster harvesting

Traditional oyster harvesting in the Gulf of Mexico relies on natural set of oyster larvae and consists of tonging oyster reefs for oysters off wild reefs, which has a significantly less destructive impact on oyster reefs than dredging (Lenihan & Peterson, 2004). Restoration efforts on publicly harvested reefs and reefs closed to harvest have entailed planting oyster shell to improve the habitat and encourage oyster settlement from natural spawns. Natural spawns typically take place from April through October if the salinity is above 6ppt and water temperatures exceed 22°C (Wallace, 2002). Settlement locations can depend on environmental conditions such as wind and ocean currents (Kim et al., 2010). The oysters that settle on the planted oyster shell are harvested by hand, tong, or by dredge in 1 to 3 years, typically after they've reached or exceeded 70 mm in shell height (*Oysters in Alabama*, n.d.). Oysters harvested this way are typically sold in shucked meat markets. Traditional harvesting has difficulty predicting the upcoming season's available crop due a yearly variation in settlement driven by water quality and oyster reef quality during the previous year's spawning season (Engle et al., 2021).

1.6 Off-bottom aquaculture

With the collapse of the GOM wild oyster population, off-bottom oyster culture was implemented using hatchery-reared seed. Off-bottom gear is comprised of cages or baskets near the surface. It protects farmed oysters from hypoxia and predation, increases access to feed, and prevents smothering via sedimentation (Wallace, 2001). Desiccation periods are employed on farmed oysters to reduce biofouling by barnacles and algae (Hood 2022).

The increased use of off-bottom culture encouraged industry to create polyploid oysters. Diploid oysters have 10 chromosomal pairs consisting of eight metacentric and two

submetacentric chromosome pairs (Leitão et al., 1999). In the 1970's, a process called "induced triploidy" was applied to oysters which involved treating newly fertilized eggs with chemicals, heat, pressure, caffeine, etc. These treatments allow genetic replication in the germ cell but prevents cellular division during maturation division (Bell, 1982). The theoretical perfect triploid oyster would have 30 chromosomes, or 15 paired chromosomes (Z. Wang et al., 1999). The most common and efficient way to create an induced triploid oyster is by using cytochalasin B (CB) to block the release of the first polar body or with 6-dimethylaminopurine (6-DMAP) to block the release of the second polar body. 6-DMAP acts on protein phosphorylation and inhibits female pronuclear condensation which means that the chromosomes are directly involved in the process (Dufresne et al., 1991). CB, on the other hand, inhibits actin polymerization which involves myofilament interference. CB is the most efficient method and will produce the most triploids, but it is a highly toxic chemical to humans. Induced triploid oysters that were produced via blocking meiosis I had a higher growth rate compared to oysters produced by blocking meiosis II (Hawkins et al., 1994; J. Stanley et al., 1984). However, commercially produced triploids via chemical induction are treated at meiosis II because triploids treated at meiosis I have lower survival and are more likely to become aneuploids (Gérard et al., 1999; Guo & Allen, 2011; Hand et al., 1998). Even while the success rate of using CB is high compared to other induction methods, this process has a low survival rate in general and often results in only 80% of the surviving embryos becoming triploids with many becoming abnormal or reverting back to diploid status after a few rounds of cellular division (Gérard et al., 1999).

In response to low success rates in induced triploids and due to concerns that chemically induced methods may not get FDA approval for use on a food product (Guo & Allen, 2011), 4Cs Breeding Technologies created a tetraploid oyster containing four complete sets of chromosomes

by finding a fecund female triploid and fertilizing the eggs with a sperm from a diploid male and retaining the second polar body using 6-DMAP to block meiosis II (Allen & Downing, 1986). Tetraploid oysters are fertile and are able to serve as broodstock for multiple generations of oysters, reducing the labor costs and increasing the efficiency compared to constantly inducing triploidy in oysters. To create mated (natural) triploid cohorts, male tetraploids are stripped of their sperm and used to fertilize a diploid oyster egg. The resulting offspring are almost 100% triploid oysters. Mated triploid Pacific oysters grew faster than meiosis II induced triploids (Wang et al., 2002). The increased performance of mated triploids over induced triploids is likely due to the origin of the third chromosome. Mated triploids receive their third chromosome from the tetraploid male while induced triploids inherit their third chromosome set from the diploid female, likely resulting in two mitochondrial genomes being passed to the offspring which can cause mitochondrial mismatch with nuclear DNA (Callam et al., 2016).

Polyploidy itself does not necessarily result in negative consequences for the individual, but the chances of abnormal development are possible (Lee et al., 2009; Storchova & Kuffer, 2008). No matter the way that triploid oysters are created, there is always the chance of chromosomal loss in polyploid animals, creating aneuploids. Mated triploids tend to result in fewer instances of aneuploids compared to induced triploids, although aneuploidy can still occur (Z. Wang et al., 1999). Aneuploidy can occur during the rapid cellular division or naturally in diploid gamete formation (Guo & Allen, 2011). Loss of chromosomes can alter the relative expression of hundreds of genes which can cause downstream consequences in cellular processes such as cell permeability and mitochondrial function (Sheltzer & Amon, 2011). Under thermal stress, triploid pacific oysters have been shown to have increased expression of stress related proteins while having reduced HSP and IAP genes compared to diploids, suggesting triploids

may be less capable of modifying their stress responses (Li et al., 2022). It can also have negative consequences such as stoichiometric imbalances resulting in over-expression of protein complexes (Kaizu et al., 2010).

Polyploidy can cause a variety of molecular changes in cell function. For example, triploid cells are usually larger due to the increase in genomic content (a larger nucleus that can be identified via DAPI staining), called polyploid gigantism (Allen & Downing, 1986; Guo & Allen, 1994; Hand et al., 1998; Wang et al., 2002). The increase in cell size without reduction in cell number contributes to polyploid animals being a larger size compared to their diploid counterpart, as hypothesized by Guo and Allen 1996 and later confirmed in several bivalve species (Guo & Allen, 1994; Tabarini, 1984; Wang et al., 2002). The larger cell volume could result in a decrease in cell efficiency and regulation but this needs to be explored further (Guo & Allen, 1994).

1.7 Anthropogenically-induced stressors

1.7.1. PFAS pollution

As discussed earlier in this introduction, the urbanization of Mobile Bay has resulted in discharge from several non-point and point sources across the delta and the bay itself (Basnyat et al., 1999, 2000; Peachey, 2003). One pollutant of major concern increasing in interest during the last decade has been the realization of per- and polyfluorinated compounds (PFAS) (Baldwin et al., 2023). While concentrations around Mobile Bay are low in comparison to high contamination sites (Hu et al., 2016; Viticoski et al., 2022), the question remains whether even low levels of PFAS are energetically expensive to depurate via the induction of detoxification

pathways (Fernández-Sanjuan et al., 2013). The PFAS contamination will be discussed more thoroughly in Chapters 2 and 3.

1.7.2. Temperature

Oysters are experiencing temperature increases via anthropogenic influences in two ways: 1) climate change and 2) farm management practices.

The impact of climate change on marine environments are undeniable and the effects on oyster physiology related to energetic cost and biological processes is well documented (Häder & Barnes, 2019; Nash et al., 2019; Rahman & Rahman, 2021). The northern GOM has seen an increase in bottom water temperatures 6.4 times faster than the concurrent increase in annual global ocean surface temperatures (Turner et al., 2017). Temperature can affect water chemistry such as pH, alkalinity, dissolved oxygen (DO), biochemical oxygen demand, and meteorological variables such as rain patterns (Dutta et al., 2018; Häder & Barnes, 2019; Rahman & Rahman, 2021).

Desiccation is a useful farm management practice that is used for biofouling control by exposing the growing cages to heat and UV light via the sun (Bodenstein et al., 2021; Hood, 2022). However, it's been observed that oyster cages can reach temperatures as high as 42°C in the peak of summer with rapid increases and decreases in temperature in comparison to the diurnal swings observed in surface water data (pers. obs.). The act of desiccation has been shown to increase oyster mortalities compared to non-desiccated oysters, but whether that is due to rapid temperature fluctuations or the act of drying is unclear (Bodenstein et al., 2021). The effects of temperature on oysters will be discussed more thoroughly in Chapters 4 and 5.

1.7.3. Salinity

Impounding on the rivers has prevented natural salinity fluctuations (Mohammed & Scholz, 2017). During droughts, more water is retained in the river by floodgates for inland agricultural and drinking water use (Leitman et al., 2016). By reducing the amount of freshwater flowing into the estuarine systems, salinities in those areas can increase to almost full-strength seawater for long periods of time increasing risk of mortalities from physiological stress related to osmoconformation (Liu & Acker, 2010; Marshall et al., 2021). It has been speculated that highly controlling the flow of rivers may have led to the collapse of the Apalachicola oyster reefs in Florida during the drought of 2012 although a direct correlation has not been drawn (Camp et al., 2015; Hintenlang et al., 2023; Liu & Acker, 2010; Oczkowski et al., 2011).

Major river impoundment also increases the risk of low salinity events. Large freshwater pulses are caused by the opening of floodgates. The flood of 2019 in the Midwest resulted in a rise in water levels in Lake Pontchartrain, LA, and, to reduce the risk of flooding the city of New Orleans, the Bonnet Caré spillway was opened twice for a total of 123 days, dropping the salinity in the Mississippi Sound to as low as 0.18-4.21ppt for over four weeks (Gledhill et al., 2020). While oysters are osmoconformers and are relatively resilient to salinity fluctuations for short periods of time by closing their valves, monitored oysters along the Louisiana and Mississippi coasts had experienced almost 100% mortality within 13 days after being relocated to the area (Gledhill et al., 2020). With the Bonnet Caré spillway opening more frequently and for longer durations, it’s likely that the wild oyster reefs along the Mississippi and Louisiana area will either recover very slowly or not recover at all. The effects of salinity on oyster behavior and metabolism will be discussed more thoroughly in Chapter 5.

1.7.4 Compounding stressors

While the effects of stressors are often looked at in single responses, many times they occur concurrently. Given that temperatures are consistently elevated in the summer months, the effects of temperature coinciding with pollution and salinity stress are of concern. When at low salinity, the negative effects of temperature are exacerbated, resulting in significant mortality in oysters (Marshall, Coxe, et al., 2021). Temperature also significantly increased mortality related to pollution exposure during increased protein synthesis (Lannig et al., 2006). PFAS bioaccumulation was found to be dependent on salinity. For instance, lower salinity resulted in a lower PFAS bioaccumulation rate in oysters (Jeon et al., 2010). As environmental parameters influence oyster physiology, observing the compounded stress effect on organismal health in controlled laboratory conditions is critical to predicting field responses (Bodenstein et al., 2023; Marshall, Casas, et al., 2021; Sinclair et al., 2020).

1.8 Assessing energetic cost of maintaining homeostasis

As discussed earlier, estuarine environmental conditions (temperature, salinity, DO, etc.) can vary widely seasonally, diurnally, and tidally (M. Byrnes et al., 2013; M. R. Byrnes et al., 2013; McPhearson, Jr, 1970; Noble et al., 1996; Orlando & Klein III, 1989; Park, Kim, et al., 2007). For example, surface water temperature swings can be greater than 10°C within 24 hours in Mobile Bay and air temperature can change even more rapidly and drastically (NOAA, 2023).

Oysters are poikilotherms, unable to regulate their internal body temperature and their internal temperatures match the surrounding environmental conditions (Hollingsworth, 1968). Homeostasis is a dynamic, self-regulating process by which organisms maintain internal stability while also adjusting to changing external conditions (Sokolova et al., 2012). Estuarine aquatic

invertebrates have developed a wide range of metabolic and behavioral adaptations to survive and adjust to these conditions to maintain homeostasis (Rahman & Rahman, 2021). In optimum conditions, an organism can devote its energy pool to somatic, gonadal development, and basal maintenance costs (Sokolova et al., 2012). In suboptimal conditions, the energy pool can be redirected to balance the increased cost of maintaining homeostasis at the risk of reducing the available energy for growth. Depending on the duration and intensity of the stressor, the energy budget of an organism can be exceeded resulting in death if the energy stores are depleted (Kooijman, 2010). Resting metabolic rate (RMR), which can be measured as a proxy for metabolic rate, is the amount of basal energy needed to carry out cellular and organismal function including protein production (Killen et al., 2021; Ramanathan, 1964). As shifts in water quality occur, the resulting change in RMR can be used to estimate the difference in energetic cost of maintaining homeostasis via biochemical, molecular, and physiological adjustment within the organism (Sokolova et al., 2012). While oysters have evolved to tolerate the wide environmental swings experienced in estuaries, climate change via anthropogenic influences are likely increasing the rapid rate and frequency of these shifts, possibly resulting in increased mortality in oysters that are unable to evolve quickly enough (Gledhill et al., 2020; Marshall, Coxe, et al., 2021; Rahman & Rahman, 2021; Root et al., 2003). While monitoring energy budget taxation alone is not enough to prevent unexpected mortality events of the eastern oyster, it can provide some insight and explanation into current and future environmental catastrophes and the resulting oyster population collapses.

1.9 Research aims and objectives

The overall goal of these studies was to investigate how specific anthropogenic stressors are impacting oyster health and mortality in Mobile Bay and Mississippi Sound coastal ecosystems, using a combination metabolic and behavioral assays.

The individual goals are as follows:

Chapter 2:

1) Quantify the rate at which eastern oysters bioaccumulate an environmentally relevant mixture of 5 PFAS compounds, 2) Quantify the rate at which they depurate this mixture, 3) Determine the energetic costs of exposure to, and depuration of, a simple PFAS mixture (PFOS + PFOA) for direct comparison to previous studies and 4) Determine the energetic costs of exposure to an environmentally relevant mixture of 5 PFAS compounds in the northern Gulf of Mexico.

Chapter 3:

1) Compare energetic costs during exposure to and depuration of PFAS at optimal and stressful temperatures and 2) determine if PFAS exposure at optimal or stressful temperatures results in an increase in production of stress response proteins.

Chapter 4:

1) Determine whether metabolic rates and occurrence of metabolic depression differ between diploid and triploid oysters exposed to acute thermal stress, 2) Examine the relationship between metabolic patterns and observable behavioral responses to thermal stress, 3) Test whether triploids exhibit a lower CTM and PPD temperature than diploids, and 4) Determine whether these differences can explain relatively higher triploid mortality in the summer months.

Chapter 5:

1) Determine if low salinity affects the metabolic patterns, behavioral responses, and functional and physiological death endpoints differently in diploid compared to triploid eastern oysters during acute thermal stress, and 2) determine whether observed responses to the combined stress of temperature and acute salinity might explain reported differences in mortality between farmed diploid and triploid oysters during the summer months.

1.10 Figures

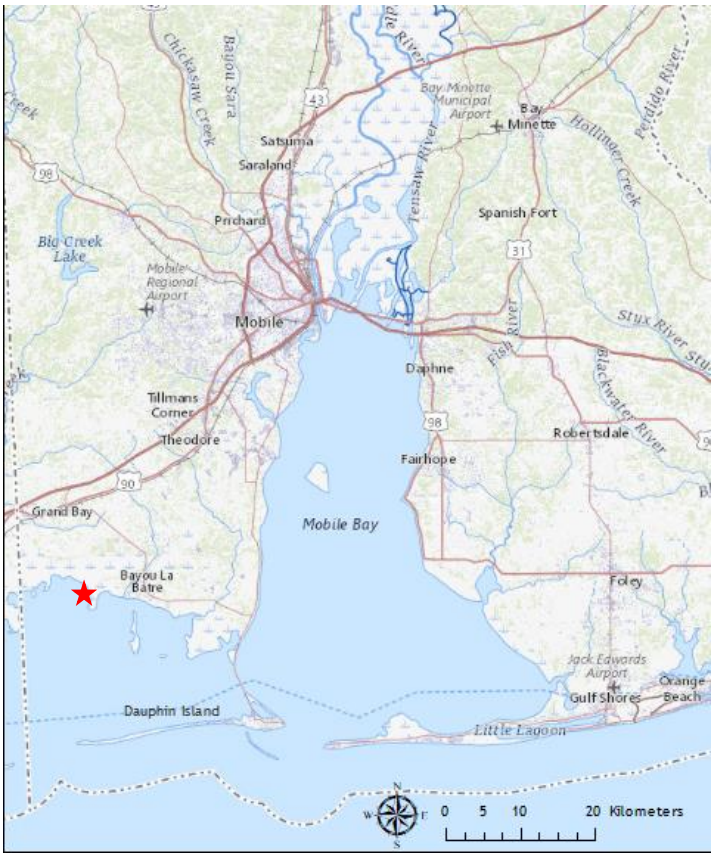

Figure 1. A map of Mobile Bay and the East Mississippi Sound detailing larger urban centers around the bay. The red star denotes the primary study area in the following research chapters. Map created by Meghan Capps.

a) b)

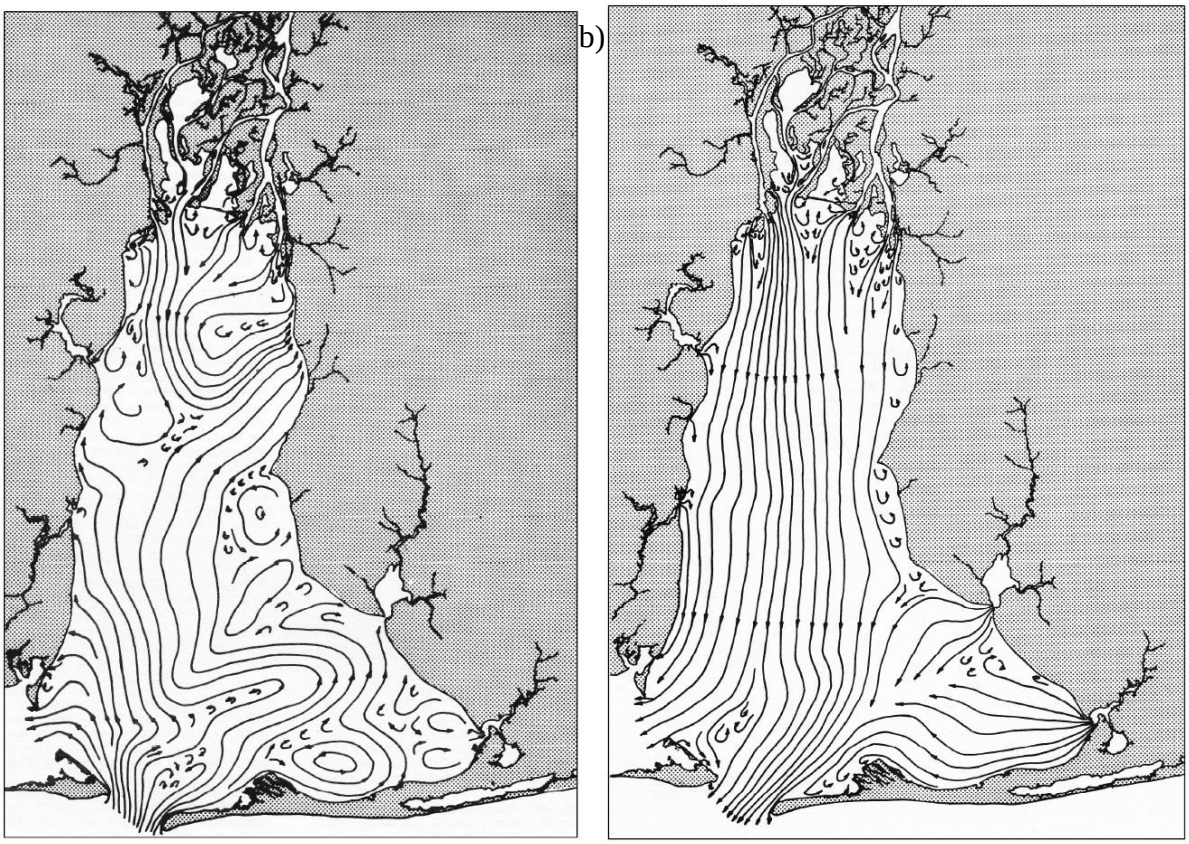

Figure 2. (a) Flood tide and (b) ebb tide surface currents before the construction of Gaillard Island (from Chermock (1974)).

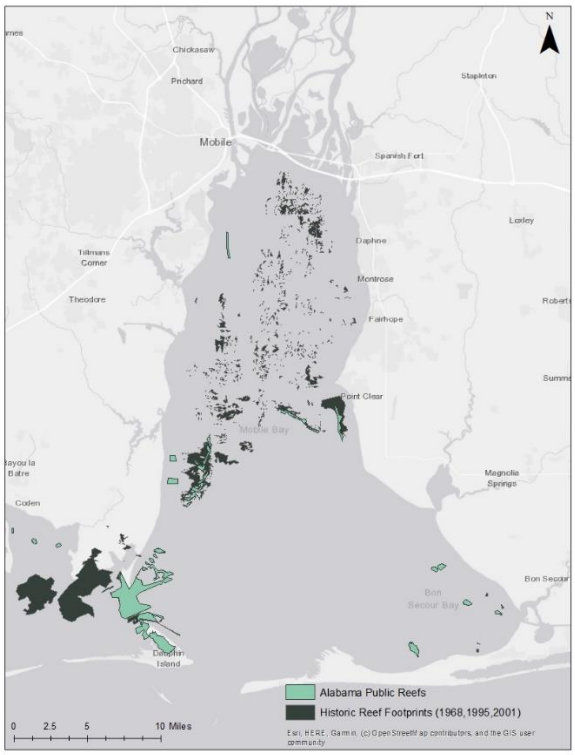

Figure 3. Locations of public reefs (light green) and historical reefs (dark green) in Mobile Bay (from Bannon & Hermann, 2020).

1.11 References

Ahmed, M. (1976). Speciation in Living Oysters. In F. S. Russell & M. Yonge (Eds.), *Advances in Marine Biology* (Vol. 13, pp. 357–397). Academic Press. https://doi.org/10.1016/S0065-2881(08)60283-7

Allen, S. K., & Downing, S. L. (1986). Performance of triploid Pacific oysters, Crassostrea gigas (Thunberg). I. Survival, growth, glycogen content, and sexual maturation in yearlings. *Journal of Experimental Marine Biology and Ecology*, *102*(2), 197–208. https://doi.org/10.1016/0022-0981(86)90176-0

AMRD. (2024, January 19). *AMRD OMS Dashboard 2023*. https://www.arcgis.com/apps/dashboards/9896b07748454e8aa2c040d2567017ec

Anderson, J. D., Karel, W. J., Mace, C. E., Bartram, B. L., & Hare, M. P. (2014). Spatial genetic features of eastern oysters (Crassostrea virginica Gmelin) in the Gulf of Mexico: Northward movement of a secondary contact zone. *Ecology and Evolution*, *4*(9), 1671–1685. https://doi.org/10.1002/ece3.1064

Arnold, A. (2023, September 8). *Baldwin County Land Use Trends: Water Quality and Quantity Patterns*. Alabama Water Resource Conference, Orange Beach.

Austin, G. (1854). *Oceanographic Survey of the Gulf of Mexico on the Circulation and Tidal Flushing of Mobile Bay Alabama, Part I* (Technical Report 28792). Office of Naval Research. https://apps.dtic.mil/sti/tr/pdf/AD0028792.pdf

Bahr, L. M., & Lanier, W. P. (1981). *The Ecology of Intertidal Oyster Reefs of the South Atlantic Coast: A Community Profile*. The Team.

Baldwin, W. S., Davis, T. T., & Eccles, J. A. (2023). Per- and Polyfluoroalkyl Substances (PFAS) and Their Toxicology as Evidenced Through Disease and Biomarkers. In V. B. Patel, V. R. Preedy, & R. Rajendram (Eds.), *Biomarkers in Toxicology* (pp. 989–1016). Springer International Publishing. https://doi.org/10.1007/978-3-031-07392-2_67

Bannon, S., & Hermann, J. (2020, Spring). Side-Scan Mapping of Mobile Bay Relic Oyster Reefs. *Alabama Current Connection*, *14*(1).

Basnyat, P., Teeter, L. D., Flynn, K. M., & Lockaby, B. G. (1999). Relationships Between Landscape Characteristics and Nonpoint Source Pollution Inputs to Coastal Estuaries. *Environmental Management*, *23*(4), 539–549. https://doi.org/10.1007/s002679900208

Basnyat, P., Teeter, L. D., Lockaby, B. G., & Flynn, K. M. (2000). The use of remote sensing and GIS in watershed level analyses of non-point source pollution problems. *Forest Ecology and Management*, *128*(1), 65–73. https://doi.org/10.1016/S0378-1127(99)00273-X

Bell, G. (1982). *The Masterpiece of Nature: The Evolution and Genetics of Sexuality*. CUP Archive.

Bible, J. M., & Sanford, E. (2016). Local adaptation in an estuarine foundation species: Implications for restoration. *Biological Conservation, 193*, 95–102. https://doi.org/10.1016/j.biocon.2015.11.015

Bodenstein, S., Casas, S. M., Tiersch, T. R., & La Peyre, J. F. (2023). Energetic budget of diploid and triploid eastern oysters during a summer die-off. *Frontiers in Marine Science*, *10*. https://www.frontiersin.org/articles/10.3389/fmars.2023.1194296

Bodenstein, S., Walton, W., & Steury, T. (2021). Effect of farming practices on growth and mortality rates in triploid and diploid eastern oysters Crassostrea virginica. *Aquaculture Environment Interactions*, *13*, 33–40. https://doi.org/10.3354/aei00387

Britton, J., & Morton, B. (1989). *Shore Ecology of the Gulf of Mexico* (1st ed.). University of Texas Press.

Buroker, N. E. (1983). Population genetics of the American oyster Crassostrea virginica along the Atlantic coast and the Gulf of Mexico. *Marine Biology*, *75*(1), 99–112. https://doi.org/10.1007/BF00392635

Byrnes, M., Berlinghoff, J., & Griffee, S. (2013). *Sediment Dynamics in Mobile Bay, Alabama: Development of an Operational Sediment Budget*. Mobile Bay national Estuary Program.

Byrnes, M. R., Rosati, J. D., Griffee, S. F., & Berlinghoff, J. L. (2013). Historical Sediment Transport Pathways and Quantities for Determining an Operational Sediment Budget: Mississippi Sound Barrier Islands. *Journal of Coastal Research*, *63 (10063)*, 166–183. https://doi.org/10.2112/SI63-014.1

Callam, B. R., Allen, S. K., & Frank-Lawale, A. (2016). Genetic and environmental influence on triploid Crassostrea virginica grown in Chesapeake Bay: Growth. *Aquaculture*, *452*, 97–106. https://doi.org/10.1016/j.aquaculture.2015.10.027

Camp, E. V., Pine, W. E., Havens, K., Kane, A. S., Walters, C. J., Irani, T., Lindsey, A. B., & Morris, J. G. (2015). Collapse of a historic oyster fishery: Diagnosing causes and identifying paths toward increased resilience. *Ecology and Society*, *20*(3). https://www.jstor.org/stable/26270266

Coogan, J., Dzwonkowski, B., Park, K., & Webb, B. (2020). Observations of Restratification after a Wind Mixing Event in a Shallow Highly Stratified Estuary. *Estuaries and Coasts*, *43*(2), 272–285. https://doi.org/10.1007/s12237-019-00689-w

Davis, J. (2018). *The Gulf: The Making of an American Sea*. Liferight.

Dufresne, L., Neant, I., St-Pierre, J., Dube, F., & Guerrier, P. (1991). Effects of 6-dimethylaminopurine on microtubules and putative intermediate filaments in sea urchin embryos. *Journal of Cell Science*, *99*(4), 721–730. https://doi.org/10.1242/jcs.99.4.721

Dutta, S. M., Mustafi, S. B., Raha, S., & Chakraborty, S. K. (2018). Biomonitoring role of some cellular markers during heat stress-induced changes in highly representative fresh water mollusc, Bellamya bengalensis: Implication in climate change and biological adaptation. *Ecotoxicology and Environmental Safety*, *157*, 482–490. https://doi.org/10.1016/j.ecoenv.2018.04.001

Eleuterius, C. (1976). *Mississippi Sound: Salinity distribution and indicated flow patterns* (MASGP-76-023). Mississippi-Alabama Sea Grant Consortium. https://repository.library.noaa.gov/view/noaa/13145

Engle, C., van Senten, J., Parker, M., Webster, D., & Clark, C. (2021). Economic tradeoffs and risk between traditional bottom and container culture of oysters on Maryland farms. *Aquaculture Economics & Management*, *25*(4), 472–503. https://doi.org/10.1080/13657305.2021.1938295

Fernández-Sanjuan, M., Faria, M., Lacorte, S., & Barata, C. (2013). Bioaccumulation and effects of perfluorinated compounds (PFCs) in zebra mussels (Dreissena polymorpha). *Environmental Science and Pollution Research International*, *20*(4), 2661–2669. https://doi.org/10.1007/s11356-012-1158-8

Fisheries, N. (2023, June 7). *Eastern Oyster | NOAA Fisheries* (New England/Mid-Atlantic, Southeast). NOAA. https://www.fisheries.noaa.gov/species/eastern-oyster

Galtsoff, P. S. (1965). *The American Oyster Crassostrea Virginica Gmelin* (Vol. 64). U.S. Fish and Wildlife Service. https://www.cambridge.org/core/journals/journal-of-the-marine-biological-association-of-the-united-kingdom/article/american-oyster-crassostrea-virginica-gmelin-by-paul-s-galtsoff-fishery-bull-fish-wild-serv-us-vol-64-480-pp-1964/1E911EB4AC9E6EFBAD57F18D6FE9BEC0

Gérard, A., Ledu, C., Phelipot, P., & Naciri-Graven, Y. (1999). *The induction of MI and MII triploids in the Pacific oyster Crassostrea gigas with 6-DMAP or CB.* https://doi.org/10.1016/S0044-8486(99)00032-0

Gledhill, J. H., Barnett, A. F., Slattery, M., Willett, K. L., Easson, G. L., Otts, S. S., & Gochfeld, D. J. (2020). Mass Mortality of the Eastern Oyster Crassostrea virginica in the Western Mississippi Sound Following Unprecedented Mississippi River Flooding in 2019. *Journal of Shellfish Research*, *39*(2), 235–244. https://doi.org/10.2983/035.039.0205

Grabowski, J. H., Brumbaugh, R. D., Conrad, R. F., Keeler, A. G., Opaluch, J. J., Peterson, C. H., Piehler, M. F., Powers, S. P., & Smyth, A. R. (2012). Economic Valuation of Ecosystem Services Provided by Oyster Reefs. *BioScience*, *62*(10), 900–909. https://doi.org/10.1525/bio.2012.62.10.10

Guo, X., & Allen, S. K. (1994). Sex determination and polyploid gigantism in the dwarf surfclam (Mulinia lateralis Say). *Genetics*, *138*(4), 1199–1206. https://doi.org/10.1093/genetics/138.4.1199

Guo, X., & Allen, S. K. A. (2011). Sex and meiosis in autotetraploid Pacific oyster, Crassostrea gigas (Thunberg). *Genome*. https://doi.org/10.1139/g97-053

Häder, D.-P., & Barnes, P. W. (2019). Comparing the impacts of climate change on the responses and linkages between terrestrial and aquatic ecosystems. *Science of The Total Environment*, *682*, 239–246. https://doi.org/10.1016/j.scitotenv.2019.05.024

Hand, R. E., Nell, J. A., & Maguire, G. (1998). Studies on triploid oysters in Australia. X. Growth and mortality of diploid and triploid Sydney rock oysters Saccostrea commercialis (Iredale and Roughley). *Journal of Shellfish Research*, *17*, 1115–1127.

Hare, M. P., & Avise, J. C. (1996). Molecular Genetic Analysis of a Stepped Multilocus Cline in the American Oyster (Crassostrea Virginica). *Evolution*, *50*(6), 2305–2315. https://doi.org/10.1111/j.1558-5646.1996.tb03618.x

Hare, M. P., Karl, S. A., & Avise, J. C. (1996). Anonymous nuclear DNA markers in the American oyster and their implications for the heterozygote deficiency phenomenon in marine bivalves. *Molecular Biology and Evolution*, *13*(2), 334–345. https://doi.org/10.1093/oxfordjournals.molbev.a025593

Hawkins, A. J. S., Day, A. J., Gérard, A., Naciri, Y., Ledu, C., Bayne, B. L., & Héral, M. (1994). A genetic and metabolic basis for faster growth among triploids induced by blocking meiosis I but not meiosis II in the larviparous European flat oyster, Ostrea edulis L. | Semantic Scholar. *Journal of Experimental Marine Biology and Ecology*. https://www.semanticscholar.org/paper/A-genetic-and-metabolic-basis-for-faster-growth-by-Hawkins-Day/f36f80d70c0738f5868f5060909abde6761aaeea

Hintenlang, L. L., Brooks, R. M., & Kane, A. S. (2023). Assessing Cumulative Stressors, State Shift, and the Current Outlook for Oyster Habitat in Apalachicola Bay, Florida. *Journal of Shellfish Research*, *42*(3), 479–489. https://doi.org/10.2983/035.042.0311

Hollingsworth, M. J. (1968). Environmental Temperature and Life Span in Poikilotherms. *Nature*, *218*(5144), Article 5144. https://doi.org/10.1038/218869a0

Hood, S. (2022). *Optimizing Desiccation as a Biofouling Control Strategy for Water-Column Cultured Oysters, Crassostrea virginica, in the Chesapeake Bay* [Dissertation]. University of Maryland.

Hoover, C. A., & Gaffney, P. M. (2005). Geographic variation in nuclear genes of the eastern oyster, Crassostrea virginica gmelin. *Journal of Shellfish Research*, *24*(1), 103–112. https://doi.org/10.2983/0730-8000(2005)24[103:GVINGO]2.0.CO;2

Hu, X., Andrews, D., Lindstrom, A., Bruton, T., Schaider, L., Grandjean, P., Lohmann, R., Carignan, C., Blum, A., Balan, S., Higgins, C., & Sunderland, E. (2016). Detection of Poly- and Perfluoroalkyl Substances (PFASs) in U.S. Drinking Water Linked to Industrial Sites, Military Fire Training Areas, and Wastewater Treatment Plants. *Environmental Science and Technology Letters*, *3*(10), 344–350. https://doi.org/10.1021/acs.estlett.6b00260

Hummell, R., & Parker, S. (1995). *Holocene Geologic History of Mobile Bay, Alabama*. Geological Survey of Alabama.

Isphording, W. C., Imsand, F. D., & Jackson, R. B. (1996). *Fluvial Sediment Characteristics of the Mobile River Delta*. *46*. http://archives.datapages.com/data/gcags/data/046/046001/0185.htm

Jackson, J. B. C., Kirby, M. X., Berger, W. H., Bjorndal, K. A., Botsford, L. W., Bourque, B. J., Bradbury, R. H., Cooke, R., Erlandson, J., Estes, J. A., Hughes, T. P., Kidwell, S., Lange, C. B., Lenihan, H. S., Pandolfi, J. M., Peterson, C. H., Steneck, R. S., Tegner, M. J., & Warner, R. R. (2001). Historical Overfishing and the Recent Collapse of Coastal Ecosystems. *Science*, *293*(5530), 629–637. https://doi.org/10.1126/science.1059199

Jacobson, J. (2018). *Mobile Harbor, Mobile, Alabama Integrated General Reevaluation Report with Supplemental Environmental Impact Statement, Mobile County, Alabama*. U.S. Army Corps of Engineers.

Jeon, J., Kannan, K., Lim, H. K., Moon, H. B., Ra, J. S., & Kim, S. D. (2010). Bioaccumulation of perfluorochemicals in Pacific oyster under different salinity gradients. *Environmental Science & Technology*, *44*(7), 2695–2701. https://doi.org/10.1021/es100151r

Karl, S. A., & Avise, J. C. (1992). Balancing Selection at Allozyme Loci in Oysters: Implications from Nuclear RFLPs. *Science*. https://doi.org/10.1126/science.1348870

Kennedy, V., Newell, R., & Eble, A. (1996). *The Eastern oyster: Crassostrea virginica*. Maryland Sea Grant.

Killen, S. S., Christensen, E. A. F., Cortese, D., Závorka, L., Norin, T., Cotgrove, L., Crespel, A., Munson, A., Nati, J. J. H., Papatheodoulou, M., & McKenzie, D. J. (2021). Guidelines for reporting methods to estimate metabolic rates by aquatic intermittent-flow respirometry. *The Journal of Experimental Biology*, *224*(18). https://doi.org/10.1242/jeb.242522

Kim, C.-K., Park, K., Powers, S. P., Graham, W. M., & Bayha, K. M. (2010). Oyster larval transport in coastal Alabama: Dominance of physical transport over biological behavior in a shallow estuary. *Journal of Geophysical Research: Oceans*, *115*(C10). https://doi.org/10.1029/2010JC006115

King, T. L., Ward, R., & Zimmerman, E. G. (2011). Population Structure of Eastern Oysters (Crassostrea virginica) Inhabiting the Laguna Madre, Texas, and Adjacent Bay Systems. *Canadian Journal of Fisheries and Aquatic Sciences*. https://doi.org/10.1139/f94-307

Kooijman, S. A. L. M. (2010). *Dynamic Energy Budget Theory for Metabolic Organization*. Cambridge University Press.

La Peyre, M. K., Eberline, B. S., Soniat, T. M., & La Peyre, J. F. (2013). Differences in extreme low salinity timing and duration differentially affect eastern oyster (Crassostrea virginica)

size class growth and mortality in Breton Sound, LA. *Estuarine, Coastal and Shelf Science*, *135*, 146–157. https://doi.org/10.1016/j.ecss.2013.10.001

Lannig, G., Flores, J. F., & Sokolova, I. M. (2006). Temperature-dependent stress response in oysters, Crassostrea virginica: Pollution reduces temperature tolerance in oysters. *Aquatic Toxicology*, *79*(3), 278–287. https://doi.org/10.1016/j.aquatox.2006.06.017

Leitman, S., Pine, W. E., & Kiker, G. (2016). Management Options During the 2011–2012 Drought on the Apalachicola River: A Systems Dynamic Model Evaluation. *Environmental Management*, *58*(2), 193–207. https://doi.org/10.1007/s00267-016-0712-4

Lenihan, H. S., & Peterson, C. H. (2004). Conserving oyster reef habitat by switching from dredging and tonging to diver-harvesting. *Fish Bulletin*, *102*(2), 298–305.

Li, Y., Jiang, K., & Li, Q. (2022). Comparative transcriptomic analyses reveal differences in the responses of diploid and triploid Pacific oysters (*Crassostrea gigas*) to thermal stress. *Aquaculture*, *555*, 738219. https://doi.org/10.1016/j.aquaculture.2022.738219

Love, G., Baker, S., & Camp, E. V. (2021). Oyster-Predator Dynamics and Climate Change. *EDIS*, *2021*(1), 5. https://doi.org/10.32473/edis-fa228-2020

Lowe, M. R., Sehlinger, T., Soniat, T. M., & Peyre, M. K. L. (2017). Interactive Effects of Water Temperature and Salinity on Growth and Mortality of Eastern Oysters, Crassostrea virginica: A Meta-Analysis Using 40 Years of Monitoring Data. *Journal of Shellfish Research*, *36*(3), 683–697. https://doi.org/10.2983/035.036.0318

Marshall, D. A., Casas, S. M., Walton, W. C., Rikard, F. S., Palmer, T. A., Breaux, N., La Peyre, M. K., Beseres Pollack, J., Kelly, M., & La Peyre, J. F. (2021). Divergence in salinity tolerance of northern Gulf of Mexico eastern oysters under field and laboratory exposure. *Conservation Physiology*, *9*(1), coab065. https://doi.org/10.1093/conphys/coab065

Marshall, D. A., Coxe, N. C., La Peyre, M. K., Walton, W. C., Rikard, F. S., Pollack, J. B., Kelly, M. W., & La Peyre, J. F. (2021). Tolerance of northern Gulf of Mexico eastern oysters to chronic warming at extreme salinities. *Journal of Thermal Biology*, *100*, 103072. https://doi.org/10.1016/j.jtherbio.2021.103072

Masaru, H., Komaru, A., Sousa, J. T. D., & Allen, S. K. (2017). Meiotic and Early Zygotic Development in Crassostrea virginica Observed through Confocal Microscopy. *Journal of Shellfish Research*, *36*(3), 699–706. https://doi.org/10.2983/035.036.0319

McPhearson, Jr, R. (1970). Hydrography of Mobile Bay and Mississippi Sound, Alabama. *Journal of Marine Science*, *1*(2), 1–83.

Mohammed, R., & Scholz, M. (2017). Critical review of salinity intrusion in rivers and estuaries. *Journal of Water and Climate Change*, *9*(1), 1–16. https://doi.org/10.2166/wcc.2017.334

Moore, J. F., Pine III, W. E., Frederick, P. c., Beck, S., Moreno, M., Dodrill, M. J., Boone, M., Sturmer, L., & Yurek, S. (2020). Trends in Oyster Populations in the Northeastern Gulf

of Mexico: An Assessment of River Discharge and Fishing Effects over Time and Space. *Marine and Coastal Fisheries*, *12*(3), 191–204. https://doi.org/10.1002/mcf2.10117

Nash, S., Johnstone, J., & Rahman, M. S. (2019). Elevated temperature attenuates ovarian functions and induces apoptosis and oxidative stress in the American oyster, Crassostrea virginica: Potential mechanisms and signaling pathways. *Cell Stress & Chaperones*, *24*(5), 957–967. https://doi.org/10.1007/s12192-019-01023-w

NOAA. (2023). *NOAA Center for Operational Oceanographic Products and Services (CO-OPS)*. https://tidesandcurrents.noaa.gov/gmap3/

Noble, M. A., Schroeder, W. W., Wiseman Jr., W. J., Ryan, H. F., & Gelfenbaum, G. (1996). Subtidal circulation patterns in a shallow, highly stratified estuary: Mobile Bay, Alabama. *Journal of Geophysical Research: Oceans*, *101*(C11), 25689–25703. https://doi.org/10.1029/96JC02506

Oczkowski, A. J., Lewis, F. G., Nixon, S. W., Edmiston, H. L., Robinson, R. S., & Chanton, J. P. (2011). Fresh Water Inflow and Oyster Productivity in Apalachicola Bay, FL (USA). *Estuaries and Coasts*, *34*(5), 993–1005. https://doi.org/10.1007/s12237-011-9383-9

Orlando, P., & Klein III, J. (1989). *Characterization of salinity and Temperature for Mobile Bay* (p. 22). National Oceanic and Atmospheric Administration.

Oysters in Alabama. (n.d.). Alabama Cooperative Extension System. Retrieved February 1, 2023, from https://www.aces.edu/blog/topics/coastal-programs/oysters-in-alabama/

Park, K., Kim, C.-K., & Schroeder, W. W. (2007). Temporal variability in summertime bottom hypoxia in shallow areas of Mobile Bay, Alabama. *Estuaries and Coasts*, *30*(1), 54–65. https://doi.org/10.1007/BF02782967

Park, K., Valentine, J. F., Sklenar, S., Weis, K. R., & Dardeau, M. R. (2007). The Effects of Hurricane Ivan in the Inner Part of Mobile Bay, Alabama. *Journal of Coastal Research*, *23*(5 (235)), 1332–1336. https://doi.org/10.2112/06-0686.1

Peachey, R. B. J. (2003). Tributyltin and polycyclic aromatic hydrocarbon levels in Mobile Bay, Alabama: A review. *Marine Pollution Bulletin*, *46*(11), 1365–1371. https://doi.org/10.1016/S0025-326X(03)00373-4

Rahman, M. S., & Rahman, M. S. (2021). Effects of elevated temperature on prooxidant-antioxidant homeostasis and redox status in the American oyster: Signaling pathways of cellular apoptosis during heat stress. *Environmental Research*, *196*, 110428. https://doi.org/10.1016/j.envres.2020.110428

Ramanathan, N. L. (1964). Reliability of estimation of metabolic levels from respiratory frequency. *Journal of Applied Physiology*, *19*(3), 497–502. https://doi.org/10.1152/jappl.1964.19.3.497

Reeb, C., & Avise, J. C. (1990). A genetic discontinuity in a continuously distributed species: Mitochondrial DNA in the American oyster, Crassostrea virginica. *Genetics*, *124*(2), 397–406.

Root, T. L., Price, J. T., Hall, K. R., Schneider, S. H., Rosenzweig, C., & Pounds, J. A. (2003). Fingerprints of global warming on wild animals and plants. *Nature*, *421*(6918), Article 6918. https://doi.org/10.1038/nature01333

Rue, C. R., Selwyn, J. D., Cockett, P. M., Gillis, B., Gurski, L., Jose, P., Kutil, B. L., Magnuson, S. F., Mesa, L. Á. L. de, Overath, R. D., Smee, D. L., & Bird, C. E. (2021). Genetic diversity across the mitochondrial genome of eastern oysters (Crassostrea virginica) in the northern Gulf of Mexico. *PeerJ*, *9*, e12205. https://doi.org/10.7717/peerj.12205

Rybovich, M., La Peyre, M., Hall, S., & La Peyre, J. (2016). Increased Temperatures Combined with Lowered Salinities Differentially Impact Oyster Size Class Growth and Mortality. *Journal Of Shellfish Research*, *35*(1), 101–113. https://doi.org/10.2983/035.035.0112

Schroeder, W. W., Cowan, J. L. W., Pennock, J. R., Luker, S. A., & Wiseman, W. J. (1998). Response of Resource Excavations in Mobile Bay, Alabama, to Extreme Forcing. *Estuaries*, *21*(4), 652–657. https://doi.org/10.2307/1353303

Sheltzer, J. M., & Amon, A. (2011). The aneuploidy paradox: Costs and benefits of an incorrect karyotype. *Trends in Genetics*, *27*(11), 446–453. https://doi.org/10.1016/j.tig.2011.07.003

Shumway, S. E. (1977). Effect of salinity fluctuation on the osmotic pressure and Na+, Ca2+ and Mg2+ ion concentrations in the hemolymph of bivalve molluscs. *Marine Biology*, *41*(2), 153–177. https://doi.org/10.1007/BF00394023

Sinclair, G. M., Long, S. M., & Jones, O. A. H. (2020). What are the effects of PFAS exposure at environmentally relevant concentrations? *Chemosphere*, *258*, 127340. https://doi.org/10.1016/j.chemosphere.2020.127340

Smith, D. (2015). *Oyster: A Gastronomic History (with Recipes)*. Harry N. Abrams.

Sokolova, I. M., Frederich, M., Bagwe, R., Lannig, G., & Sukhotin, A. A. (2012). Energy homeostasis as an integrative tool for assessing limits of environmental stress tolerance in aquatic invertebrates. *Marine Environmental Research*, *79*, 1–15. https://doi.org/10.1016/j.marenvres.2012.04.003

Stanley, J. G., & Sellers, M. A. (1986). *Species profiles: Life histories and environmental requirements of coastal fishes and invertebrates (Gulf of Mexico)—American oyster* (82; US Fish and Wildlife Service Biological Report, p. 25).

Stanley, J., Hidu, H., & Allen, S. K. (1984). *Growth of American oysters increased by polyploidy induced by blocking meiosis I but not meiosis II*. https://www.sciencedirect.com/science/article/pii/0044848684900723

Stumpf, R. P., Gelfenbaum, G., & Pennock, J. R. (1993). Wind and tidal forcing of a buoyant plume, Mobile Bay, Alabama. *Continental Shelf Research*, *13*(11), 1281–1301. https://doi.org/10.1016/0278-4343(93)90053-Z

Summers, J. K. (2001). Ecological condition of the estuaries of the Atlantic and Gulf coasts of the United States. *Environmental Toxicology and Chemistry*, *20*(1), 99–106. https://doi.org/10.1002/etc.5620200109

Tabarini, C. L. (1984). Induced triploidy in the bay scallop, Argopecten irradians, and its effects on growth and gametogenesis. *Aquaculture*. https://doi.org/10.1016/0044-8486(84)90362-4

Theuerkauf, S. J., Burke, R. P., & Lipcius, R. N. (2015). Settlement, Growth, and Survival of Eastern Oysters on Alternative Reef Substrates. *Journal of Shellfish Research*, *34*(2), 241–250. https://doi.org/10.2983/035.034.0205

Turner, R. E., Rabalais, N. N., & Justić, D. (2017). Trends in summer bottom-water temperatures on the northern Gulf of Mexico continental shelf from 1985 to 2015. *PLOS ONE*, *12*(9), e0184350. https://doi.org/10.1371/journal.pone.0184350

U.S. Census Bureau. (2020). Retrieved October 10, 2023, from https://data.census.gov/

US Department of Commerce, N. (2023). *Temperature and Precipitation Graph for Mobile*. NOAA's National Weather Service. Retrieved October 10, 2023, from https://www.weather.gov/mob/climate_kmob

Varney, R. L., Galindo-Sánchez, C. E., Cruz, P., & Gaffney, P. M. (2009). Population Genetics of the Eastern Oyster Crassostrea virginica (Gmelin, 1791) in the Gulf of Mexico. *Journal of Shellfish Research*, *28*(4), 855–864. https://doi.org/10.2983/035.028.0415

Viticoski, R. L., Wang, D., Feltman, M. A., Mulabagal, V., Rogers, S. R., Blersch, D. M., & Hayworth, J. S. (2022). Spatial distribution and mass transport of Perfluoroalkyl Substances (PFAS) in surface water: A statewide evaluation of PFAS occurrence and fate in Alabama. *The Science of the Total Environment*, *836*, 155524. https://doi.org/10.1016/j.scitotenv.2022.155524

Wallace, R. K. (2001). Cultivating the Eastern Oyster, Crassostrea virginica. *Southern Regional Aquaculture Center*, 4.

Wallace, R. K. (2002). *Oysters in Alabama*. Auburn University Marine Extension and Research Center Sea Grant Extension.

Wang, Z., Guo, X., Allen, S., & Wang, R. (2002). *Heterozygosity and body size in triploid Pacific oysters, Crassostrea gigas Thunberg, produced from meiosis II inhibition and tetraploids*. https://doi.org/10.1016/S0044-8486(01)00845-6

Waterborne Commerce of the United States (p. 98). (2010). [National Summary]. U.S. Army Corps of Engineers.

Wiberg, P. L., Taube, S. R., Ferguson, A. E., Kremer, M. R., & Reidenbach, M. A. (2019). Wave Attenuation by Oyster Reefs in Shallow Coastal Bays. *Estuaries and Coasts*, *42*(2), 331–347. https://doi.org/10.1007/s12237-018-0463-y

CHAPTER 2
PFAS BIOACCUMULATION, DEPURATION, AND ASSOCIATED ENERGETIC COSTS IN THE EASTERN OYSTER (*Crassostrea virginica*)

2.1 Introduction

Per- and polyfluorinated chemicals (PFAS) are a class of man-made chemicals that are widespread and persistent in the environment (US EPA, 2016). PFAS is used in manufacturing and has been linked to industrial sites, military fire training areas, and wastewater treatment plants (Hu et al., 2016). PFAS molecules- particularly those with long carbon chains (i.e. >6c)- have the ability to bind to proteins and fats, increasing the likelihood of bioaccumulation in organisms that are exposed to them (Jeon et al., 2010). Human populations are primarily exposed to PFAS through dietary intake and contaminated drinking water. Exposure has been associated with reduced birthweight, endocrine disruption, and cancers in humans (Panieri et al., 2022). PFASs have been found in low concentrations in marine and freshwater habitats world-wide (Giesy and Kannan, 2001; Kannan et al., 2005, 2002), but studies showing effects at ecologically relevant concentrations are limited (Sinclair et al., 2020).

Benthic organisms such as filter-feeders may be chronically exposed to biocontaminants through water and food. Potential cellular toxicities at high water concentrations make PFAS of particular concern if they bioaccumulate in filter feeders such as oysters (Aquilina-Beck et al., 2020). PFAS bioaccumulation in filter feeders increases the risk of biomagnification in predators including humans (De Silvia et al., 2021; Kannan et al., 2005). Although PFOS and PFOA manufacturing have been voluntarily phased out in the United States, these two PFAS are still found in U.S. waterways in water and sediment (ATSDR, 2018; White et al., 2015). In addition to PFOS and PFOA, over 9,000 PFAS compounds have been identified with that number increasing as detection sensitivity increases (CDC, 2022). Previous studies by our research group

have documented detectable levels of PFOS, PFOA, PFBS, PFBA, PFPeA, PFHpA, PFNA, and PFHxA in the water around Mobile Bay, AL, a major port in the Gulf of Mexico (Strozier et al., unpublished data).

As sessile filter feeders, oysters are chronically exposed to ambient PFAS and other contaminants in the water column. The amount of PFAS that accumulates in bivalve tissue is dependent on environmental factors including salinity and PFAS concentration (Fernández-Sanjuan et al., 2013; Jeon et al., 2010). The ability of some PFAS to bioaccumulate more readily than others is determined in large part by chemical composition. The longer and more linear a PFAS compound is, the more likely it is to bind to proteins (Benskin et al., 2009; Houde et al., 2008; Lau, 2015). For example, linear PFOS bioaccumulates more rapidly than complex PFOS with multiple carbon branches (Aquilina-Beck et al., 2020). The functional group also plays a role in bioaccumulation. Even though they both have 8-carbon chains, PFOS has a higher bioaccumulation factor than PFOA due to the sulfonic acid versus carboxylic acid on the compound. Although oysters bioaccumulate PFAS within their tissues, the Pacific oyster (*Magallana (Crassostrea) gigas*) has been shown to be very efficient at eliminating PFAS from their tissues via depuration, reducing the risk of high levels of bioaccumulation (Jeon et al., 2010).

Stressors, including pollutants, can increase metabolic costs and reduce the amount of energy remaining for maintenance and basic functions in aquatic ectotherms including crustaceans and bivalves (Goodchild et al., 2019; Rowe et al., 2001; Smolders et al., 2004). The multixenobiotic resistance (MXR) system is a defense mechanism that bivalves have evolved to actively lower the intracellular concentration of many toxins using high molecular membrane proteins, similar to the multidrug resistance (MDR) system in mammals (Gottesman and Pastan,

1993; Minier and Moore, 1996). The MXR system has been well characterized and studied in mussels and is induced by contaminants such as Methyl methanesulfonate (MMS) and Dimethyl sulfoxide (DMSO) in mussel larvae (McFadzen et al., 2000). The production and maintenance of these proteins in response to toxic chemicals is metabolically expensive (Calow, 1991).

Because the eastern oyster (*Crassostrea virginica*) is a keystone species as well as a commercial aquaculture species, it is important to examine the potential for PFAS to negatively affect an oyster's energetic health. A decrease in energetic health can decrease growth and reproduction and increase the chances of mortality and loss of oyster reefs or crop value for oyster farmers. Not only could this reduce habitat that many species rely on for food and shelter, major oyster loss results in a loss in other ecosystem services oysters provide including wave attenuation, denitrification, and water clarity (Grabowski et al., 2012).

The goals of this study were to 1) quantify the rate at which eastern oysters bioaccumulate an environmentally relevant mixture of 5 PFAS compounds, 2) quantify the rate at which they depurate this mixture, 3) determine the energetic costs of exposure to, and depuration of, a simple PFAS mixture (PFOS + PFOA) for direct comparison to previous studies and 4) determine the energetic costs of exposure to an environmentally relevant mixture of 5 PFAS compounds in the northern Gulf of Mexico.

2.2 Materials and methods

2.2.1 Chemical stock and working solutions

We first created individual stock solutions containing a nominal 20,000µg/L of PFOS (Synquest Laboratories, Product 6164-3-08, purity 97%, Alachua, FL, USA), PFOA (BeanTown Chemical, Product BT139610, purity ≥95%, Hudson, NH, USA), PFHxA (Matrix Scientific, Cat.

101777-248, purity ≥95%, Columbia, SC, USA), PFBS (Synquest Laboratories, Cat. 6164-3-09, purity 97%, Alachua, FL, USA), or PFPeA (Alfa Aesar, Cat. AAB21567-06, purity 97%, Tewksbury, MA, USA) in reverse osmosis deionized (RODI) water in 1 L HDPE bottles and stored them at -20°C.

In addition to the individual stock solutions, a 5-PFAS mixture working solution was created by combining 50mL (PFOS, PFOA) and 100mL (PFHxA, PFBS, PFPeA) of each of the previously described stock solutions and then diluting the resultant mix with 700ml of DI water for a final nominal concentration of 1,667µg/L per compound and stored it at 4°C.

A 2-PFAS mixture working solution was created by adding .05L each of the PFOS and PFOA stock solutions to .9L of RO/DI water for a total volume of 1L and a concentration of 1,000µg/L for each compound and a combined concentration of 2,000 µg/L.

2.2.2 Bioaccumulation and Depuration of 5-PFAS Mixture

2.2.2.1 Collection and initial processing of study animals

Adult oysters (60-70mm in height) for bioaccumulation experiments were collected from off-bottom oyster baskets at the Grand Bay Oyster Park, Grand Bay, AL on 17 November 2021. Water temperature at time of collection was 21.5°C. Because oysters are hermaphroditic and not sexually dimorphic, the sex of each individual was unknown. Following collection, oysters were placed in a cooler between moist paper towels. Ice packs were added above and below the paper towels to reduce the temperature of the cooler during shipping, as per standard oyster shipping practice. The cooler was shipped overnight to E. W. Shell Fisheries Center, Auburn University, AL.

Upon arrival, the ice packs were removed, and the internal air temperature of the cooler (10°C) was raised to ambient laboratory air temperature (23°C) over 8 hours. Oysters were scrubbed with a soft bristle brush and deionized (DI) water and rinsed with 16ppt synthetic seawater (SSW) made with Crystal Sea® Marinemix (Marine Enterprises International, LLC., Baltimore, MD, USA) dissolved in DI water to remove biofouling organisms like algae and barnacles. Tougher barnacles were scraped from the shell using a stainless-steel spatula. Oysters were weighed, shell height and length recorded, and tagged with 8 X 4 mm external Hallprint shellfish tags (Hallprint, Hindmarsh Valley, South Australia). Oysters were then placed in 14L of 16ppt SSW. Water temperature was increased 1°C every two hours until laboratory holding temperatures were reached (28°C). After 24 hours of acclimation in a common trough, oysters were randomly assigned and placed in recirculating acclimation upwellers containing 75L of 16ppt SSW at 28°C. Minimal mortality (<10%) was observed throughout the processing and acclimation period.

Upwellers were constructed of plastic totes with a recirculation pump. Bacterial biofilters consisting of bioballs were established for >2 weeks prior to the arrival of experimental oysters. Each upweller was given a ration of three parts Reed Mariculture 1800® Shellfish Diet and one-part Nanno 3600 (Reed Mariculture Inc., Campbell, CA, USA) once every hour based on the estimated tissue wet weight of the upweller population (tissue wet mass = ~40% of the whole animal wet mass). The wet tissue weight of the population was multiplied by .036 to estimate the appropriate volume of algae to feed per day (Helm and Bourne, 2004). pH was measured once a week using a handheld pH meter (Oakton® pH30 pH Tester, Vernon Hills, IL, USA) and ammonia, nitrite, and nitrates were measured using either 7 in 1 aquarium test strips (Stript Health) and Tetra® EasyStrips™ Ammonia Test Strips (Blacksburg, VA, USA) or an EcoSense

YSI 9300 Photometer (Yellow Spring, OH, USA). Water changes were completed if ammonia or nitrite concentrations exceeded 1mg/L.

2.2.2.2 PFAS exposure

A 28-day bioaccumulation and subsequent five-day depuration trial was conducted by exposing oysters to a mixture of PFOS, PFOA, PFBS, PFPeA, and PFHxA at a nominal concentration of 1.7µg/L each (cumulative PFAS concentration of 8.5µg/L) in SSW (28°C, 16ppt) in a Coleman cooler containing 70 L of SSW. Internal walls of the cooler were made of polypropylene plastic. A complete water change, with addition of appropriate amounts of PFAS from the stock solution, was conducted every other day to maintain water quality and minimize changes in PFAS concentrations. After 28 days of exposure, the oysters were moved to an uncontaminated 120qt Coleman cooler with 70 L of SSW without PFAS for 5 days. Depuration water was changed every 24 hours to remove any PFAS depurated from the oysters. During exposure and depuration, oysters were fed 75mL daily ration of three parts Shellfish Diet 1800 and one part Nanno 3600 split into hourly feedings using a GHL Doser 2 (GHL, Germany).

Water samples were collected every 48 hours during the duration of the exposure in HDPE sample bottles to monitor PFAS concentrations in the water. Duplicate samples were collected prior to each water change when concentrations were presumably at their lowest levels. All water samples were stored frozen at -20°C until analysis.

At eight times during the exposure period (Day 0, 2, 4, 7, 10, 14, 20, 28) and at three times during the depuration period (Day 1, 3, 5), three oysters were randomly chosen from the cooler to monitor PFAS tissue concentrations. Live oysters were shucked and their tissues were rinsed with DI water. Wet tissues were weighed and stored at -80°C until analysis for PFAS.

2.2.1.3 Analysis of water and oyster tissue samples for PFAS

Water sample preparation

Experimental water samples were thawed and spiked with an internal standard (MPFOS, 1 ng/mL) and subjected to the Solid Phase Extraction (SPE) cleanup procedure. SPE has four stages: conditioning, loading, washing, and eluting. Oasis WAX 6cc Vac cartridges (150mg, 30µm) were pre-conditioned by passing 4mL 0.1% ammonium hydroxide (NH_4OH) in methanol solution, 4mL methanol, and 4mL of liquid chromatography water in order and the fractions discarded. The cartridge was then loaded with sample and eluted at the rate of 1 drop/sec, discarding the flowthrough. The cartridge was then washed with 4mL of 25mM ammonia acetate buffer (4 pH) to remove any remaining organics, and the fraction discarded. The PFAS retained on the cartridge was eluted by using 2 mL methanol followed by 2mL of 0.1% NH_4OH in methanol. These two fractions were combined and filtered through a glass-fiber nylon membrane syringe filter (Andwin Scientific 0.25µm). Filtered samples were aliquoted out and spiked again with internal standard (MPFOS, 1ng/mL).

For each experimental time period, duplicate water samples (50+50mL) were combined and spiked with internal standards prior to solid phase extraction. The samples were subjected to SPE cleanup and eluted with extraction solvent (4mL of 0.1% NH4OH in methanol + 2mL of methanol). The extract was concentrated under vacuum and reconstituted with water/methanol (90:10%, v/v) and diluted further for analysis.

Tissue sample preparation and extraction

Tissue samples were freeze-dried for 96 hours using a HarvestRight Scientific Freeze Dryer (HarvestRight, North Salt Lake, Utah, USA). Dried samples were weighed and placed in 50mL centrifuge tubes and stored at -80°C until analysis. Samples from 3 oysters per sampling period were spiked with internal standard and extracted with 30mL of 0.1% alkaline methanol. Samples were sonicated for an hour at 60Hz and then shaken on an orbital shaker (250 rpm) for 16 hrs. The homogenates were centrifuged for 15 min at 13,000 rpm. The obtained extracts were concentrated under vacuum and diluted with 50mL LC grade water. After SPE cleanup, samples were eluted with 4mL of 0.1% NH_4OH in methanol + 2mL methanol. Finally, the extracts were concentrated and diluted in methanol and water (90:10,v/v) for further analysis.

Water and tissue sample analysis

Water and dry tissue PFAS concentration was quantified on an ultra-high performance liquid chromatography, triple quadruple mass spectrometer (UHPLC-MS/MS) (Agilent Technologies, Santa Clara, CA, USA). Blanks were processed along with the samples and experimental solvent blanks were analyzed with each batch to test carryover effect during purification and analysis.

Bioaccumulation factor and percent PFAS elimination calculations

Bioaccumulation factor (BAF) was calculated using the following formula where C_{biota} (µg/kg wet weight) is the concentration of each PFAS in the whole wet tissue weight of the oyster and C_{water} (µg/L) is the concentration of each PFAS in the culture water.

$$BAF\ (L/kg\ wet\ weight) = C_{biota}/C_{water}$$

Bioaccumulation factors were calculated for each of two periods: Days 4-10 and Days 20-28. Within each period, mean tissue and mean water concentrations were used for calculations.

Because PFAS fell below detection limits in extracted tissue samples within 24 hours of oysters being transferred to clean water (see Results), we could not calculate PFAS elimination rates. To estimate the approximate detection limit per gram of oyster dry weight, the detection limit of extracted samples (ng/mL) was multiplied by the volume of extracted sample and then divided by the dry weight (g) of oyster tissue from which it had been extracted and reported as µg PFAS/g dry oyster tissue weight.

2.2.3 Energetic costs of exposure and depuration

A 10-day exposure and subsequent one-day depuration trial was conducted to measure energetic costs of exposure and subsequent depuration to a 2-compound mixture (PFOS plus PFOA) for comparison to previous studies. A 10-day exposure trial was also conducted to measure energetic costs of an environmentally relevant, 5-compound PFAS mixture on oysters. The exposure time in both trials was limited to 10 days to measure effects during the period of maximum PFAS tissue concentrations (see results of bioaccumulation trials).

2.2.3.1 Oyster intake and acclimation

Adult oysters (56-80mm in height) for energetic cost experiments were collected on 18 August 2020 from off-bottom oyster baskets at Grand Bay Oyster Park, Grand Bay, AL. Oysters were packed, shipped, cleaned, and acclimated to laboratory conditions (28°C, 18ppt, 12:12 h; light-dark, pH 8) for > 2 weeks in upwellers and SSW as described previously. During this time,

oysters were observed spawning in the upwellers over a two-day period (August 20- August 22). A water change was conducted post-spawn to prevent water quality degradation.

Following acclimation, oysters were randomly assigned to three exposure groups and total wet mass of each oyster was recorded. Exposure groups were as follows: Control (no PFAS; 10 oysters), 5µg PFOS/L + 5µg PFOA/L (10µg PFAS/L; 20 oysters) and 2µg/L each of PFOS + PFOA + PFBS + PFPeA + PFHxA (10µg PFAS/L; 10 oysters). Oysters were exposed to their respective PFAS concentrations for 10 days in exposure chambers made of HDPE plastic and containing 2L of 16ppt salinity SSW at 28°C. Chamber water was completely changed every 24 hrs and the appropriate amount of PFAS added to each batch of new water. For the PFOS + PFOA exposure group, 30ml of the PFOS/PFOA working stock solution (see previous section) was diluted to 6L with SSW for a final concentration of 5µg/L of each compound (10µg/L combined) and used to fill the appropriate exposure chambers. For the 5-PFAS exposure group, 27.89mL of the 5-PFAS working stock solution was diluted to 28 L with SSW for a final concentration of 2µg/L each (10µg/L combined) and used to fill the appropriate exposure chambers.

Oysters were fed a ration of 36mL Reed Mariculture Shellfish Diet and 12mL of Reed Mariculture nano 3600 algae diluted in 35ppt SSW to a total volume of 250mL Each oyster was batch fed volumes of diluted algae based on their wet weight twice daily (1.35 - 2.13mL).

2.2.3.2 Respirometry

On Day 11 of the exposure regime, mass-specific respiration rates (MO_2) were measured for 10 control oysters in clean SSW, 10 oysters exposed to PFOS + PFOA (10µg PFAS/L) measured in clean water, 10 oysters in PFOS + PFOA water (10µg PFAS/L), and 10 oysters in

PFOS + PFOA + PFBS + PFPeA +PFHxA water (10µg PFAS/L) to estimate metabolic costs of ongoing exposure to PFAS. On Day 11 we also measured respiration rates of an additional 10 oysters that had been transferred from the PFOS + PFOA treatment to clean water in order to estimate the metabolic costs of depuration. This was performed for direct comparison to PFAS depuration costs previously documented for zebra mussels exposed to PFOS+PFOA mixtures (Fernández-Sanjuan et al., 2013).

Because we could not measure respiration of all oysters on the same day, we staggered the starting dates for exposure and respirometry for individual oysters in order to meet the exposure regime described above (i.e. exposure was initiated on different dates for different oysters). To conduct a given respirometry trial, two oysters were collected from the Control, four oysters from the PFOS+PFOA exposure, and two oysters from the 5-PFAS exposure at Day 10 of exposure for those respective oysters. Trials were repeated until we had run at least 10 oysters from each exposure group.

Each respirometry trial tested four treatments: control, ongoing exposure to PFOS+PFOA, depuration of PFOS+PFOA, and ongoing exposure to the 5-PFAS solution. Treatments were randomly assigned to one of four bins held in a water bath kept at 28°C. Each bin contained 28L of 16ppt SSW with supplemental aeration, but no food. The appropriate amount of PFAS was added to the PFOS+PFOA and the 5-PFAS exposure bins. No PFAS was added to the control or PFOS+PFOA depuration bins. Temperature sensors were placed in the bins furthest to the left and right of the trough to account for any temperature differences within the water bath. Bin placement was randomly assigned before each trial. Tubing, pumps, chambers, and bins had been previously chlorinated with a 1% bleach solution to reduce ambient

oxygen demand from bacteria, and then rinsed thoroughly with tap water to remove any residual chlorine.

On Day 10 of exposure, water in the test chambers was changed at 09:00 and no food was added to initiate a 24-hour fasting period prior to collecting respiration data for analysis. Oysters assigned to each treatment (2 per treatment) were placed in respirometry chambers within the appropriate treatment bin (2 respirometry chambers per bin) at 19:00 on Day 10, oriented with the flat valve facing upwards, and allowed to acclimate to the chambers overnight. No food was added to the respirometry system during acclimation or the subsequent respiration measurement periods. Respiration rates were measured using an 8-chamber fiber-optic respirometry system with AutoResp™ 2.3.0 software (Loligo® Systems, Viborg, Denmark). Each acrylic respirometry chamber was fitted with two Eheim® submersible 300 L/h pumps (Eheim GmbH & Co., Deizisau, Germany). The flush pump brought fresh, oxygenated water into the chamber to replace oxygen-depleted water and flush out waste metabolites between measurement cycles. The closed pump recirculated water through a closed loop that included the chamber and a flow-through oxygen cell with a fiber-optic dissolved oxygen (DO) sensor (Fig. 4). Probes were calibrated using a two-point calibration (0% and 100%) prior to each experimental run. The closed pump was left on during the entire experiment, while the flush pump was only turned on between measurement periods.

Following placement in the chambers, oysters were allowed to draw down the oxygen for 12.5 min during a measurement period which was followed by a 13 min flushing period. This flush-measurement cycle was repeated for the entire experiment (including the overnight acclimation) at 28°C and a 12-hr light: 12-hr dark cycle with dissolved oxygen never declining below 80% saturation during measurement periods. Data collection for analysis began on Day 11

at 09:00 (2 hours after lights turned on) – after the overnight acclimation. Data collection ended at 18:00 on Day 11. Oysters were then shucked, and wet tissue mass was recorded. All tissues were stored at -20°C until they could be freeze dried, after which dry tissue mass was recorded.

During each trial, respiration rate (mgO_2/kgWWW/h) was calculated for individual oysters during each measurement period by AutoResp™ software using the formula:

$$\text{RMR (mg } O_2\text{/kgWWW/h)} = \frac{V([O_2]_{t0} - [O_2]_{t1})}{t \times WWW}$$

where:

$[O_2]_{t0}$ = DO at time t0 (mg O_2/L)

$[O_2]_{t1}$ = DO at time t1 (mg O_2/L)

V = respirometer volume (L) – volume of oyster (L)

t = time t1 (h) – time t0 (h)

WWW = whole oyster wet weight (g)

Background oxygen consumption (mgO_2/empty chamber/h) from sources such as bacteria was measured in chambers without oysters present for ~1 h before and after each run using the same formula but without oyster mass included. The background respiration rate before and after the run was then plotted and a linear regression run through the initial and final data points. Background oxygen consumption at a given time point was then estimated from the linear regression. Mass specific oyster respiration rates (mgO_2/kgWWW/h) were then multiplied by oyster kgWWW to convert to mgO_2/occupied chamber/h. Estimated control respiration was then subtracted from oyster respiration measured at each given point in time. The resultant value was then divided by oyster dry tissue weight (kgDTW) to yield the corrected mass specific respiration rate for each oyster (mgO_2/kgDTW/h).

2.2.3.3 Respiration data analysis

To account for effects of periodic valve closure on respiration rates, we analyzed respiration data using two approaches (Fig. 5). The first approach estimated mean MO_2 for open, actively respiring oysters. Data points during periods of time when oysters were presumed to have been affected by valve closures were removed from this dataset. A data point was considered affected by a closure or partial closure event if the MO_2 value was below 40% of the mean of all data for a given oyster and/or if the R^2 value associated with that measurement cycle was < 0.90. The second approach estimated the cumulative oxygen consumption regardless of closure status. For this approach, we retained all respiration data and calculated area under the curve (AUC) using the Area Below Curve function in SigmaPlot13. MO_2 estimates associated with an R^2 below 0.9 were removed from the dataset as these could be unreliable measurements (Chabot et al., 2021).

2.2.4 Statistical analysis

We used a Shapiro-Wilk test to check normality and a Brown-Forsythe test to check equal variance before performing a one-way ANOVA (SigmaPlot 13) to test for differences among treatments in mean respiration rate (RMR) when open, as well as to test for differences in cumulative respiration rate (AUC) among treatments. A linear regression was used to test if PFAS concentrations in the water had significantly increased or decreased during the 28-Day exposure period.

2.3 Results

2.3.1 Bioaccumulation and depuration of 5-PFAS mixture

Concentrations of PFOS, PFOA, PFHxA, PFBS, and PFPeA in ambient water samples averaged across the entire 28-day exposure period were below the nominal value of 1.7µg/L for each compound (Table 1). Daily concentrations of each compound also tended to fall below 1.7µg/L, with PFOS and PFOA concentrations frequently below 1µg/L (Fig. 6 A-D). There was no significant relationship between concentration in exposure water and time for any PFAS compound (general linear regression: $R^2 < .243$, $p > .05$) for all cases.

Concentrations of all PFAS compounds were below detectable limits in tissues of the three oysters sacrificed and sampled just prior to exposure in the laboratory. We did not observe any mortality of control or treatment oysters during the 28-day exposure period. Concentrations of PFOS, PFOA, and PFHxA in oyster tissues increased and then leveled off within four days of exposure. This was followed by a decline at ~ Day 14 (Fig. 6 A-C). Conversely, PFPeA exhibited fluctuating concentrations from Day 2 onwards (Fig. 6 D).

Bioaccumulation factors were calculated for two separate periods: Day 4-10 and Day 20-28 to reflect the two phases of bioaccumulation we noticed from the samples. In both cases, PFOS had the highest bioaccumulation factor followed by PFOA, PFPeA, and PFHxA respectively. The BAF for Day 4-10 was higher than for Day 20-28 (Table 1, Fig. 7 A,B). This pattern was driven by a reduction in the mean PFAS body burden over time rather than a reduction in PFAS concentrations in the ambient water. (Fig. 7 A-D). Following the 28-day exposure period, tissue concentrations of all PFAS compounds fell below detectable limits (.0025– .01049µg PFAS/gDW) within 24 hours of being placed in clean water. The detection limits were as follows: .00766µg PFPeA/g DW, .00743µg PFHxA/g DW, .00248µg PFOA/ g

DW, and .01049µg PFOS/gDW. Note that detection limits are calculated per g dry tissue weight whereas tissue concentration in Fig. 6 are reported per kg wet tissue weight.

2.3.2 Energetic cost of exposure and depuration

There was no significant difference in mean respiration rates among control oysters, oysters that were exposed to PFOS+PFOA or the 5-PFAS mixture, and oysters that were allowed to depurate PFOS+PFOA in clean water for 24 hours ($F_{(3,33)} = 0.476$, $p = .701$)(Fig. 8 A).

There was also no difference in cumulative oxygen consumption (i.e. AUC) among control oysters, oysters that were exposed to PFOS+PFOA or 5-PFAS mixture, and oysters that were allowed to depurate PFOS+PFOA in clean water for 24 hours ($F_{(3,35)} = 0.129$, $p = .942$) (Fig. 8 B).

2.4 Discussion

Our results show that oysters do accumulate PFAS in their tissues at concentrations an order of magnitude higher than seen in the environment. However, the low BAF value for PFOS, PFOA, PFPeA, and PFHxA do not fit the limits of what the USEPA considers as a chemical with tendencies to accumulate within organisms (BAF >1000). BAF for PFBS could not be quantified due to background interference in the tissue samples. BAF values below 1000 have been previously observed in PFOS and PFOA in bivalves (Aquilina-Beck et al., 2020; Fernández-Sanjuan et al., 2013; Jeon et al., 2010). With the exception of PFPeA, PFAS bioaccumulation patterns didn't follow the typical temporal pattern seen in other studies that used higher concentrations. For example, when oysters were exposed to individual concentrations of 6-7µg/L of PFOS, PFOA, PFDA and PFUnDA, body burden concentrations increased throughout the

entire 28-day uptake period while our study at lower concentrations (<2µg/L) of PFOS and PFOA saw a decrease in body burden from days 20-28 after an initial spike at Day 4. This decline in body burden could not be explained by decreasing PFAS water concentration as shown by the linear regression model. This suggests that internal depuration mechanisms, such as the MXR detoxification system, may have taken approximately 10-14 days to fully develop and reach a steady state with accumulation when individual PFAS concentrations were below 2µg/L. If oysters are chronically exposed to fairly constant concentrations in the environment, PFAS concentrations in the soft tissues may remain at a relatively low steady state. However, if PFAS exposure is sporadic, concentrations in soft tissues may rise and fall over time with the highest body burden concentrations occurring within a few days after an exposure event.

Our findings support the conclusions of other studies: bioaccumulation is low at concentrations under 10µg/L due to depuration kinetics in bivalves, and that bioaccumulation is dependent on chemical structure (Jeon et al., 2010). The higher bioaccumulation factors seen in this study in PFOS and PFOA compared to PFPeA and PFHxA, which have shorter carbon chains, are supported by previous studies that show that chain has have an impact on bioaccumulation rates (Jeon et al., 2010). The functional group also plays a role in bioaccumulation evidenced by the difference between bioaccumulation factors between PFOS and PFOA, both of which are 8-carbon chains. In other bivalve species, PFOS has shown a consistently higher BAF, which has a sulfonic acid for its functional group, compared to PFOA which contains a carboxylic acid, regardless of exposure concentration and is consistent with our findings (Fernández-Sanjuan et al., 2013; Jeon et al., 2010). Our data has shown that longer chained PFAS have a high affinity for tissues and have a higher risk of bioaccumulation. PFOS body burdens in wild oyster tissue have been surveyed in the early 2000's at both the Gulf of

Mexico and the Chesapeake Bay, but with the introduction of over 12,000 different PFAS compounds and their precursors to aquatic systems around the world, a survey of current concentrations of many different PFAS compounds is needed (Giesy and Kannan, 2001; Kannan et al., 2002; Viticoski et al., 2022).

The multixenobiotic resistance (MXR) system may explain why oysters were able to depurate PFAS rapidly, even though these chemicals only came into production in the mid-20th century (Mueller and Yingling, 2020). The MXR system is a defense mechanism that bivalves evolved to actively lower the intracellular concentration of many naturally occurring toxins using high molecular membrane proteins, similar to the multidrug resistance (MDR) system in mammals (Gottesman and Pastan, 1993; Minier and Moore, 1996). The MXR system has been well characterized and studied in bivalves and is induced by other toxins such as Methyl methanesulfonate (MMS) and dimethyl sulfoxide (DMSO) in mussel larvae (McFadzen et al., 2000). P-glycoprotein, an MXR-like protein, has been observed at higher concentrations in oysters during warm months, indicating that the MXR system may also be used as an adaptive response to natural stressors such as temperature in the summer (Keppler and Ringwood, 2001). It is also possible that chronic exposure to PFAS compounds since at least the late 1990s (Kannan et al. 2002) has contributed to depuration efficiency observed in the current population. Oysters in contaminated areas are more likely to be adapted to those pollutants and are more resilient when a spill occurs compared to those in pristine environments (Bard, 2000).

In the eastern oyster, PFAS depuration did not appear to be energetically expensive after exposure to a PFOS plus PFOA mixture at 8.5µg/L. In contrast, zebra mussels exposed to a mix of PFOS plus PFOA at concentrations as low as 1µg/L had significantly higher respiration rates than controls while depurating (Fernández-Sanjuan et al., 2013). The lack of a significant

increase in oyster respiration rate suggests that some marine bivalves such as oysters have a more efficient depuration mechanism than freshwater bivalves such as zebra mussels. If so, sublethal effects of PFAS exposure related to energetic costs may vary widely among bivalve taxa.

This study tested for acute (i.e. 10-day exposure) effects and did not address potential energetic costs of oysters chronically exposed to PFAS over months or years. Wild oysters collected from Florida that had the highest PFAS body burden had the lowest condition indices, suggesting that there may be long term energetic costs to PFAS depuration (Lemos et al., 2022). However, field surveys relating PFAS exposure to body condition of oysters in ambient conditions should be treated with caution as there are many confounding factors that influence oyster health and physical characteristics including salinity, wave action, tidal action, reproductive activity, and disease that may be present but not quantified.

Although we found no indication of energetic stress, exposure to PFAS can induce other molecular stress. For example, biomarkers such as glutathione, stress protein expression, and lipid peroxide assays are often employed when looking for cellular impacts of contaminants (Aquilina-Beck et al., 2020; Fernández-Sanjuan et al., 2013), but have not been used for ecologically relevant concentration exposures (i.e. <300ng/L in Mobile Bay region) (Viticoski et al., 2022). These assays should be utilized for oysters exposed to PFAS exposure at ecologically relevant concentrations of PFAS to explore other cellular costs associated with homeostasis. Measuring the energetic cost of compounded stressors such as pollutants and high temperatures in laboratory trials should also be investigated to understand the combined stress oysters experience at farms and reefs (Fig. 9).

As filter feeders, oysters have been shown to remove contaminants, such as microplastics and heavy metals, from the water column and bio-deposit them on the seafloor improving the overall water quality, but potentially decreasing sediment quality and increasing exposure risks of benthic organisms (Björk et al., 2000; Craig et al., 2022; Dobson and Mackie, 1998; Liu et al., 2023; Piarulli and Airoldi, 2020; Prince et al., 2021). Although oysters have been shown to rapidly depurate PFAS from their tissues, the final destination of depurated PFAS is not well understood and likely to vary among compounds. If a given PFAS compound remains relatively water soluble and is reintroduced to the water column post-depuration, oysters are not likely to strongly impact water quality with regard to that compound. However, if PFAS is assimilated into feces or pseudofeces and deposited onto the seafloor, oysters may serve to improve water quality while at the same time increasing local sediment contamination. Transfer of PFAS from the water column to the sediments may increase absorption or ingestion by benthic aquatic invertebrates and increase the biomagnification risk of persistent contaminants around large populations of bivalves (Liu et al., 2023; Prince et al., 2021). Further studies examining the fate and transport of depurated PFAS by marine bivalves should be undertaken to understand the potential ecological impacts on local ecosystems.

2.5 Tables

Table 1. Concentrations of individual components of the 5-PFAS mixture in water across the 28-day bioaccumulation assay, and in water and oyster tissue in Days 4-10 and Days 20-28 of the exposure period. All concentrations are given as mean (SE). Bioaccumulation factors (BAF) in oyster tissue are also given for Days 4-10 and Days 20-28.

	Days 0-28	**Days 4-10**			**Days 20-28**		
	Water	**Water**	**Oyster**		**Water**	**Oyster**	
	µg/L	**µg/L**	**µg /kgWTW**	**BAF**	**µg/L**	**µg /kgWTW**	**BAF**
PFPeA	1.6 (.05)	1.6 (.05)	25.0 (3.91)	15.3	1.6 (.11)	18.7 (2.83)	12.0
PFHxA	1.5 (.05)	1.5 (.05)	12.6 (1.78)	8.1	1.5 (.09)	3.7 (.51)	2.5
PFOA	0.7 (.06)	0.7 (.08)	40.4 (5.70)	61.4	0.7 (.13)	7.2 (.86)	10.1
PFOS	0.7 (.15)	0.6 (.16)	41.1 (4.33)	75.4	0.9 (.42)	17.2 (4.46)	19.7
PFBS	2.1 (.08)	2.2 (.06)	-	-	1.8 (.14)	-	-

2.6 Figures

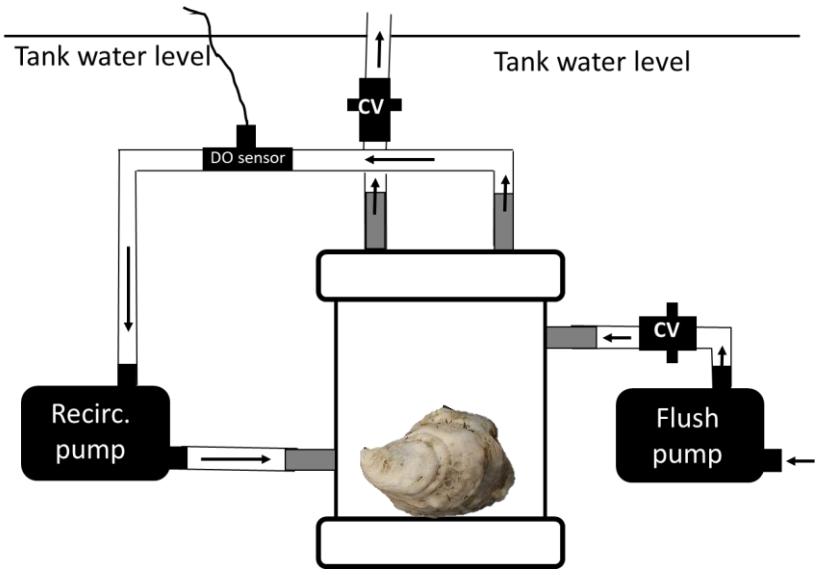

Figure 4. A schematic of the respirometry components. Modified from Haney et al. (2020).

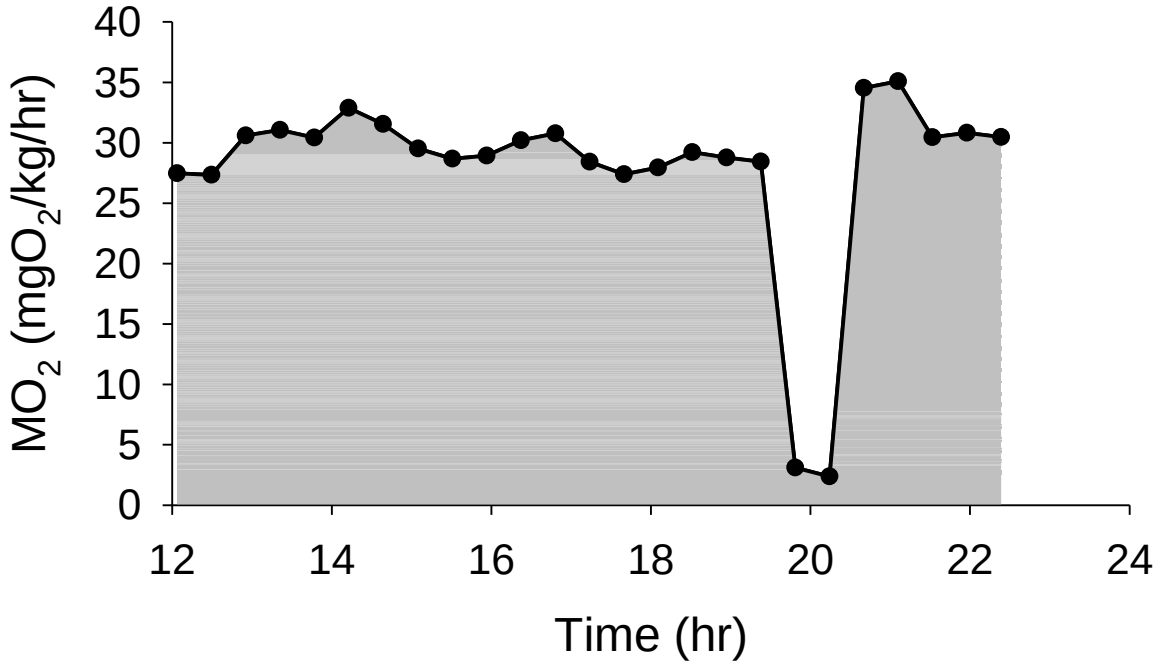

Figure 5. Example of oyster respirometry data showing a presumed closure event at 20 hours. Oyster was acclimated overnight for 12 hours prior to collection of data from analysis. The two data points at ~20 hrs were removed from the dataset when calculating mean respiration rate of open oysters. The entire data set was used when calculating area under the curve (cumulative oxygen consumption), indicated by grey shading.

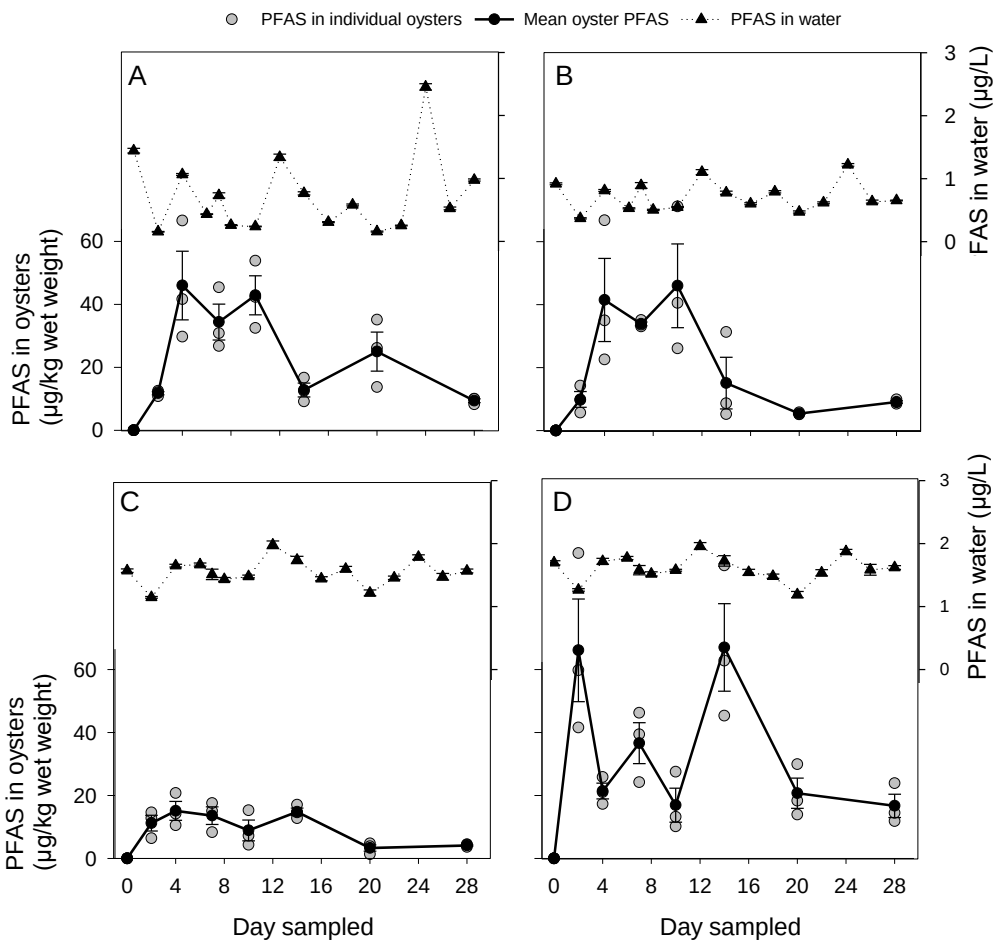

Figure 6. PFAS concentrations (µg/kg wet weight) measured in oyster tissue and ambient water (µg/L) throughout the exposure period for A) PFOS, B) PFOA, C) PFHxA, and D) PFPeA. Error bars represent ± 1 SE.

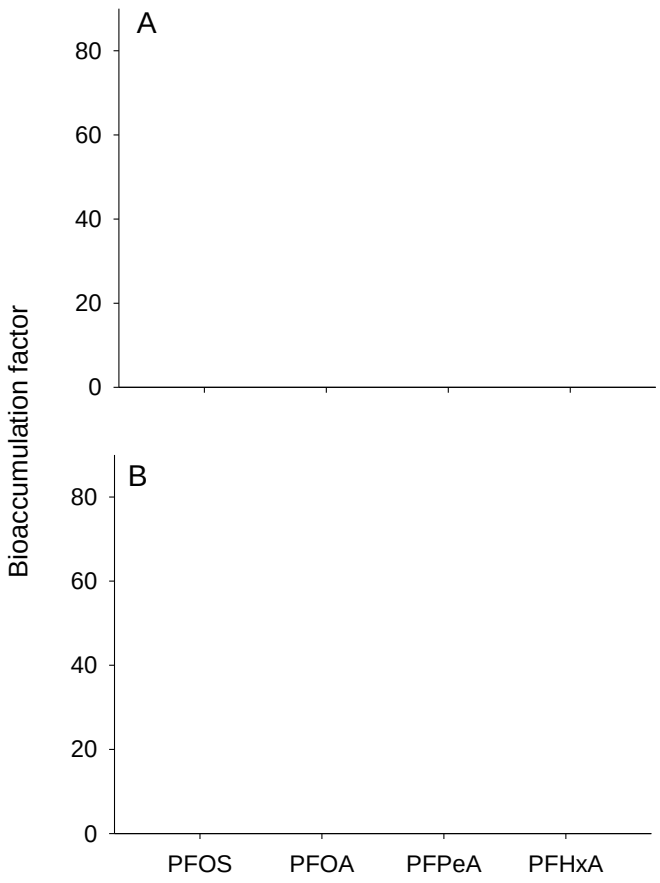

Figure 7. Bioaccumulation factors calculated for PFPeA, PFHxA, PFOA, and PFOS of oysters sampled A) between Days 4 through 10 and B) between Days 20-28 of exposure to the 5-PFAS mixture. Due to analytical issues, we were not able to calculate body burdens or bioaccumulation factors for PFBS.

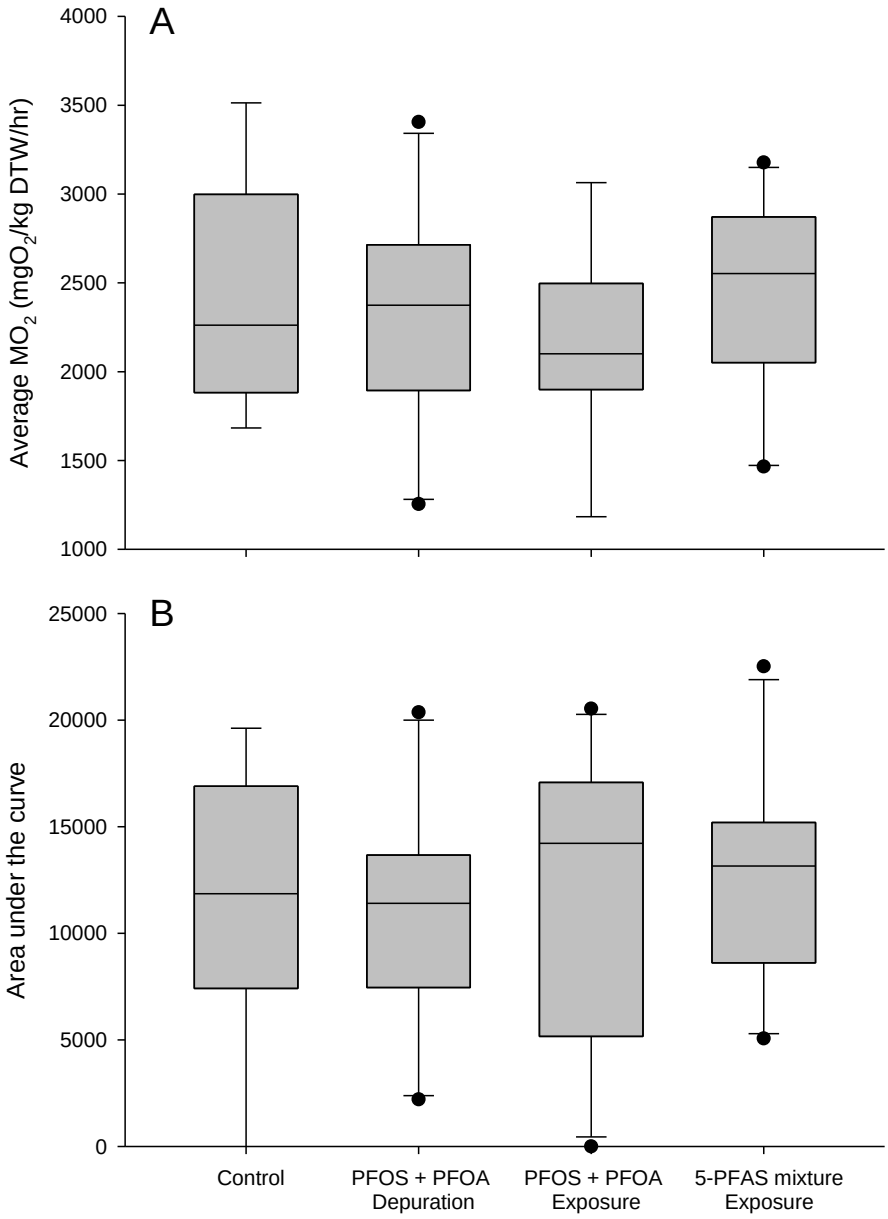

Figure 8. A) Mean respiration rates of open oysters in the following categories: control (no PFAS exposure); depurating (12 hrs after exposure to PFOS and PFOA); exposed to a mixture of PFOS and PFOA; and exposed to a 5-PFAS mixture. B) Area under the curve for respiration of oysters under the same conditions as top panel and inclusive of presumed closure events.

2.7 References

Aquilina-Beck, A. A., Reiner, J. L., Chung, K. W., DeLise, M. J., Key, P. B., & DeLorenzo, M. E. (2020). Uptake and Biological Effects of Perfluorooctane Sulfonate Exposure in the Adult Eastern Oyster Crassostrea virginica. *Archives of Environmental Contamination and Toxicology*, *79*(3), 333–342. https://doi.org/10.1007/s00244-020-00765-4

ATSDR. (2018). *Toxicological Profile for Perfluoroalkyls*. ATSDR.

Bard, S. (2000). Multixenobiotic resistance as a cellular defense mechanism in aquatic organisms. *Aquatic Toxicology*, *48*(4), 357–389. https://doi.org/10.1016/S0166-445X(00)00088-6

Benskin, J. P., Holt, A., & Martin, J. W. (2009). Isomer-specific biotransformation rates of a perfluorooctane sulfonate (PFOS)-precursor by cytochrome P450 isozymes and human liver microsomes. *Environmental Science & Technology*, *43*(22), 8566–8572. https://doi.org/10.1021/es901915f

Björk, M., Gilek, M., Kautsky, N., & Näf, C. (2000). In situ determination of PCB biodeposition by Mytilus edulis in a Baltic coastal ecosystem. *Marine Ecology Progress Series*, *194*, 193–201. https://doi.org/10.3354/meps194193

Calow, P. (1991). Physiological costs of combating chemical toxicants: Ecological implications. *Comparative Biochemistry and Physiology. C, Comparative Pharmacology and Toxicology*, *100*(1–2), 3–6. https://doi.org/10.1016/0742-8413(91)90110-f

CDC. (2022, September 15). *Per- and polyfluoroalkyl substances (PFAS)*. https://www.cdc.gov/niosh/topics/pfas/default.html

Chabot, D., Zhang, Y., & Farrell, A. P. (2021). Valid oxygen uptake measurements: Using high r2 values with good intentions can bias upward the determination of standard metabolic rate. *Journal of Fish Biology*, *98*(5), 1206–1216. https://doi.org/10.1111/jfb.14650

Craig, C. A., Fox, D. W., Zhai, L., & Walters, L. J. (2022). In-situ microplastic egestion efficiency of the eastern oyster Crassostrea virginica. *Marine Pollution Bulletin*, *178*, 113653. https://doi.org/10.1016/j.marpolbul.2022.113653

De Silva, A. O., Armitage, J. M., Bruton, T. A., Dassuncao, C., Heiger-Bernays, W., Hu, X. C., Kärrman, A., Kelly, B., Ng, C., Robuck, A., Sun, M., Webster, T. F., & Sunderland, E. M. (2021). PFAS Exposure Pathways for Humans and Wildlife: A Synthesis of Current Knowledge and Key Gaps in Understanding. *Environmental Toxicology and Chemistry*, *40*(3), 631–657. https://doi.org/10.1002/etc.4935

Dobson, E. P., & Mackie, G. L. (1998). Increased deposition of organic matter, polychlorinated biphenyls, and cadmium by zebra mussels (Dreissena polymorpha) in western Lake Erie.

Canadian Journal of Fisheries and Aquatic Sciences, *55*(5), 1131–1139. https://doi.org/10.1139/f97-321

Fernández-Sanjuan, M., Faria, M., Lacorte, S., & Barata, C. (2013). Bioaccumulation and effects of perfluorinated compounds (PFCs) in zebra mussels (Dreissena polymorpha). *Environmental Science and Pollution Research International*, *20*(4), 2661–2669. https://doi.org/10.1007/s11356-012-1158-8

Giesy, J. P., & Kannan, K. (2001). Global distribution of perfluorooctane sulfonate in wildlife. *Environmental Science & Technology*, *35*(7), 1339–1342. https://doi.org/10.1021/es001834k

Goodchild, C. G., Simpson, A. M., Minghetti, M., & DuRant, S. E. (2019). Bioenergetics-adverse outcome pathway: Linking organismal and suborganismal energetic endpoints to adverse outcomes. *Environmental Toxicology and Chemistry*, *38*(1), 27–45. https://doi.org/10.1002/etc.4280

Gottesman, M. M., & Pastan, I. (1993). Biochemistry of multidrug resistance mediated by the multidrug transporter. *Annual Review of Biochemistry*, *62*, 385–427. https://doi.org/10.1146/annurev.bi.62.070193.002125

Grabowski, J. H., Brumbaugh, R. D., Conrad, R. F., Keeler, A. G., Opaluch, J. J., Peterson, C. H., Piehler, M. F., Powers, S. P., & Smyth, A. R. (2012). Economic Valuation of Ecosystem Services Provided by Oyster Reefs. *BioScience*, *62*(10), 900–909. https://doi.org/10.1525/bio.2012.62.10.10

Helm, M. M., & Bourne, N. (2004). *The hatchery culture of bivalves: A practical manual*. http://www.fao.org/3/y5720e/y5720e09.htm#bm09..3.2.2

Houde, M., Czub, G., Small, J. M., Backus, S., Wang, X., Alaee, M., & Muir, D. C. G. (2008). Fractionation and Bioaccumulation of Perfluorooctane Sulfonate (PFOS) Isomers in a Lake Ontario Food Web. *Environmental Science & Technology*, *42*(24), 9397–9403. https://doi.org/10.1021/es800906r

Hu, X., Andrews, D., Lindstrom, A., Bruton, T., Schaider, L., Grandjean, P., Lohmann, R., Carignan, C., Blum, A., Balan, S., Higgins, C., & Sunderland, E. (2016). Detection of Poly- and Perfluoroalkyl Substances (PFASs) in U.S. Drinking Water Linked to Industrial Sites, Military Fire Training Areas, and Wastewater Treatment Plants. *Environmental Science and Technology Letters*, *3*(10), 344–350. https://doi.org/10.1021/acs.estlett.6b00260

Jeon, J., Kannan, K., Lim, H. K., Moon, H. B., Ra, J. S., & Kim, S. D. (2010). Bioaccumulation of perfluorochemicals in Pacific oyster under different salinity gradients. *Environmental Science & Technology*, *44*(7), 2695–2701. https://doi.org/10.1021/es100151r

Kannan, K., Hansen, K. J., Wade, T. L., & Giesy, J. P. (2002). Perfluorooctane sulfonate in oysters, Crassostrea virginica, from the Gulf of Mexico and the Chesapeake Bay, USA.

Archives of Environmental Contamination and Toxicology, *42*(3), 313–318. https://doi.org/10.1007/s00244-001-0003-8

Kannan, K., Tao, L., Sinclair, E., Pastva, S. D., Jude, D. J., & Giesy, J. P. (2005). Perfluorinated compounds in aquatic organisms at various trophic levels in a Great Lakes food chain. *Archives of Environmental Contamination and Toxicology*, *48*(4), 559–566. https://doi.org/10.1007/s00244-004-0133-x

Keppler, C. J., & Ringwood, A. H. (2001). Expression of P-glycoprotein in southeastern oysters, Crassostrea virginica. *Marine Environmental Research*, *52*(1), 81–96. https://doi.org/10.1016/s0141-1136(00)00263-4

Lau, C. (2015). Perfluorinated Compounds: An Overview. In J. C. DeWitt (Ed.), *Toxicological Effects of Perfluoroalkyl and Polyfluoroalkyl Substances* (pp. 1–21). Springer International Publishing. https://doi.org/10.1007/978-3-319-15518-0_1

Lemos, L., Gantiva, L., Kaylor, C., Sanchez, A., & Quinete, N. (2022). American oysters as bioindicators of emerging organic contaminants in Florida, United States. *Science of The Total Environment*, *835*, 155316. https://doi.org/10.1016/j.scitotenv.2022.155316

Liu, Q., Liao, Y., Zhu, J., Shi, X., Shou, L., Zeng, J., Chen, Q., & Chen, J. (2023). Influence of biodeposition by suspended cultured oyster on the distributions of trace elements in multiple media in a semi-enclosed bay of China. *Journal of Hazardous Materials*, *443*, 130347. https://doi.org/10.1016/j.jhazmat.2022.130347

McFadzen, I., Eufemia, N., Heath, C., Epel, D., Moore, M., & Lowe, D. (2000). Multidrug resistance in the embryos and larvae of the mussel Mytilus edulis. *Marine Environmental Research*, *50*(1–5), 319–323. https://doi.org/10.1016/s0141-1136(00)00057-x

Minier, C., & Moore, M. N. (1996). Induction of multixenobiotic resistance in mussel blood cells. *Marine Environmental Research*, *42*(1), 389–392. https://doi.org/10.1016/0141-1136(96)87093-0

Mueller, R., & Yingling, V. (2020). *History and Use of Per- and Polyfluoroalkyl Substances (PFAS)*. Interstate Technology Regulatory Council.

Panieri, E., Baralic, K., Djukic-Cosic, D., Buha Djordjevic, A., & Saso, L. (2022). PFAS Molecules: A Major Concern for the Human Health and the Environment. *Toxics*, *10*(2), Article 2. https://doi.org/10.3390/toxics10020044

Piarulli, S., & Airoldi, L. (2020). Mussels facilitate the sinking of microplastics to bottom sediments and their subsequent uptake by detritus-feeders. *Environmental Pollution*, *266*, 115151. https://doi.org/10.1016/j.envpol.2020.115151

Prince, K. D., Crotty, S. M., Cetta, A., Delfino, J. J., Palmer, T. M., Denslow, N. D., & Angelini, C. (2021). Mussels drive polychlorinated biphenyl (PCB) biomagnification in a coastal food web. *Scientific Reports*, *11*(1), 9180. https://doi.org/10.1038/s41598-021-88684-9

Rowe, C. L., Hopkins, W. A., Zehnder, C., & Congdon, J. D. (2001). Metabolic costs incurred by crayfish (Procambarus acutus) in a trace element-polluted habitat: Further evidence of similar responses among diverse taxonomic groups. *Comparative Biochemistry and Physiology Part C: Toxicology & Pharmacology*, *129*(3), 275–283. https://doi.org/10.1016/S1532-0456(01)00204-6

Sinclair, G. M., Long, S. M., & Jones, O. A. H. (2020). What are the effects of PFAS exposure at environmentally relevant concentrations? *Chemosphere*, *258*, 127340. https://doi.org/10.1016/j.chemosphere.2020.127340

Smolders, R., Bervoets, L., De Coen, W., & Blust, R. (2004). Cellular energy allocation in zebra mussels exposed along a pollution gradient: Linking cellular effects to higher levels of biological organization. *Environmental Pollution*, *129*(1), 99–112. https://doi.org/10.1016/j.envpol.2003.09.027

US EPA, O. (2016, March 30). *Basic Information on PFAS* [Overviews and Factsheets]. US EPA. https://www.epa.gov/pfas/basic-information-pfas

Viticoski, R. L., Wang, D., Feltman, M. A., Mulabagal, V., Rogers, S. R., Blersch, D. M., & Hayworth, J. S. (2022). Spatial distribution and mass transport of Perfluoroalkyl Substances (PFAS) in surface water: A statewide evaluation of PFAS occurrence and fate in Alabama. *The Science of the Total Environment*, *836*, 155524. https://doi.org/10.1016/j.scitotenv.2022.155524

White, N. D., Balthis, L., Kannan, K., De Silva, A. O., Wu, Q., French, K. M., Daugomah, J., Spencer, C., & Fair, P. A. (2015). Elevated levels of perfluoroalkyl substances in estuarine sediments of Charleston, SC. *Science of The Total Environment*, *521–522*, 79–89. https://doi.org/10.1016/j.scitotenv.2015.03.078

CHAPTER 3
ENERGETIC COSTS AND GENE EXPRESSION OF THE EASTERN OYSTER (*Crassostrea virginica)* WHEN EXPOSED TO PFAS DURING THERMAL STRESS

3.1 Introduction

PFAS are a classification of man-made chemicals that are considered an emerging contaminant of concern (US EPA, 2016). These chemicals have been observed bioaccumulating in tissues of wildlife and humans when ingested (Giesy & Kannan, 2001). Areas of high industrial development tend to have higher levels of PFAS found in the soil and ground water due to their use in manufacturing (US EPA, 2016). Many of these chemicals are discharged into riverine systems that eventually flow into estuaries around the Gulf of Mexico (Viticoski et al., 2022). Mobile Bay, AL is an estuary located at the mouth of the Mobile-Tensaw River Delta and has historically been an area for industrial manufacturing including chemical, aviation/aerospace, and other manufacturing industries. In 2020, sampled tributaries in Mobile Bay exhibited a mean cumulative concentration of 24.7ng/L of detected PFAS compounds (PFPeA, PFHxA, PFOA, PFOS) as they entered the bay (Viticoski et al., 2022). This is similar to the levels detected in coastal systems including Miami Beach, FL (4.4ng/L), Biscayne Canal Number C-8, FL in 2021 (115.98ng/L) (X. Li et al., 2022), and along the Atlantic coast in Brevard County, FL in 2021 (61.2ng/L) (Griffin et al., 2022).

Oysters are exposed to PFAS as they draw water into their mantle cavity and across their gills for respiration and feeding. Exposure to PFOS (a prevalent type of PFAS) at concentrations ≥ 3,000µg/L has been shown to cause increases in some cell stress biomarkers (i.e. Malondialdehyde) in the eastern oyster (*Crassostrea virginica*) (Aqualina-Beck et al., 2020). Upon transfer to clean seawater, oysters were able to depurate 96% of accumulated PFOS within 48 hours (Aqualina-Beck et al., 2020). Although bivalves appear to be efficient at depurating

PFAS (Fernández-Sanjuan et al., 2013; Jeon et al., 2010), there is some evidence that PFAS depuration incurs significant energetic costs, possibly due to induction of the MXR detoxification system. For example, zebra mussel (*Dreissena polymorpha*) respiration rates showed a significant increase during depuration of a mixture of PFOS and PFOA at combined concentrations ≥ 2µg/L (Fernández-Sanjuan et al., 2013).

In previous experiments, neither a PFOS + PFOA mixture at 5µg/L each (cumulative concentration = 10µg/L) nor an ecologically relevant mixture of PFAS (2µg/L of each PFBS, PFOA, PFOS, PFPeA, PFHxA; cumulative concentration = 10µg/L) were found to be energetically expensive for oysters to depurate (see Chapter 2). However, in natural environments, oysters may be exposed to multiple, concurrent stressors, including periods of high temperature (>30°C) (Marshall et al., 2021). High temperature events in the Mobile Bay area occur frequently in the summer months, often reaching over 33°C where oyster aquaculture is located (Fig. 9). The optimal temperature range for the eastern oyster is ~ 20-30°C (Stanley & Sellers, 1986) and temperatures above the optimal can result in reduced ability to tolerate other forms of stress (Coxe et al., 2023; Hégaret et al., 2003; Marshall et al., 2021). While PFAS exposure and depuration did not incur energetic costs at an optimal temperature of 28°C in our previous study, it is possible that exposure to, and depuration of, PFAS is more costly at higher temperatures.

Thermal and chemical stressors can increase the amount of energy required to maintain homeostasis (Bodenstein et al., 2023; Calow, 1991; Pouvreau et al., 2006). Molecular chaperones are enhanced in cells that have experienced or are currently recovering from a protein perturbing stress such as heat shock or chemical exposure (Feige et al., 1996). PFOA exposure at 200µg/L significantly depressed immune effector molecules and significantly increased genes that were

related to oxidative responses in *Ruditapes philippinarum* (F. Li et al., 2024). High temperatures can increase energetic demand due to the production of protein cascades such as heat shock proteins (HSPs) whose function is to repair damage from heat stress (Ghaffari et al., 2019). *HSP70* is a molecular chaperone whose function is to stabilize protein intermediates which are usually aggregate-prone (Feige et al., 1996). Among the many HSPs utilized in a cell, *HSP70* is high on the hierarchical model of chaperone mediated protein folding. Proteins first interact with HSP70 before being passed to other molecular chaperones such as *HSP60* to mediate the final stages of protein folding (Liberek et al., 1991). *HSP70* acts not only as a folding assistant but also stabilizes damaged proteins or assists in protein denaturing and cleaning the cell of damaged and possibly hazardous unfolded proteins (non-native conformation) (Feige et al., 1996). *HSP70* upregulation has been seen in oysters exposed to cadmium (Ivanina et al., 2008) and oysters who were exposed to elevated temperatures (Nash et al., 2019).

The blcl-2-associated X apoptosis regulator (*bax*) gene is a pro-apoptotic member that plays a critical role in regulating apoptosis during uncontrolled cell growth or cell death. It exists in the cell cytoplasm until it is activated by an upregulation of death signals such as BH3 expressed on the mitochondrial membrane (Carpenter & Brady, 2022). Exposure to Atrazine significantly increased *bax* expression in common carp (Wang et al., 2019). Thermal stress increases the rate of apoptosis and *bax* expression in mammalian tissues (Kvitt et al., 2016).

P53 is a cellular tumor antigen used for cell regulation (Lebordais et al., 2021). Contaminants may increase the prevalence of neoplasia (uncontrolled and abnormal growth of cells) if they compromise immune function which can be indicated by downregulated *p53* protein expression (Rivlin et al., 2011; Smolarz et al., 2005). For instance, *p53* expression was found to significantly increase in *Crassostrea virginica* exposed to nanoplastics combined with

arsenic (Lebordais et al., 2021). Because of this *p53* protein expression is commonly used as a marker for environmental research.

During the summer months, oysters in the northern Gulf of Mexico are likely to be exposed to a combination of thermal stress and a mixture of PFAS compounds. To better reflect the energetic impact of PFAS and temperature exposure in oysters in Mobile Bay, total PFAS concentrations were decreased from Chapter 2 (10µg/L) to a more ecologically relevant concentration (1µg/L). The goals of this study therefore were to 1) compare energetic costs during exposure to and depuration of PFAS at optimal and stressful temperatures and 2) determine if PFAS exposure at optimal or stressful temperatures results in an increase in production of stress response proteins.

3.2 Methods

3.2.1 Oyster collection, shipment, and intake

Adult diploid oysters (60-70mm height) were collected on 17 November 2021 from off-bottom oyster baskets at Grand Bay Oyster Park, Grand Bay, AL. Because oysters are hermaphroditic and not sexually dimorphic, the sex of each individual was unknown.

Oysters were placed in a cooler between moist paper towels in preparation for shipping. Ice packs were placed above and below the paper towels to reduce the temperature of the cooler during shipping. The cooler was shipped overnight to E. W. Shell Fisheries Center, Auburn University, AL. Upon arrival, the ice packs were removed, and the internal temperature of the cooler (10°C) was raised to ambient temperature (21°C) over 12 hours. Oysters were then scrubbed to remove algae and barnacles and submerged in a super saturated salt solution with gentle agitation for 6 minutes to reduce the number of oyster blister worms burrowed in the shell,

which compromise shell structure and contribute to unnecessary background oxygen consumption. Oysters were then tagged with 8 X 4 mm external Hallprint shellfish tags (Hallprint, Hindmarsh Valley, South Australia) secured with super glue and placed in randomly assigned holding upwellers containing 75 L of 16ppt SSW. The temperature was increased from 21°C to 28°C by 1°C/day. Less than 1% mortality was observed during and after acclimation to laboratory conditions.

3.2.2 Holding conditions

Upwellers were constructed using a holding basket (internal plastic tote), bio balls and a heater within an insulated container. Water was pumped from the internal basket to the external container where it flowed back into the internal basket via a screened opening underneath. Two air stones were added for extra water movement and aeration (See Chapter 2). Bacterial biofilters in the upwellers were established for >2 weeks prior to the arrival of experimental oysters. Each upweller was provided a ration of three-parts Reed Mariculture 1800® Shellfish Diet and one-part Nanno 3600 (Reed Mariculture Inc., Campbell, CA, USA) once every hour based on the assumed wet weight of the upweller population calculated above (see Chapter 2).

Oysters were acclimated to laboratory conditions (28°C, 12:12 h; light dark, pH 8) for > 2 weeks. Within 48 hours of being placed in upwellers, oysters were observed spawning and a water change was conducted on all upwellers after the oysters were no longer releasing gametes to maintain water quality.

3.2.3 Temperature treatment

Following acclimation to laboratory holding conditions, groups of eight oysters were randomly assigned to one of four respirometry trials using a random number generator. To initiate a given trial, four of the eight oysters were kept at 28℃ and the other four were brought to 33°C by raising temperatures at a rate of 1℃/day in acclimation upwellers specific to that temperature. Each acclimation upweller was equipped with a biological filter and an air stone. The oysters were then held at their respective temperatures (28°C or 33°C) in 75L upwellers for 2 weeks to acclimate them to experimental temperatures. Because all individuals could not be run at the same time in a single trial, oyster temperature acclimation was staggered through time so that each temperature acclimation period was exactly two weeks for each successive trial.

3.2.4 Chemical stock solutions

We first created five separate stock solutions containing a nominal 20,000µg/L of PFOS (Synquest Laboratories, Product 6164-3-08, purity 97%, Alachua, FL, USA), PFOA (BeanTown Chemical, Product BT139610, purity ≥95%, Hudson, NH, USA), PFHxA (Matrix Scientific, Cat. 101777-248, purity ≥95%, Columbia, SC, USA), PFBS (Synquest Laboratories, Cat. 6164-3-09, purity 97%, Alachua, FL, USA), and PFPeA (Alfa Aesar, Cat. AAB21567-06, purity 97%, Tewksbury, MA, USA) in RODI water in 1 L HDPE bottles and stored them at -20°C. Prior to experiments, a 5-PFAS stock solution was created by combining 100 ml of each previously described stock solution (PFOS, PFOA, PFHxA, PFBS, and PFPeA) and then diluting the resultant mix with 700 ml of DI water for a final nominal concentration of 1,667µg/L per compound (cumulative concentration = 8,335µg PFAS/L) and stored at 4°C.

3.2.5 10-Day exposure to PFAS

Following acclimation to experimental temperatures, 4 oysters per temperature were assigned to a control or exposure treatment using a random number generator. Exposure groups were as follows: Control (no PFAS) or 0.2µg/L each of PFOS + PFOA + PFBS + PFPeA + PFHxA (1µg PFAS/L total) to be measured in contaminated water. Oysters were exposed to their respective PFAS concentrations for 10 days in exposure chambers made of HDPE plastic and containing 1.5L of 16ppt SSW at 28°C or 33°C depending on assigned treatment. Target temperatures during exposure was maintained by placing the exposure chambers in water baths. Chamber water was completely changed every 24 hours and the appropriate amount of PFAS working stock added to the exposure treatment to obtain the PFAS target concentration described previously. Oysters were batch fed 1.35-2.13 mL of Shellfish Diet 1800 and Reed Mariculture Nano 3600 (3:1) based on their wet weight twice daily. During the 10-day exposure, oysters suffered one mortality in the 28°C Control group and one mortality in the 28°C Treatment group.

3.2.6 Energetic costs of exposure and depuration

An 84cm by 152cm fiberglass trough was partitioned in half using foam boarding sealed with waterproof tape to create two water baths. The temperature of each water bath was alternated between 28°C and 33°C in consecutive runs such that each half was used to test both temperatures. During a given run, the appropriate temperature in each bath was maintained via a Finnex heating element equipped with an InkBird temperature controller. Two 45L polypropylene totes were placed in each half of the water bath (i.e. two totes per temperature, four totes total) with one tote serving as the PFAS exposure treatment and the other as the control (Fig. 10). Each bin contained 28L of 16ppt SSW with supplemental aeration and two respirometry chambers. The treatment bins were spiked with PFAS to target concentrations of

1µg/L total PFAS at ~18:00 on Day 0 of a given trial. At ~19:00, a single oyster was placed in each of two individual respirometry chambers held within the appropriate treatment bin (28°C, 33°C; PFAS exposed, or PFAS unexposed; two oysters per treatment, 8 oysters total). Oysters were oriented with the flat valve facing upwards and allowed to acclimate to the chambers overnight. No food was added to the respirometry system during acclimation or the following measurement periods to facilitate a 24-hour fasting period.

Resting Metabolic Rate (RMR) of fasted oysters within each trial was measured using an 8-chamber fiber-optic respirometry system with AutoResp™ 2.3.0 software (Loligo® Systems, Viborg, Denmark). Each acrylic respirometry chamber was fitted with two Eheim® submersible 300 L/h pumps (Eheim GmbH & Co., Deizisau, Germany). The flush pump brought fresh, oxygenated water into the chamber to replace oxygen-depleted water and flush out waste metabolites. The closed pump recirculated water through a closed loop that included the chamber and a flow-through oxygen cell with a fiber-optic dissolved oxygen (DO) sensor

Figure(See Chapter 2). Probes were calibrated using a two-point calibration (0% and 100%) prior to each experimental run. The closed pump was left on during the entire experiment, while the flush pump was only turned on between measurement periods.

During each respirometry cycle, oysters were allowed to draw down the oxygen for 9 min during a given measurement period (closed pump only) which was followed by a 16.5 min flushing period (flush pump on). This open-closed cycle was repeated for the entire trial (including the overnight acclimation) under a 12-hr light: 12-hr dark cycle. Dissolved oxygen never fell below 80% saturation during closed respirometry periods. Collection of oyster respirometry data for analysis was initiated at 09:00 (2 hours after lights turned on) the morning after acclimation to the chamber and ended at ~20:00 that same day. Oysters were then removed

from chambers, shucked, and wet tissue mass recorded. A 4mmx4mm section of gill tissue was excised from each oyster and stored on ice for immediate RNA extraction for gene expression analysis. The remaining tissue was frozen at -20°C.

Respiration rate (mL O_2/kgWWW/h) was calculated for each oyster during each measurement period by AutoResp™ software using the formula:

$$\text{RMR (mg } O_2\text{/kgWWW/h)} = \frac{V([O_2]_{t0} - [O_2]_{t1})}{t \times WWW} \text{ where}$$

$[O_2]_{t0}$ = DO at time t0 (mg O_2/L)

$[O_2]_{t1}$ = DO at time t1 (mg O_2/L)

V = respirometer volume (L) – volume of oyster (L)

t = time t1 (h) – time t0 (h)

WWW = whole oyster wet weight (g)

Background oxygen consumption from bacteria was measured in chambers without oysters present for ~1h before and after each trial using the same formula but without oyster mass included to yield mgO_2/empty chamber/h. Background oxygen consumption at any given time point within the trial was then estimated from a linear regression. Shell background oxygen consumption was estimated using the MO_2 readings during valve closures periods throughout the experiment and were averaged and subtracted from the mgO_2/occupied chamber/h values to remove background oxygen consumption from the microbial community on the shell. In instances where there were no recorded valve closures during respirometry, the oyster was processed as above, and the two empty valves were placed back into the chamber for an hour-long closed period to estimate microbial background. The background respiration rate before and

after the run was then plotted and a linear regression run through the initial and final data points. Mass specific oyster respiration rates (mgO_2/kgWWW/h) were then multiplied by oyster kgWWW to convert to mgO_2/occupied chamber/h. Estimated control respiration was then subtracted from oyster respiration measured at each given point in time. The resultant value was then divided by oyster wet tissue weight (kgWTW) to yield the corrected mass specific respiration rate for each oyster (mgO_2/kgWTW/h). MO_2 estimates where the relationship between DO and time exhibited an R^2 value of <0.9 were removed from dataset as being an unreliable estimate (Chabot et al., 2021), unless that measurement was identified as a closure.

Cumulative respiration was calculated via the Area Below Curve Macro function in Sigma plot, v 14. RMR was calculated by removing data during suspected closure events and averaging all remaining values together for each individual (see Chapter 2).

The proportion of open measurements was calculated by taking the number of measurements identified as being collected when the oyster was actively respiring (open) for an individual and dividing it by the total number of measurements collected during that run (open plus closed).

3.2.7 RNA extraction and cDNA synthesis

Equal amounts of gill tissue from each individual was homogenized using 2-mercaptoethanol in TRK lysis buffer and a VWR® pellet mixer with VWR® disposable pestles. Total RNA from the homogenate was extracted using the E.Z.N.A. Total RNA Kit I (Omega Bio-Tek®). The total RNA concentration was measured using a NanoDrop One (Thermo Fisher Scientific®). RNA extracts were stored at -80°C. All RNA samples were diluted to the same concentration (40ng/µl) using ultra-pure water. Complementary DNA (cDNA) was synthesized

using a high-capacity cDNA reverse transcription kit (Thermo Fisher Scientific®). All cDNA was synthesized at the same time and stored at -20°C.

3.2.8 qPCR assays

Quantitative polymerase chain reaction (qPCR) was used to measure relative messenger RNA (mRNA) in the following genes: heat shock protein 70 (*HSP70*), blcl-2-associated X apoptosis regulator (*bax*), and *p53*. β-actin and elongation factor 1 alpha (*ef1α*) were included as reference genes. Primer sets were synthesized by Thermo-Fisher. Primers were validated for single band amplification using a hot start PCR-to-gel Taq master mix, 2X (VWR®). qPCR was conducted using PowerUp™ SYBR™ Green Master Mix (Applied Biosystems, Waltham, MA, USA) on a Thermo Fisher Scientific Applied Biosystems QuantStudio5 qPCR thermocycler (Applied Biosystems, Waltham, MA, USA), with the cycle settings of 50°C for 2 min, 95°C for 2 min, followed by 40 cycles of 95°C for 15 sec, 55°C for 15 sec, 72°C for 60 sec.

Specific primer sets were obtained from the literature and verified for single bands using a reference oyster sample (Table 2).

3.2.9 Delta Delta CT calculations

The average delta CT values were raised to the power of 2. The average delta CT values of each individual was then divided by the average power of the control group to calculate the delta delta CT.

3.2.10 Statistical analysis

To test for differences in mean RMR between oysters exposed to PFAS x temperature treatments, a two-way analysis of variation (ANOVA) was conducted on the log average RMR to meet normality assumptions using exposure and temperature as the independent variables. To compare cumulative oxygen consumption between treatments, a two-way ANOVA was used where area under the curve (AUC) was the dependent variable with temperature and exposure groups as the independent variables. To compare proportion of open measurements between treatments, data were transformed via a Box-Cox transformation to meet normality assumptions, and a two-way ANOVA was used where temperature and exposure groups were the independent variables.

To test for differences in gene expression between oysters exposed to PFAS × temperature treatments, each delta delta CT value was normalized to the control at 28°C relative expression to the protein of interest and log transformed to meet normality assumptions. A two-way ANOVA was then used to compare relative expression of each target gene between all four treatment groups. To test if PFAS exposure within temperature treatments affected gene expression, delta delta CT values were then normalized to the control of each temperature treatment and an independent t-test was used on the log transformed delta delta CT values to compare fold-change of each gene of interest between control and treatment values at each temperature.

3.3 Results

3.3.1 Respiration

There was no significant interaction between temperature and PFAS exposure ($F_{(1,26)}$ = .171, p = .683) on respiration rate (Fig. 11 A). Higher temperature had a significant increase in

respiration rate ($F_{(1,26)}$ = 7.986, p = .009), but respiration rate was not significantly altered by PFAS exposure ($F_{(1,26)}$ = .0057, p = .941) (Fig. 11 B,C).

There was also no significant interaction between temperature and PFAS exposure ($F_{(1,26)}$ = .763, p = .391) on mean oxygen consumption as measured by AUC (Fig. 12 A). There was no significant effect of temperature ($F_{(1,26)}$ = 2.393, p = .134) or PFAS exposure ($F_{(1,26)}$ = 0.421, p = .522) on mean oxygen consumption (Fig. 12 B,C).

There was no significant interaction between PFAS exposure and temperature on the proportion of open measurements observed during the course of the trials ($F_{(1,26)}$ = .134, p = .717) (Fig. 13 A).There was no effect of PFAS exposure ($F_{(1,26)}$ = .232, p = .634) or temperature ($F_{(1,26)}$ = .728, p = .401) on proportion of measurements oysters were open (Fig. 13 B,C).

3.3.2 Gene expression

When gene expression was normalized against the unexposed oysters at 28°C, there was no significant effect of exposure ($F_{(1,26)}$ = .587, p = .451), temperature ($F_{(1,26)}$ = .501, p = .485), or their interaction ($F_{(1,26)}$ = 1.400, p = .247) on the fold-change of *bax* (Fig. 14 A,B). There was no significant effect of exposure ($F_{(1,26)}$ = .264, p = .612), temperature ($F_{(1,26)}$ = 1.215, p = .280) and no interaction between temperature and exposure ($F_{(1,26)}$ = 1.222, p = .279) on the fold-change of *HSP70* (Fig. 14 C,D). There was also no significant effect of exposure ($F_{(1,26)}$ = 2.480, p = .127), temperature ($F_{(1,26)}$ = .0686, p = .795) or their interaction ($F_{(1,26)}$ = .0569, p = .813) on *p53* fold-change (Fig. 14 E,F).

When relative expression of treatment oysters was normalized to control oysters at their respective temperatures, there was no significant difference in fold-change in *bax* (t(12) = .315, p = .758), *HSP70* (t(12) = .983, p = .345), or *p53* (t(12) = 1.250, p = .235) between control and

exposed oysters at 28°C (Fig. 15 A,C,E) There was also no significant difference in fold-change in *bax* ($t(14) = -1.330$, $p = .205$), *HSP70* ($t(14) = .494$, $p = .629$), and *p53* ($t(12) = .884$, $p = .392$) between control and exposed oysters at 33°C (Fig. 15 B,D,F).

3.4 Discussion

3.4.1 Influence of temperature and PFAS on metabolism

Exposure to contaminants can increase RMR of organisms due to the costs associated with detoxification (Ivanina et al., 2008). We expected that costs associated with detoxification might be particularly evident at high, stressful temperatures. When oysters were exposed to temperatures above their optimum, mean respiration rates of oysters increased, as expected. However, we found no evidence that exposure to an ecologically relevant mixture of PFAS further increased the energetic burden of cellular maintenance.

The lack of an energetic response to PFAS exposure at high temperature may be because the high temperature (33ºC) was less stressful than expected. Bivalves often increase the frequency of valve closure as a mechanism to reduce costs of thermal stress (Clements et al., 2018). We expected that the frequency of valve closures would increase at high temperatures, resulting in a decrease in cumulative oxygen consumption as oysters lose access to ambient oxygen when closed. However, neither valve-closure frequency nor cumulative oxygen consumption changed as temperatures increased above the optimal range for oysters (20–30°C (Stanley & Sellers, 1986)).

Given that cumulative PFAS concentrations in Mobile Bay are likely below the target concentration in this study (Viticoski et al., 2022), PFAS exposure is likely not increasing energetic demand of wild or farmed oysters at temperatures ≤ 33ºC. However, subsequent

studies (see Chapter 5) have shown that thermal stress, as evidenced by increased valve closure, increases dramatically as temperatures increase from 33ºC to 38ºC. Thus, we cannot preclude energetic effects of PFAS exposure at warmer temperatures than tested in the current study.

3.4.2 Impacts of PFAS on gene expression

In previous studies, the cellular impacts of PFAS exposure in bivalves have been shown via other biomarker assays (Aquilina-Beck et al., 2020; Fernández-Sanjuan et al., 2013; Liu et al., 2014; Liu & Gin, 2018). PFOS was shown to significantly increase the percentage of destabilized cells in oysters at concentrations at and above 3,000µg/L (Aquilina-Beck et al., 2020). PFOS, PFOA, PFNA, and PFDA were found to have significant spontaneous cytotoxicity and reduce hemocyte cell viability at concentrations at and above 100µg/L in green mussels, although the effects were reversed when animals were placed in clean water (Liu & Gin, 2018). This suggests that at high concentrations, bivalves have a reduced immune response to disease, which could result in higher mortalities from disease, and has been discussed in other reviews (Baldwin et al., 2023). In Manila clams, 200 µg/L resulted in an immunological response (F. Li et al., 2024) although these concentrations are orders of magnitude above what has been observed in waters entering Mobile Bay (Viticoski et al., 2022).

In this study, exposure to an environmentally relevant mixture of PFAS at a cumulative concentration of 1µg/L did not cause a significant increase in expression of protein biomarkers indicative of cellular stress and detoxification at temperatures within or above the optimal range previously reported for oysters (Stanley & Sellers, 1986). The lack of increased production of potentially energetically expensive biomarkers might explain why exposure to PFAS was not found to be energetically expensive at a cumulative concentration (1µg/L) higher than the mean

concentration (24.7ng/L) previously reported to be entering Mobile Bay (Viticoski et al., 2022). Elevated temperatures (33°C) also did not cause a significant change in protein production, suggesting that at an optimal salinity, oysters can tolerate a temperature 7°C above their optimal temperature for at least a short period of time without triggering production of the biomarkers tested. However, increased respiration rate can be taxing on organismal health, and chronic exposure to high temperatures induces severe effects that are not apparent during acute exposure. For example, wild Louisiana and Texas oysters held at 33.3°C experienced an earlier LT50 compared to those same lines held at 28.9°C (Marshall et al., 2021). Given that the LAFT line used in the current study was selectively bred for growth, thermal tolerance may differ from wild lines, but this has not been examined for GOM oysters.

Cells did not generate large quantities of *HSP70* when exposed to PFAS, indicating that there was not significant damage to proteins when exposed to environmentally relevant mixtures at concentrations above what has been measured in tributaries around Mobile Bay. *Bax* is a protein that is used to signal that a cell requires destruction by apoptosis. Because there was no significant *bax* expression change when exposed to PFAS, acute exposure to PFAS did not likely result in immediate neoplasia. *P53* is a protein that assists in cell replication and, because *p53* expression did not undergo a significant change during exposure, low concentrations of PFAS are likely not negatively impacting cell replication. Significant increases in respiration rates in combination with a significant change in gene expression would have indicated that low concentrations of PFAS are affecting the oyster in a way that requires major cellular intervention. However, the results from this study suggest that mixtures of PFAS characteristic of Mobile Bay are not likely to impact cellular and energetic health. when at cumulative concentrations ≤ 1 µg/L.

3.4.3 Comparison with field studies

Synergistic effects of pollutants on oyster health are of major concern for oyster populations in areas with large urban centers. Sampling oysters for PFAS body burden in contaminated areas is an optimal method to assess in-situ exposure to bioavailable PFAS due to their filter feeding behaviors (Wang et al., 2022). However, assessing the degree of stress caused by PFAS exposure and uptake in the field is more problematic. While field trials have suggested PFAS (.61-134.8ng/gWTW) and PAH (<.328-1021ng/gWTW) exposure may negatively impact oyster body weight and size in wild oyster reefs around the Florida peninsula, field conditions make it difficult to tease contaminant effects apart from other ecological and biological factors that can also cause changes in body weight and size (Lemos et al., 2022). Oyster aquaculture takes place in coastal estuarine environments where oysters are often exposed to multiple environmental stressors (wave energy, nutritional availability, salinity fluctuations, dissolved oxygen, disease etc.) and pollutants (PFAS, PAH, heavy metals, etc.) simultaneously that could be impacting health in addition to the contaminant in question (Lemos et al., 2022). Assessing the health effects of specific chemicals on wild and farmed oysters sampled directly from the natural environment should be approached with caution, as environmental influence (wave energy, water temperature, etc.) can greatly alter other soft tissue and shell characteristics.

3.5 Tables

Table 2. *Crassostrea virginica* targeted gene functions and optimized primer sets for qPCR. Housekeeping genes are denoted with a *.

Associated cell functions	**Gene names**	**Abbreviations**	**Accension #**	**Forward (F) Reverse (R) primers**	**Citation**
Apoptosis	Bcl-2-associated X apoptosis regulator	*bax*		F: AGTAAACCCGAGTGCAAACCA R: GACCCCAGTTGTAAACACCATC	Lebordais et al., 2021
Cell cycle regulation	Tumor protein P53	*p53*		F: ATGAAGACTCGTACACCCTCAC R: TCTCTGCTTGAACTACCACCTC	Lebordais et al., 2021
Protein stabilization	Heat shock protein	*HSP70*	AJ271444	F: CACATCTGGGAGGTGAGGA R: CTCAAATCTGGCTCGTGTGA	Nash et al., 2019
	Beta-actin	β-actin*	X75894.1	F: CCCACACAGTCCCCATCTAC R: CTCCTGCTCGAAGTCCAAAG	Nash et al., 2019
	Elongation factor 1A	*ef1α**	AB122066	F: ACATTGCTCTGTGGAAGTTCG R: CTCCTGCTCGAAGTCCAAAG	Wang et al., 2010

3.6 Figures

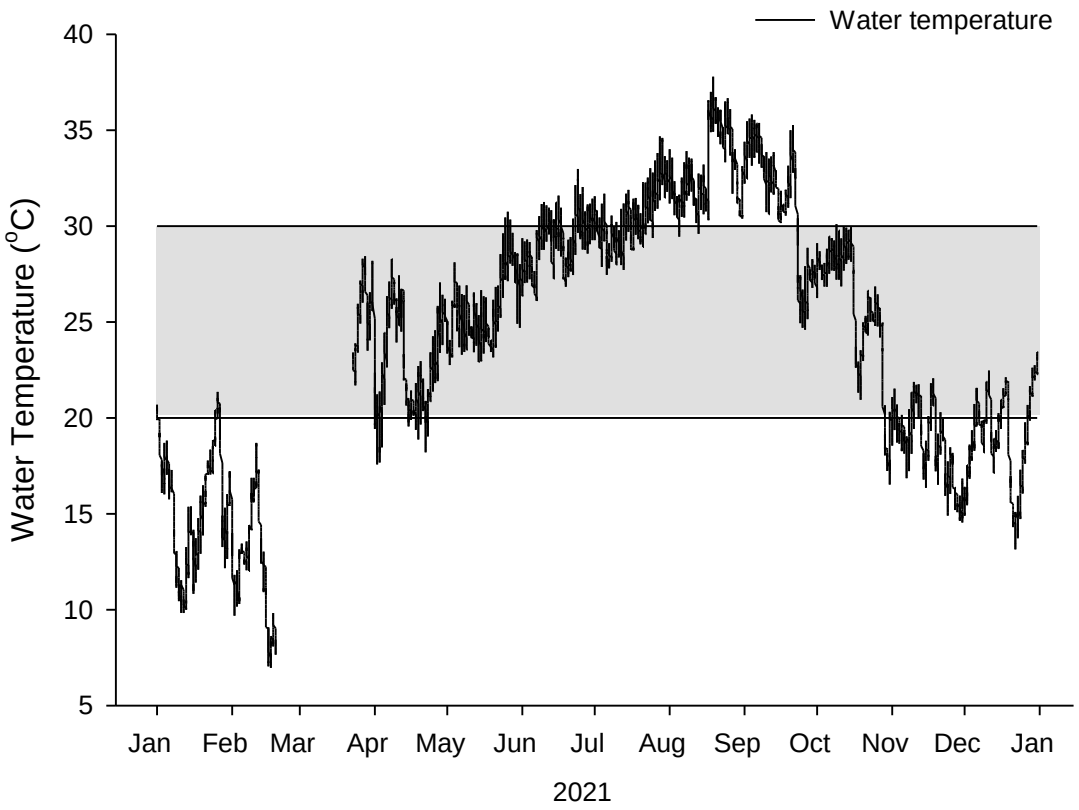

Figure 9. Water temperature collected by an Onset HOBOLogger deployed at Grand Bay Oyster Park (Bayou la Batre, AL) in 2021. Horizontal lines and shaded box denote the upper and lower optimal range for oysters.

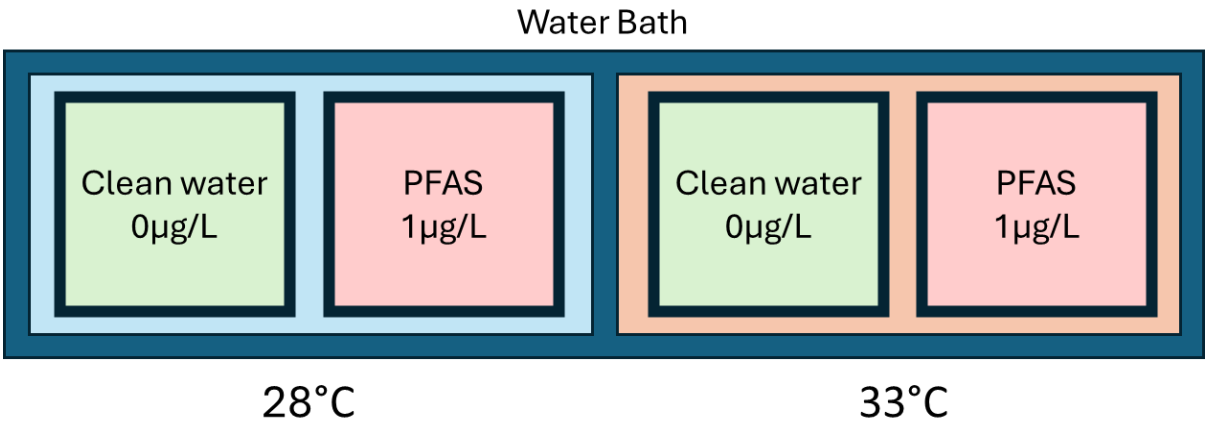

Figure 10. Schematic of water bath, and exposure design during respirometry assay.

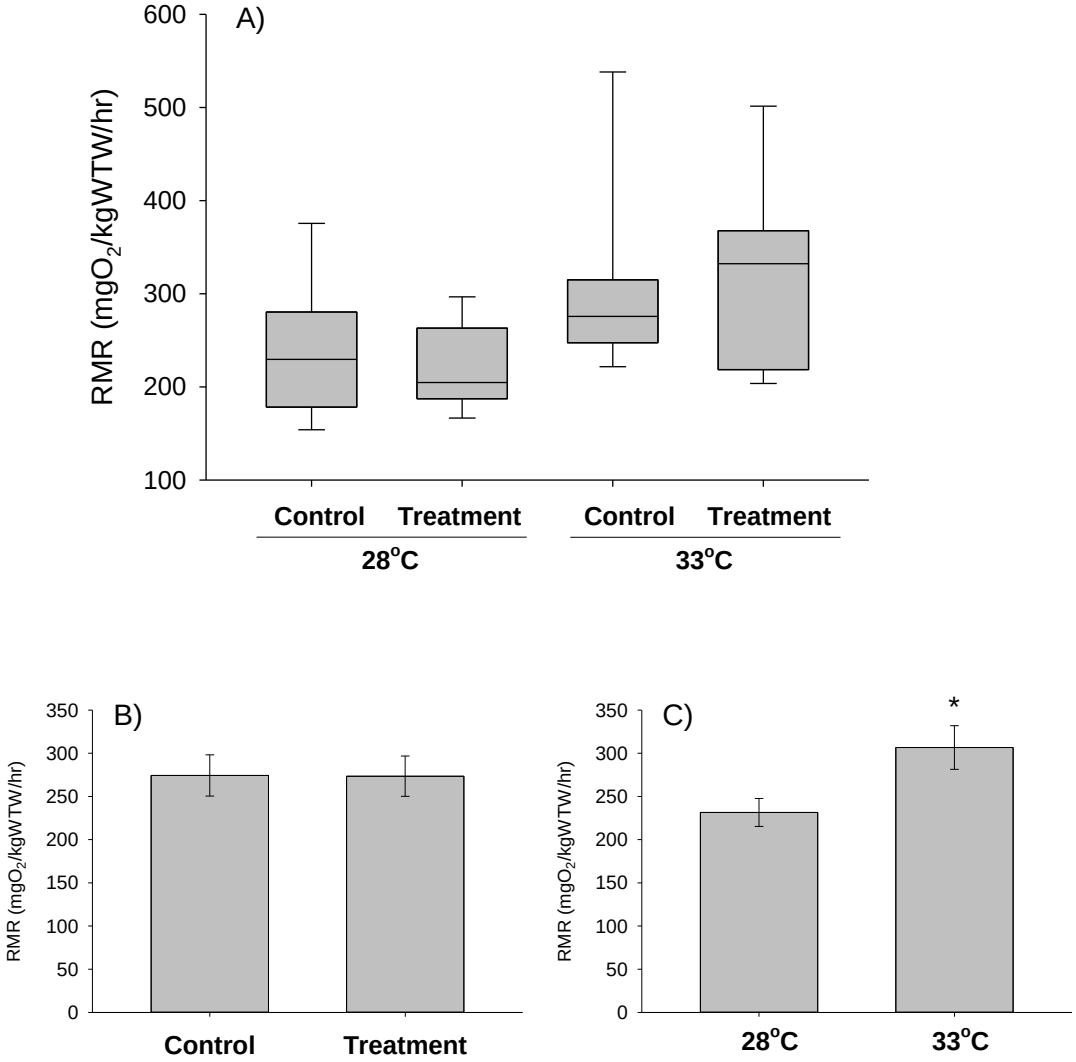

Figure 11. Mean resting metabolic rates (RMR) of open oysters. A) Boxplot displaying RMR for all categories. The horizontal line represents median value with the upper and lower limits representing the upper Q3 and lower Q1 quartile. Error bars indicate the maximum and minimum values. B) Mean RMR of control and exposure oysters regardless of temperature. C) Mean RMR values oysters at 28°C and 33°C regardless of exposure to PFAS. Error bars represent standard error. Significant differences among and between categories are indicated by an asterisk.

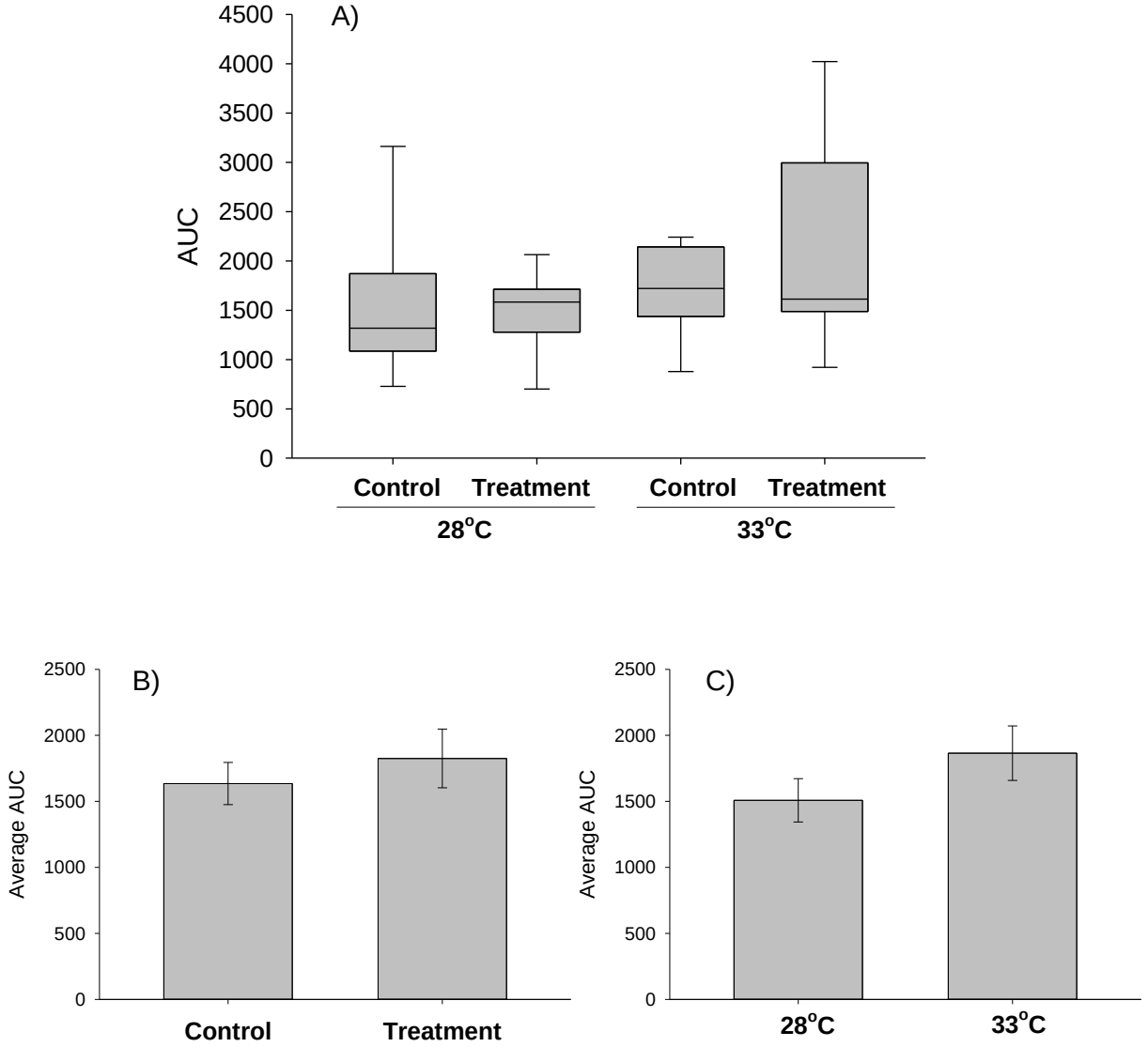

Figure 12. Area under the curve (AUC) of RMR, representing cumulative oxygen consumption of oysters including open and closed periods. A) Boxplot showing mean AUC for all categories B) Mean AUC estimates for control and exposed oysters regardless of temperature C) Mean AUC estimates for oysters at 28°C and 33°C regardless of exposure to PFAS. Error bars denote standard error of the mean for each category.

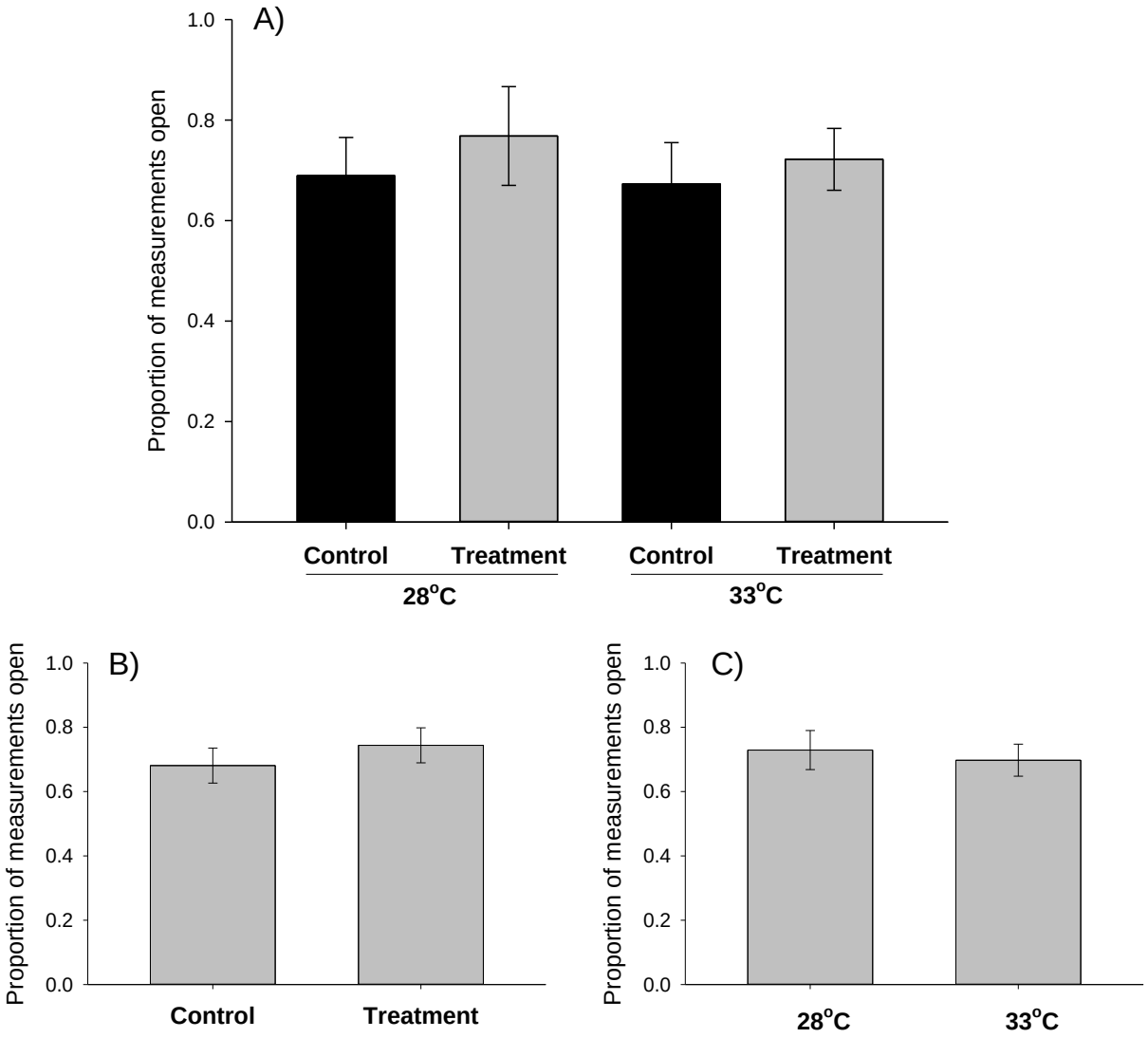

Figure 13. Mean proportion of measurements identified as being from open oysters during respirometry. A) Bar graph showing mean proportion of measurements open for all categories B) Mean proportion open estimates for control and exposed oysters regardless of temperature C) Mean proportion open estimates for oysters at 28°C and 33°C regardless of exposure to PFAS. Error bars denote standard error of the mean for each category.

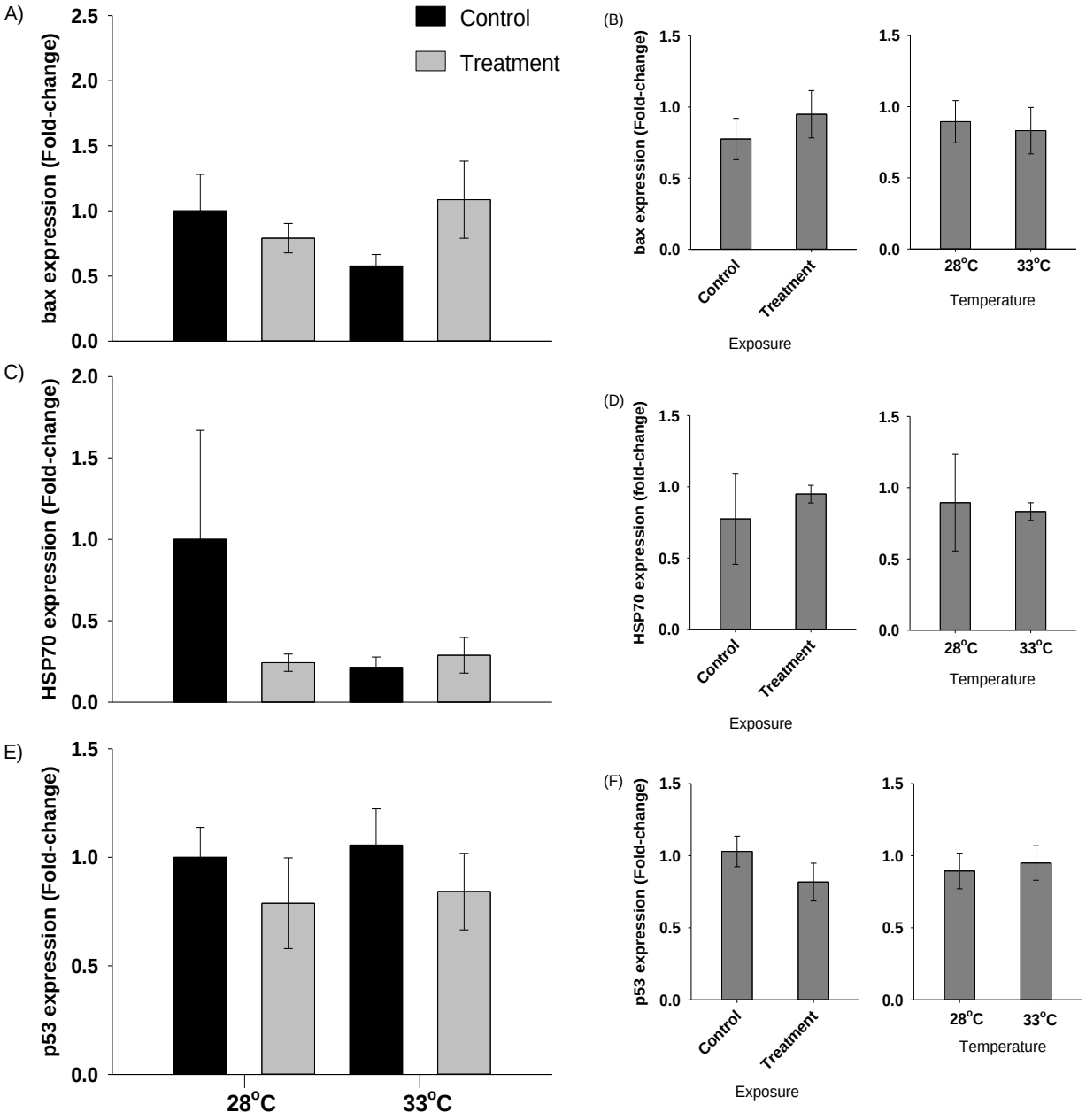

Figure 14. Fold-change of the stress genes A) *bax* C) *HSP70*, and E) *p53* normalized to the control oysters at 28°C for all exposure × temperature categories. Fold-change of the stress genes B) *bax* D) *HSP70*, and F) *p53* for the main effects (Exposure and Temperature) from the two-way repeated measures analysis. Each expression value is normalized to the control for that treatment (28°C), resulting in an expression of 1 for the 28°C control value. Error bars represent the standard error of the mean for each treatment.

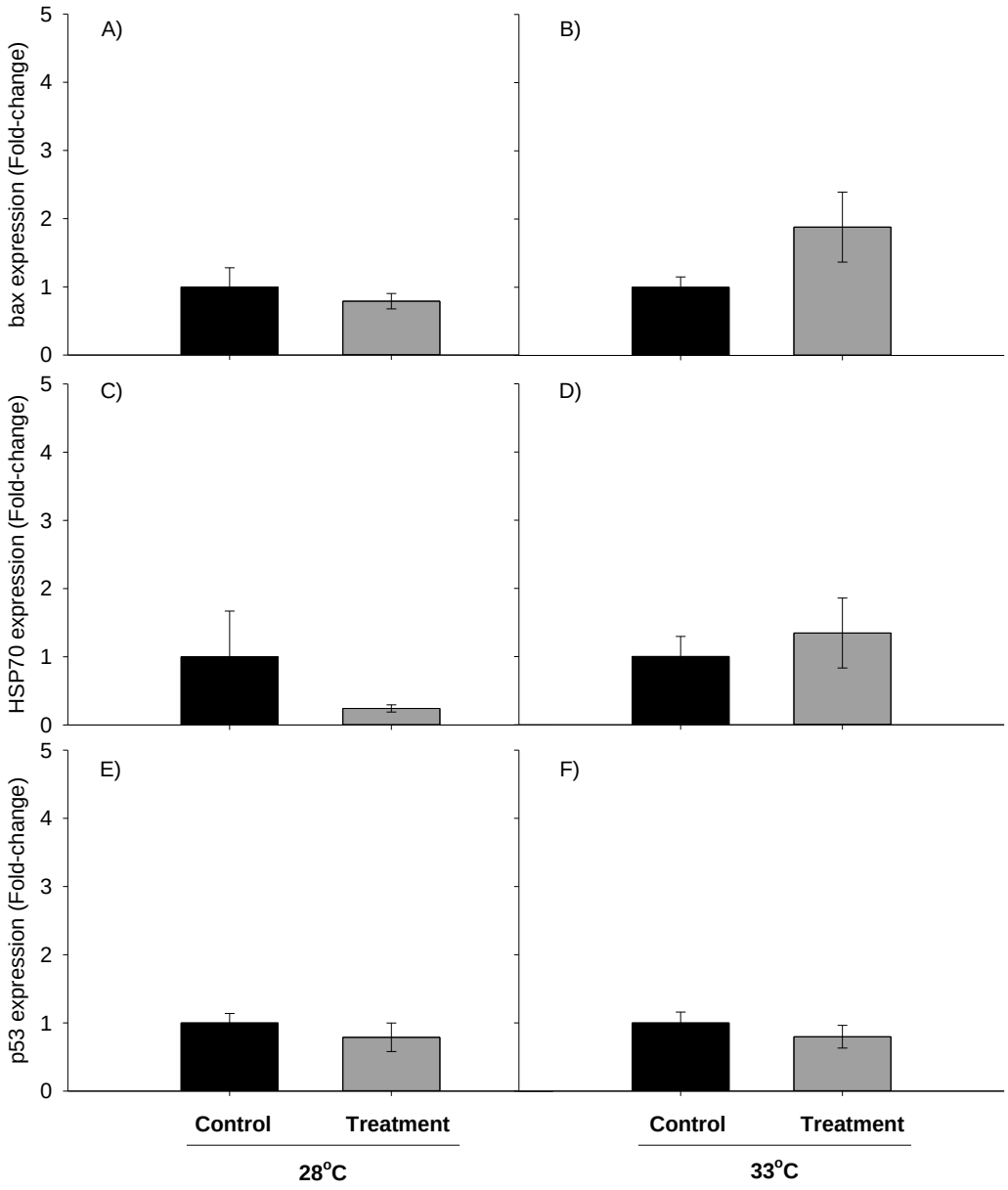

Figure 15. Fold-change of stress genes normalized to the control oysters at each temperature after 10 days of PFAS exposure compared to control oysters of each respective temperature. Each expression value is normalized to the control for that temperature, resulting in an expression of 1 for each control value. A) *bax* at 28°C; B) *bax* at 33°C; C) *HSP70* at 28°C; D) *HSP70* at 33°C E) *p53* at 28°C; F) *p53* at 33°C. Error bars represent the standard error of the mean for each treatment.

3.7 References

Aquilina-Beck, A. A., Reiner, J. L., Chung, K. W., DeLise, M. J., Key, P. B., & DeLorenzo, M. E. (2020). Uptake and Biological Effects of Perfluorooctane Sulfonate Exposure in the Adult Eastern Oyster Crassostrea virginica. *Archives of Environmental Contamination and Toxicology*, *79*(3), 333–342. https://doi.org/10.1007/s00244-020-00765-4

Baldwin, W. S., Davis, T. T., & Eccles, J. A. (2023). Per- and Polyfluoroalkyl Substances (PFAS) and Their Toxicology as Evidenced Through Disease and Biomarkers. In V. B. Patel, V. R. Preedy, & R. Rajendram (Eds.), *Biomarkers in Toxicology* (pp. 989–1016). Springer International Publishing. https://doi.org/10.1007/978-3-031-07392-2_67

Bodenstein, S., Casas, S. M., Tiersch, T. R., & La Peyre, J. F. (2023). Energetic budget of diploid and triploid eastern oysters during a summer die-off. *Frontiers in Marine Science*, *10*. https://www.frontiersin.org/articles/10.3389/fmars.2023.1194296

Calow, P. (1991). Physiological costs of combating chemical toxicants: Ecological implications. *Comparative Biochemistry and Physiology. C, Comparative Pharmacology and Toxicology*, *100*(1–2), 3–6. https://doi.org/10.1016/0742-8413(91)90110-f

Carpenter, R., & Brady, M. F. (2022). BAX Gene. In *StatPearls*. StatPearls Publishing. http://www.ncbi.nlm.nih.gov/books/NBK555927/

Chabot, D., Zhang, Y., & Farrell, A. P. (2021). Valid oxygen uptake measurements: Using high r2 values with good intentions can bias upward the determination of standard metabolic rate. *Journal of Fish Biology*, *98*(5), 1206–1216. https://doi.org/10.1111/jfb.14650

Clements, J. C., Comeau, L. A., Carver, C. E., Mayrand, É., Plante, S., & Mallet, A. L. (2018). Short-term exposure to elevated pCO2 does not affect the valve gaping response of adult eastern oysters, Crassostrea virginica, to acute heat shock under an ad libitum feeding regime. *Journal of Experimental Marine Biology and Ecology*, *506*, 9–17. https://doi.org/10.1016/j.jembe.2018.05.005

Coxe, N., Mize, G., Casas, S., Peyre, M. K. L., Lavaud, R., Callam, B., Rikard, S., & Peyre, J. L. (2023). Hypoxia and Anoxia Tolerance in Diploid and Triploid Eastern Oysters at High Temperature. *Journal of Shellfish Research*, *42*(1), 29–43. https://doi.org/10.2983/035.042.0104

Feige, U., Morimoto, R. I., Yahara, I., & Polla, B. S. (Eds.). (1996). *Stress-Inducible Cellular Responses*. Birkhauser.

Fernández-Sanjuan, M., Faria, M., Lacorte, S., & Barata, C. (2013). Bioaccumulation and effects of perfluorinated compounds (PFCs) in zebra mussels (Dreissena polymorpha). *Environmental Science and Pollution Research International*, *20*(4), 2661–2669. https://doi.org/10.1007/s11356-012-1158-8

Ghaffari, H., Wang, W., Li, A., Zhang, G., & Li, L. (2019). Thermotolerance Divergence Revealed by the Physiological and Molecular Responses in Two Oyster Subspecies of

Crassostrea gigas in China. *Frontiers in Physiology*, *10*. https://www.frontiersin.org/articles/10.3389/fphys.2019.01137

Giesy, J. P., & Kannan, K. (2001). Global distribution of perfluorooctane sulfonate in wildlife. *Environmental Science & Technology*, *35*(7), 1339–1342. https://doi.org/10.1021/es001834k

Griffin, E. K., Aristizabal-Henao, J., Timshina, A., Ditz, H. L., Camacho, C. G., da Silva, B. F., Coker, E. S., Deliz Quiñones, K. Y., Aufmuth, J., & Bowden, J. A. (2022). Assessment of per- and polyfluoroalkyl substances (PFAS) in the Indian River Lagoon and Atlantic coast of Brevard County, FL, reveals distinct spatial clusters. *Chemosphere*, *301*, 134478. https://doi.org/10.1016/j.chemosphere.2022.134478

Hégaret, H., Wikfors, G. H., & Soudant, P. (2003). Flow cytometric analysis of haemocytes from eastern oysters, Crassostrea virginica, subjected to a sudden temperature elevation: II. Haemocyte functions: aggregation, viability, phagocytosis, and respiratory burst. *Journal of Experimental Marine Biology and Ecology*, *293*(2), 249–265. https://doi.org/10.1016/S0022-0981(03)00235-1

Ivanina, A. V., Cherkasov, A. S., & Sokolova, I. M. (2008). Effects of cadmium on cellular protein and glutathione synthesis and expression of stress proteins in eastern oysters, Crassostrea virginica Gmelin. *Journal of Experimental Biology*, *211*(4), 577–586. https://doi.org/10.1242/jeb.011262

Jeon, J., Kannan, K., Lim, H. K., Moon, H. B., Ra, J. S., & Kim, S. D. (2010). Bioaccumulation of perfluorochemicals in Pacific oyster under different salinity gradients. *Environmental Science & Technology*, *44*(7), 2695–2701. https://doi.org/10.1021/es100151r

Kvitt, H., Rosenfeld, H., & Tchernov, D. (2016). The regulation of thermal stress induced apoptosis in corals reveals high similarities in gene expression and function to higher animals. *Scientific Reports*, *6*(1), Article 1. https://doi.org/10.1038/srep30359

Lebordais, M., Gutierrez-Villagomez, J. M., Gigault, J., Baudrimont, M., & Langlois, V. S. (2021). Molecular impacts of dietary exposure to nanoplastics combined with arsenic in Canadian oysters (Crassostrea virginica) and bioaccumulation comparison with Caribbean oysters (Isognomon alatus). *Chemosphere*, *277*, 130331. https://doi.org/10.1016/j.chemosphere.2021.130331

Lemos, L., Gantiva, L., Kaylor, C., Sanchez, A., & Quinete, N. (2022). American oysters as bioindicators of emerging organic contaminants in Florida, United States. *Science of The Total Environment*, *835*, 155316. https://doi.org/10.1016/j.scitotenv.2022.155316

Li, F., Gong, X., Zhou, Y., Geng, Q., Jiang, Y., Yao, L., Qu, M., & Tan, Z. (2024). Integrated evidence of transcriptional, metabolic, and intestinal microbiota changes in Ruditapes philippinarum due to perfluorooctanoic acid-induced immunotoxicity. *Science of The Total Environment*, *916*, 170341. https://doi.org/10.1016/j.scitotenv.2024.170341

Li, X., Fatowe, M., Cui, D., & Quinete, N. (2022). Assessment of per- and polyfluoroalkyl substances in Biscayne Bay surface waters and tap waters from South Florida. *Science of The Total Environment*, *806*, 150393. https://doi.org/10.1016/j.scitotenv.2021.150393

Liberek, K., Skowyra, D., Zylicz, M., Johnson, C., & Georgopoulos, C. (1991). The Escherichia coli DnaK chaperone, the 70-kDa heat shock protein eukaryotic equivalent, changes conformation upon ATP hydrolysis, thus triggering its dissociation from a bound target protein. *The Journal of Biological Chemistry*, *266*(22), 14491–14496.

Liu, C., Chang, V. W. C., & Gin, K. Y. H. (2014). Oxidative toxicity of perfluorinated chemicals in green mussel and bioaccumulation factor dependent quantitative structure–activity relationship. *Environmental Toxicology and Chemistry*, *33*(10), 2323–2332. https://doi.org/10.1002/etc.2679

Liu, C., & Gin, K. Y.-H. (2018). Immunotoxicity in green mussels under perfluoroalkyl substance (PFAS) exposure: Reversible response and response model development. *Environmental Toxicology and Chemistry*, *37*(4), 1138–1145. https://doi.org/10.1002/etc.4060

Lowe, M. R., Sehlinger, T., Soniat, T. M., & Peyre, M. K. L. (2017). Interactive Effects of Water Temperature and Salinity on Growth and Mortality of Eastern Oysters, Crassostrea virginica: A Meta-Analysis Using 40 Years of Monitoring Data. *Journal of Shellfish Research*, *36*(3), 683–697. https://doi.org/10.2983/035.036.0318

Marshall, D. A., Coxe, N. C., La Peyre, M. K., Walton, W. C., Rikard, F. S., Pollack, J. B., Kelly, M. W., & La Peyre, J. F. (2021). Tolerance of northern Gulf of Mexico eastern oysters to chronic warming at extreme salinities. *Journal of Thermal Biology*, *100*, 103072. https://doi.org/10.1016/j.jtherbio.2021.103072

Nash, S., Johnstone, J., & Rahman, M. S. (2019). Elevated temperature attenuates ovarian functions and induces apoptosis and oxidative stress in the American oyster, Crassostrea virginica: Potential mechanisms and signaling pathways. *Cell Stress & Chaperones*, *24*(5), 957–967. https://doi.org/10.1007/s12192-019-01023-w

Pouvreau, S., Bourles, Y., Lefebvre, S., Gangnery, A., & Alunno-Bruscia, M. (2006). Application of a dynamic energy budget model to the Pacific oyster, Crassostrea gigas, reared under various environmental conditions. *Journal of Sea Research*, *56*(2), 156–167. https://doi.org/10.1016/j.seares.2006.03.007

Rivlin, N., Brosh, R., Oren, M., & Rotter, V. (2011). Mutations in the p53 Tumor Suppressor Gene. *Genes & Cancer*, *2*(4), 466–474. https://doi.org/10.1177/1947601911408889

Smolarz, K., Thiriot-Qui´, C., & Wolowicz, M. (2005). Recent trends in the prevalence of neoplasia in the Baltic clam Macoma balthica (L.) from the Gulf of Gdańsk (Baltic Sea)*. *Oceanologia*, *47*(1), 61–74.

Stanley, J. G., & Sellers, M. A. (1986). *Species profiles: Life histories and environmental requirements of coastal fishes and invertebrates (Gulf of Mexico)—American oyster* (82; US Fish and Wildlife Service Biological Report, p. 25).

US EPA, O. (2016, March 30). *Basic Information on PFAS* [Overviews and Factsheets]. US EPA. https://www.epa.gov/pfas/basic-information-pfas

Viticoski, R. L., Wang, D., Feltman, M. A., Mulabagal, V., Rogers, S. R., Blersch, D. M., & Hayworth, J. S. (2022). Spatial distribution and mass transport of Perfluoroalkyl Substances (PFAS) in surface water: A statewide evaluation of PFAS occurrence and fate in Alabama. *The Science of the Total Environment*, *836*, 155524. https://doi.org/10.1016/j.scitotenv.2022.155524

Wang, Q., Ruan, Y., Jin, L., Lu, G., Ma, L., Yeung, L. W. Y., Wang, W.-X., & Lam, P. K. S. (2022). Oysters for legacy and emerging per- and polyfluoroalkyl substances (PFASs) monitoring in estuarine and coastal waters: Phase distribution and bioconcentration profile. *Science of The Total Environment*, *846*, 157453. https://doi.org/10.1016/j.scitotenv.2022.157453

Wang, S., Zhang, Q., Zheng, S., Chen, M., Zhao, F., & Xu, S. (2019). Atrazine exposure triggers common carp neutrophil apoptosis via the CYP450s/ROS pathway. *Fish & Shellfish Immunology*, *84*, 551–557. https://doi.org/10.1016/j.fsi.2018.10.029

CHAPTER 4
DIFFERENCES IN TOLERANCE AND RESPONSES TO THERMAL STRESS BETWEEN DIPLOID AND TRIPLOID EASTERN OYSTERS (*Crassostrea virginica*) FROM THE NORTHERN GULF OF MEXICO

4.1 Introduction

Oyster aquaculture and wild harvesting are economically important industries in the Gulf of Mexico (GOM). In 2020, the GOM alone landed over 9 million pounds of oysters valued at over 59 million dollars, accounting for 62% of the total weight of oysters landed in the United States and making up 40% of the total oyster revenue (NOAA, 2020). Traditional oyster production has relied on harvesting oysters off wild reefs or capturing natural set spat and planting them on-bottom in a managed location. With the recent introduction of new culture techniques, semi-intensive off-bottom oyster farming is now feasible in the GOM (Supan, 2002, p. 20, 2014; Walton et al., 2013).

The emergence of an off-bottom farming industry has increased the demand for production of triploid oysters in hatcheries. Triploid oysters can be created by breeding a female diploid oyster with a male tetraploid oyster to create a mated triploid, or by chemically inducing triploidy (chemical triploids) via preventing a polar body release after fertilization of a diploid egg by diploid sperm (Gérard et al., 1999). Triploid oysters are considered a superior product to diploid oysters because of their faster growth rate and superior meat quality during the summer spawning season (Wadsworth, Wilson, et al., 2019). Currently, the majority of eastern oyster seed requested in the GOM by producers for the half shell market are triploids which are then grown in semi-intensive off-bottom cages (S. Rikard, personal communication, 2023). The shift in production from diploid to triploid seed is dependent on triploids performing well through the growing season, but the two decades has seen a concerning trend towards decreased survival of

triploid oysters over a typical growing season compared to diploid oysters in the same growing area (Wadsworth, Casas, et al., 2019; Wadsworth, Wilson, et al., 2019).

Alabama and Louisiana farmers in the north Gulf of Mexico (nGOM) have reported sudden and unexpected mortality events in farmed oysters. Studies comparing diploid and triploid survival noted that triploid oysters were experiencing proportionately higher mortality than diploids across most farm sites studied (Bodenstein et al., 2023; Wadsworth, Casas, et al., 2019). Amongst diploid oysters, it has been well documented that summer mortality events primarily affect reproductively mature oysters (60-70mm) (Burge et al., 2007; Wadsworth, Casas, et al., 2019). Likewise, triploid mortality events are primarily impacting near market-sized oysters (50-70 mm) as they enter their first summer (Matt & Allen, 2021; Wadsworth, Casas, et al., 2019). There is a great need to investigate differences and similarities between diploid and triploid oysters in physiological responses to environmental stressors, tolerance to different environmental parameters and the mechanisms behind tolerance. Common environmental stressors at oyster farms include periods of prolonged low salinity, high surface water temperature, disease, predation, and hypoxic events. Unexpected mortality events observed at oyster farms are likely caused by exposure to multiple simultaneous stressors (Marshall et al., 2021).

Metabolism is a valuable metric to examine energy use and stress in invertebrates. Unlike obligate aerobic ectotherms, facultative anaerobes such as bivalves can suppress their metabolism by mechanisms such as valve closure and switching to anaerobic respiration as temperatures increase. Anaerobic respiration is less efficient and suppresses ATP turnover rates below baseline rates but can prevent a collapse of cellular process during periods of thermal stress (Boutilier and St.-Pierre, 2000; Vadjedsameie et al. 2021). In bivalves, this can produce a

pattern where metabolic rate (as represented by heart rate or respiration) temporarily decreases and then recovers with increasing temperature, or a pattern where metabolism increases with temperature until it reaches a peak (RMR_{peak}), after which metabolic rates decreases with further increases in temperature. The decline post-RMR_{peak} has been termed respiratory suppression or metabolic depression (Anestis et al., 2007; Vajedsamiei et al., 2021). It has been suggested that a reduction in metabolic rate may be an adaptation to cope with thermal stress and delay the lethal effects of temperature (Miller & Stillman, 2012; Verberk et al., 2016). Temperature fluctuations are frequently experienced in intertidal bivalves and thus they have adapted mechanisms to depress their metabolism to cope with thermal stress via increased closures (Hui et al., 2020; Vajedsamiei et al., 2021). An increased frequency of closures at high temperatures likely represents shifts from aerobic to anaerobic metabolism which results in a reduction in ATP turnover (Anestis et al., 2007).

Behavioral endpoints in bivalves can also be indicators of thermal metabolic stress (Galbraith et al., 2012). At a certain temperature, termed the critical thermal maximum (CTM) loss of organismal coordination occurs and the organism can no longer escape the lethal environmental conditions (Lutterschmidt & Hutchison, 1997). In response to thermal stress, freshwater mussels exhibit the following CTM behaviors: extreme gaping behavior, mantle tissue relaxation, and unresponsiveness to probing (Galbraith et al., 2012). Oyster behavioral responses to thermal stress include valve closures (Clements et al., 2018) followed by gaping with no response to tactile stimulation at CTM. However very few studies denote where actual behavioral signs of thermal stress and death occur in relation to metabolic stress in oysters (Clements et al., 2018; Vajedsamiei et al., 2021).

The main goals of this study were to determine 1) whether metabolic rates and occurrence of metabolic depression differ between diploid and triploid oysters exposed to acute thermal stress, 2) Examine the relationship between metabolic patterns and observable behavioral responses to thermal stress, 3) Test whether triploids exhibit a lower CTM and PPD temperature than diploids, and 4) Determine whether these differences can explain relatively higher triploid mortality in the summer months.

4.2 Methods

4.2.1 Oyster farm temperature

An Onset HOBO logger (Onset, Bourne, MA, USA) was deployed at the Auburn University Shellfish Lab farm in Grand Bay Oyster Park, Bayou La Batre, Alabama from January 2021 to December 2021. The logger was submerged approximately 20cm below the water surface. The logger was periodically retrieved from the farm and replaced with a clean logger to reduce background interference by biofouling. Abnormalities in the HOBO logger data were identified as extended periods with no variation of temperature, as well as values outside the range of what is reasonably expected for the Gulf of Mexico at that time of the year (-5°C to 45°C: ARCOS, 2023). These temperatures were removed from the dataset as they were assumed to be most likely due to a failed calibration or biofouling on the sensor.

4.2.2 Oyster lineage

Oysters are known to have a high degree of local adaptation (Bible & Sanford, 2016; Burford et al., 2014) and environmental tolerance can be directly influenced by genetics passed from broodstock (Callam et al., 2016). To minimize differences based on parentage, we created

half-sibling lines that used the same maternal diploid broodstock crossed with diploid males to produce diploid offspring and crossed with tetraploid males to produce triploid offspring. Female broodstock used in this experiment were from a commercially available lines produced at the Auburn University Shellfish Laboratory with parentage derived from Louisiana, Alabama, Florida, and Texas (LAFT) wild oysters. Diploids were produced using LAFT males resulting in a 2MLAFT21 (LAFT X LAFT) cohort. Triploids were produced by fertilizing LAFT females using Louisiana (GNL) tetraploid male sperm resulting in a 3MLAFTLA21 (LAFT X GNL) cohort. Diploid and triploid fertilization occurred at the same time using the same egg pool. Resulting half-sibling oyster cohorts were set on microcultch and raised at Grand Bay Oyster Park, AL until they reached experimental size. Research animals were not desiccated during the growth period, which is a standard method to control biofouling. To control growth and to remove epibionts and mortalities from the population, oysters were periodically tumbled according to Auburn University Shellfish Lab (AUSL) standard management practices.

4.2.3 Oyster collection

Half-sibling diploid and triploid hatchery-raised, single-set adult oysters (65-75mm shell height) were collected in January 2022 from off-bottom long-line BST baskets (Cowell, South Australia) suspended from lines at Grand Bay Oyster Park (30° 22’ 30” N, 88° 18’ 53” W). Oysters were transported back to AUSL by boat. To remove epibionts, oysters were scrubbed of all biofouling organisms such as barnacles and algae. They were then placed in a freshwater dip for 20 minutes with gentle agitation and transferred to a hypersaline salt dip for an additional 8 minutes with gentle agitation and were then placed on a flat surface cup-side down and allowed to dry overnight to remove shell-burrowing annelids. The following morning, diploid and triploid

oyster cohorts were split into two groups of equal numbers and placed equidistant from each other within two holding upwellers (i.e. each upweller contained a mix of diploids and triploids) sharing a sump with the cupped valve facing down. After a day of recovery from handling stress, each oyster was assigned an identification number via an 8X4mm external Hallprint shellfish tag (Hallprint, Hindmarsh Valley, South Australia) secured with super glue.

4.2.4 Holding conditions

Upwellers were constructed containing bio balls and shredded PVC as the biofilter media. A holding basket (plastic tote) with a screened opening underneath was included as the internal container. A mesh screen as the holding basket was situated over the biofiltration media. Two upwellers were placed within a fiberglass trough containing 300L of water that acted as the shared sump. Water was pumped from the sump to the internal container where it flowed into the holding basket via the screened opening and back into the shared sump. One air stone was placed in each upweller to provide extra aeration and water movement (Fig. 16). Bacterial biofilters in the upwellers were established for >1mo prior to the arrival of experimental oysters. The upwellers contained natural seawater adjusted to 18±1ppt salinity using Instant Ocean® Sea Salt (Blackburg, VA, USA) and dechlorinated municipal water. Acclimation temperatures were set to 25±1°C via two 800W Finnex Deluxe tube heaters (with guard) plugged into an Aqua Logic Temperature Controller TC11 (Aqua Logic Inc., Dan Diego, CA, USA). The shared sump was batch fed 15mL of LPB algae diet (Reed mariculture, Campbell, CA) three times a week to maintain body condition but not promote growth. Oysters were acclimated to laboratory conditions (25°C, 12:12 h; light dark, pH 8) for >2 weeks prior to experiments.

4.2.5 Oxygen consumption assay

Respiration was measured with an 8-chamber fiber-optic respirometry system and Auto-Resp^{TM} 2.3.0 software (Loligo Systems®, Viborg, Denmark). Chambers were made of acrylic and were 250ml in volume. Each chamber was equipped with two Eheim® submersible 300L/h pumps (Eheim GmbH & Co., Deizisau, Germany): One pump was designated as the flush pump to circulate oxygenated water into the chamber and the other was designated the recirculation pump which constantly circulated water through the chamber. A flow-through oxygen cell with an optical dissolved oxygen (DO) sensor was connected to the recirculation tubing for each chamber to measure real time dissolved oxygen readings (Fig. 17).

To reduce background oxygen consumption from bacteria, the tank and all associated respirometry equipment were disinfected before each run by soaking overnight in a weak bleach solution in tap water. The tank was then drained and thoroughly rinsed with tap water before being set up for the next run. Chambers, tubing, and pumps were submerged in a ~400L fiberglass trough filled with 200L of 18ppt ambient sea water filtered through a 1µm filter bag. Water was aerated using air stones to maintain ~100% saturation. Water temperature was set to the acclimation temperature (25±1°C) controlled by an 800W Finnex Deluxe tube heater (with guard) plugged into an Aqua Logic Temperature Controller TC11 (Aqua Logic Inc., Dan Diego, CA, USA).

For a given respirometry trial, three diploid and three triploid oysters were randomly selected and placed in the respirometry tank with no food at 09:00 on Day 0 to facilitate a 24-hour fasting period. Oysters were then assigned to random respiration chambers (one oyster per chamber) at approximately 12:00 and allowed to acclimate to the chambers overnight. A 12:12 light:dark cycle was maintained throughout each trial, with lights turning off at 19:00 and turning

back on at 07:00. Respiration measurement cycles occurred throughout the acclimation period, but only measurements taken after 09:00 on Day 1 were used for analysis to allow oysters ~2h to adjust to lights turning on. The respirometry cycle for each chamber consisted of a flush period, wait period and a measurement period. During the flush period, both the flush and recirculating pumps were turned on and tank water was flushed through each chamber. During the wait period, the flush pump was turned off while the recirculating pump stayed on, creating a closed system. The wait period was used to remove the initial parabolic curve as the dissolved oxygen dropped such that the subsequent measurement period is comprised of the period where DO decreases linearly. The cycle then repeated after each measurement period. The flush period was typically 500 seconds and allowed sufficient time for chamber water to return to ~100% saturation between measurement periods. The wait period was set at 100 seconds. The measurement period ranged from 350 – 200 seconds, depending on temperature, and was adjusted such that the DO in the chambers never fell below 80% saturation.

Starting at 10:00 on Day 1, the trough temperature was increased at a rate of 2°C per hour. Trials ended at 46°C, at which concurrent behavioral response trials were ended (see description in the next section). After the conclusion of each trial, oysters were shucked, and the wet tissue was recorded. Tissues were then frozen at -20°C and subsequently oven dried for 48 hours to obtain dry tissue weight. Shells were airdried for 1 week at 20°C to find dry shell weight. Four trials were conducted, using different oysters for each trial, for a total of 12 oysters per ploidy. AutoResp software calculated respiration rate for every measurement cycle using the following formula:

$$\text{RMR } (mgO_2/kgWWW/h) = \frac{V\left([O_2]_{t0} - [O_2]_{t1}\right)}{t \times WWW} \text{ where}$$

$[O_2]_{t0}$ = DO at time t0 (mg O_2/L)

$[O_2]_{t1}$ = DO at time t1 (mg O_2/L)

V = respirometer volume (L) – volume of oyster (L)

t = time t1 (h) – time t0 (h)

WWW = whole oyster wet weight (g)

4.2.5.1 Correcting for background respiration

Within each trial, one chamber contained no oysters and was used as a control to estimate background oxygen consumption of bacteria using the same formula as above but without oyster mass included to yield mgO_2/empty chamber/h. A second chamber contained the shucked shells of one diploid and one triploid oyster (4 valves total) to account for background consumption of bacteria and residual invertebrate communities associated with the oyster shells as temperatures increased.

To correct for bacterial and shell community background respiration, MO_2 values of chambers containing shells were converted to chamber values (mgO_2/shell chamber/h) by using the same formula as above taking into account the amount of water displaced by the shell (mgO2/shell chamber/h). Because the shell background chamber contained two sets of shells (4 valves), the average of one set (2 valves) of shells was determined by subtracting the bacterial chamber MO_2 (mgO_2/shell chamber/h) and dividing the resulting shell background without bacteria by 2 to obtain the average oxygen consumption of one set of shells. The bacterial MO_2 was then added back to the single shell respiration estimate.

Mass specific oyster respiration rates (mgO_2/kgWWW/h) were then multiplied by oyster kgWWW to convert to mgO_2/occupied chamber/h. Estimated bacterial and shell community

oxygen consumption described in the previous paragraph was then subtracted from oyster respiration measured at each given temperature point. The resultant value was then divided by oyster dry tissue weight (kgDTW) to yield the corrected mass specific respiration rate for each oyster (mgO_2/kgDTW/h).

4.2.5.2 Defining valve closures and unreliable measurements

We identified measurement periods as part of a valve closure when the corrected respiration rate for that measurement period was either ≤ 0 or was <50% of the respiration rate recorded prior to the decline (Fig. 18). Outside of the identified closure periods, any measurement period where the linear relationship between DO and temperature exhibited an R^2 < .9 was considered unreliable and automatically removed prior to analysis unless the measurement was identified as a closure (Chabot et al., 2021). The resulting values were considered the resting metabolic rate (RMR) at that measurement point for an individual.

Closure analysis was done by first identifying the number of closed measurements that were recorded within each integer ± 5°C temperature bin (i.e., 28±5°C, 29±5°C, etc.). The number of "closed" measurements was then divided by the number of total measurements within each bin to calculate the proportion of closed measurements at each integer temperature for each individual. To evaluate changes in closure frequency, proportion closed values within 5°C before metabolic peak (29-33°C) and proportion closured values within 5°C after metabolic peak (34-38°C) within ploidies were then averaged to find proportion closed pre- and post-RMR_{peak}.

4.2.5.3 Temperature quotient (Q10)

For each individual oyster, the mean respiration rate was calculated from all open and reliable estimates obtained within the 25±0.5°C (initial temperature) and 32±0.5°C (temperature just before metabolic peak) temperature bins. A temperature quotient (Q10) was then calculated for each individual using the following equation described in Lampert 1984:

$$Q10 = (R2/R1)^{(10/(T2-T1))}$$

R1: Respiration rate at 25°C

R2: Respiration rate at 32°C

T1: Initial temperature

T2: Final temperature

4.2.6 Behavior, functional death, and physical death

An insulated test chamber was filled with 75L of ambient seawater heated to 25°C. For each trial, salinity was adjusted to 18±.2ppt. An air stone and pump were used to keep water circulating and oxygenated throughout the assay. An 800W Finnex titanium heater bar (Chicago, IL, USA) was affixed to the center of the chamber via suction cups. Diploid and triploid oysters were evenly placed on both sides of the heater bar. Water temperature was increased 2°C every hour and oysters were checked every half hour for the onset of behavioral endpoints. Temperature recorded when oysters showed signs of critical thermal maximum (CTM: gaping and no response to probing) or presumed physical death (PPD: gaping, mantle retraction, and no response to probing). Water temperature was increased until 100% of oysters showed mantle tissue retraction or water temperatures reached 46°C to account for oysters that had expired but were held closed by suction, which was later verified by shucking post-experiment and

examining mantle tissue for reactions to probing. PPD_{temp} was not recorded for oysters that had this occur. At the end of each trial, oysters were removed from the test container and shucked. Tissue wet weight was recorded, and tissues stored frozen at -20°C to be later dried in a Fisher Scientific Isotemp Oven (Waltham, MA, USA) at 80°C for 48 hrs before being weighed on a AL204 Mettler Toledo analytical balance (Columbus, OH, USA) to obtain dry tissue weight. Empty shell was airdried at 20°C for 1 week to find dry shell weight.

4.2.7 Condition index

Condition index was calculated using the following equation (Abbe & Albright, 2003):

CI=[dry meat mass (g)/(whole oyster wet weight(g)-dry shell weight (g))]*100

4.2.8 Statistical analysis

We used a t-test to test for differences in initial RMR between diploids and triploids at 25°C – the temperature to which they had been acclimated prior to the thermal ramp. To determine the relationship between respiration rate of open oysters and temperature, respiration estimates from measurement periods identified as containing a valve closure were first removed from the RMR dataset as described previously. Then, for each oyster ploidy class, a thermal performance curve (TPC) was created by fitting a smoothing spline (SS) model to a plot of RMR vs temperature. The selection of the smoothing parameter (λ) was based on the restricted maximum likelihood (REML) method to ensure the compromise between the smoothness of the function and the lack of fit (Berry & Helwig, 2021). The fitted SS models were used to predict RMR at temperatures from 24.25 – 46.66ºC with an interval of .001ºC. For each oyster ploidy class, 95% confidence intervals (95% CI) of predicted RMR curves were created via

bootstrapping (Efron & Tibshirani, 1993) implemented in the boot package (version 1.3-28; Canty and Ripley, 2021). Data were resampled with replacement 1,000 times, with the SS model re-fitted to these data each time, and the 95% CIs were determined from the 2.5^{th} and 97.5^{th} percentiles. $RMR_{peak\ temperature}$ was determined as the temperature where the maximum metabolic rate was predicted by the spline. T_{upper} and T_{lower} were calculated by identifying the upper 90% of the predicted RMR rate above and below the maximum RMR rate ($RMR_{peak\ rate}$) respectively (Fig. 19). Statistical analyses for RMR data were conducted using R software for windows (version 4.1.1; R Core team, 2021).

Differences in proportion closed was analyzed using a two-way ANOVA and a Tukey's test was used to compare proportion closed between diploid and triploid oysters pre- and post-$RMR_{peak\ temp}$ to identify how metabolic stress post-$RMR_{peak\ temp}$ changed the proportion closed. Because there was no significant difference in $RMR_{peak\ temp}$ between diploids and triploids we used the mean $RMR_{peak\ temp}$ of diploids and triploids combined (34°C) as the breakpoint between pre- and post-$RMR_{peak\ temp}$ for both ploidies in this analysis.

The likelihood of exhibiting CTM and PPD were analyzed using the survival analysis methods. Kaplan-Meier survival analyses were used to determine the median CTM_{temp} and PPD_{temp} for each oyster ploidy class, and log-rank tests were used to compare probabilities of CTM and PPD between ploidy groups. Statistical significance was set at P-value < .05, and data were presented as the mean ± *SD*. Survival analyses were performed in SAS® version 9.4 (*SAS*, 2013). A mixed-model analysis of covariance (ANCOVA) was used to test the effects of mass, shell height, and condition index on CTM and PPD.

4.3 Results

4.3.1 Site specific environmental parameters

Surface water temperatures exhibited expected seasonal trends with increasing temperature from winter to summer. Average monthly temperatures ranged from a low of 12.4°C in February up to a high of 32.9°C in August. The greatest fluctuation between the highest and lowest observed temperature in any given month was ~10°C (Fig. 20).

4.3.2 Effects of temperature on metabolism

After acclimation to a constant temperature for >2 weeks, RMR did not significantly differ between diploids (1157.5±169.8) and triploids (1265.8±100.9) ($t(16) = -.514$, $p = .614$) at the initial temperature of 25°C just prior to each temperature ramp (Table 4; Fig. 21). As temperatures began to increase, RMR of diploid oysters as modeled by the spline was consistently higher than that of triploids, but with the lower 95% CI of diploids frequently overlapping the upper 95% CI of triploids (Fig. 22 C). The temperatures at which T_{lower}, $RMR_{peak\ temp}$, and T_{upper} occurred did not differ between diploids and triploids (Table 3, Fig. 22 A,B). However, $RMR_{peak\ rate}$ of diploids was significantly higher than that of triploids as evidenced by non-overlapping confidence intervals (Table 3, Fig. 22 C). There was no significant difference in Q10 between diploids (1.6±.15) and triploids (1.44±.16) as RMR increased towards RMR_{peak} from 25-32°C ($t(10) = .427$, $p = .678$) (Table 4).

4.3.3 Behavioral endpoints

A two-way ANOVA revealed that there was a statistically significant effect of ploidy on closing frequency, with triploids having a higher proportion closed compared to diploids ($F_{(1,44)} = 5.018$, $p = .030$). There was also a significant effect of pre-/post-RMR_{peak} category on closing

frequency with oysters closing more frequently after surpassing $RMR_{peak\ temp}$ than before reaching $RMR_{peak\ temp}$ ($F_{(1,44)}$=10.340, p = .002). There was no significant interaction between ploidy and pre-/post-RMR category $F_{(1,44)}$ = 1.449, p = .235. (Table 5, Fig. 23).

There was no significant difference in the mean temperature at which diploid (43.5±0.3°C) and triploid (42.8±0.4°C) oysters reached CTM (Log-rank test: $\chi^2_{(1)}$ = .45, p = .2311). There was also no significant difference in the temperature at which diploid (44.4±.2°C) and triploid (44.3±.2°C) oysters reached PPD (Log-rank test: $\chi^2_{(1)}$ = .45, p = .5033) (Table 4, Fig. 24 A,B).

There were no significant effects of oyster mass, shell height, or condition index on CTM or PPD (p > .05). There was a significant effect of acclimation upweller ID on PPD (p = .0145). However, because equal numbers of diploid and triploid oysters were placed in each upweller, container effects did not affect the overall conclusions.

4.4 Discussion

Oysters are an important economic and ecological bivalve in coastal communities (Grabowski et al., 2012; Petrolia et al., 2022). Given that farmed oyster populations across the United States coasts are experiencing sudden mortality events and that some of these events appear to be disproportionately affecting triploids (Bodenstein et al., 2021; Callam et al., 2016; Guevelou et al., 2019; Wadsworth, Casas, et al., 2019), testing for physiological and behavioral differences between the ploidies during thermal stress may explain the difference in triploid and diploid mortality during these events.

4.4.1 Metabolic and behavioral patterns prior to metabolic depression

Resting metabolic rate typically shows a high degree of variability within and among species. The relative advantages and disadvantages of relatively high or low RMR are the subject of much discussion and research (Burford et al., 2014). For example, it has been hypothesized that individuals with a high RMR have greater fitness when environmental conditions are favorable, whereas individuals with a lower RMR are favored under unfavorable conditions such as a limited food supply (Burton et al., 2011). In our study, RMR was highly variable within ploidies, making it difficult to tease out differences between diploids and triploids as evidenced by the frequent overlap in confidence intervals. However, the degree of overlap was minimal as RMR increased towards its peak, with diploid RMR consistently higher than triploid RMR. The lower RMR in triploids is likely driven by inefficient gas exchange across the cell membrane in larger cells as theorized in embryonic triploid fish (Atkins & Benfey, 2008). However, this does not necessarily indicate an immediate disadvantage for triploids. A trend towards a lower RMR for triploids suggests that they require less energy to meet their basic metabolic needs and would be less susceptible to food limitation than diploids as temperatures rise to the point that metabolic depression is induced. Reduced susceptibility to food limitation based on a lower RMR has also been hypothesized for freshwater mussel species that differ in RMR (Haney et al. 2020). This advantage might be offset if triploids closed more frequently than diploids and thus spent less time feeding, but there was no difference in closure frequency between ploidies as temperatures rose towards $RMR_{peak\ temp}$. Similarly, the advantage could be offset if the magnitude of the increase in RMR with increasing temperature was greater for triploids, but this was not the case. We found no difference in Q10 between diploids and triploids as temperature rose towards $RMR_{peak\ temp}$. Finally, the advantage could be offset if triploids RMR continued rising past the temperature at which RMR began declining for diploids, but we found no difference between

$RMR_{peak\ temp}$ between diploids and triploids. The conclusion that triploids have an energetic advantage over diploids as temperatures rise towards $RMR_{peak\ temp}$ is further supported by recent scope for growth studies, which found that triploids obtained more surplus energy than diploids and thus had an energetic advantage at the temperature (28^{o}C) and salinity (15ppt) tested (Bodenstein et al. 2023).

4.4.2 Metabolic and behavioral patterns after metabolic depression

Valve closure, indicative of metabolic depression, is a common bivalve response to thermal stress (Anestis et al., 2007; Philipp & Abele, 2010; Sokolova et al., 2012). During closure events, oxygen in ambient waters is no longer available until they open again. By temporarily switching to periods of anaerobic respiration, aquatic invertebrates suppress their metabolism and are able to reduce the cellular demand for energy induced by temperature via a reduction in ATP turnover and metabolic substrates (Boutilier & St-Pierre, 2000; Pörtner, 2012; Ritchie, 2018; Vajedsamiei et al., 2021). In our study, frequency of closure events increased significantly for triploid oysters after $RMR_{peak\ temp}$. There was also a trend of increasing closure frequency for diploids after $RMR_{peak\ temp}$, but this difference was not significant.

Although increases in valve closure are a common response of bivalves to stressful temperatures, there are tradeoffs to this behavior. Reduced ATP turnover also reduces ATP available for protein production, which may have negatively impacted the supply of key thermal stress related proteins such as *HSP70*, a protein used to repair protein damage from stress caused by temperature, pollution, etc. (Feige et al., 1996; Meng et al., 2018; Sokolova et al., 2000). Anaerobic respiration in bivalves leads to the accumulation of toxic metabolic byproducts such as pyruvate, lactate, octopine, succinate, alanine, acetate, propionate, and CO_2, which can be flushed out of oyster tissues quickly upon valve opening but may have detrimental effects during

prolonged exposure (de Zwaan & Wijsman, 1976). Closures also reduce the amount of food bivalves accumulate and retain due to reduction in filtering activity (Vajedsamiei et al., 2021). As a result, increased closures during prolonged or dramatic acute thermal stress at critically high temperature exposure may prevent oysters from obtaining the energy they need to upkeep thermal stress protein production, possibly contributing to mortality events recorded during late spring and early summer (Wadsworth, Casas, et al., 2019). However, experiencing moderate thermal fluctuations around metabolic depression temperatures is not necessarily a detriment to growth. Cyclical thermal fluctuation-mediated metabolic suppression and recovery in *Mytilus edulis* may promote growth by increasing feeding rates while metabolism is still being actively suppressed (Vajedsamiei et al., 2021).

Metabolic depression via a reduction in aerobic respiration (i.e. a reduction in RMR of open oysters) and/or increasing reliance on anaerobic respiration (i.e. an increase in frequency of valve closure) are thought to be adaptations to reduce thermal stress and delay the lethal effects of temperature (Anestis et al., 2007; Philipp & Abele, 2010; Sokolova et al., 2012). In the case of diploid and triploid oysters, CTM and PPD did not occur immediately after $RMR_{peak\ temp}$. In oysters, CTM was delayed until temperatures had increased by a further 8-10^{o}C higher. The fact that CTM was delayed, rather than occurring immediately after $RMR_{peak\ temp}$ supports the hypothesis that metabolic depression after $RMR_{peak\ temp}$ is a mechanism for coping with thermal stress. However, although triploids closed more frequently than diploids above $RMR_{peak\ temp}$, this did not give them an additional advantage. There was no difference in CTM or PPD between ploidies.

Although PPD generally occurred only ~1^{o}C higher than CTM, follow-up experiments indicated the two endpoints were distinct, and provided further support that metabolic depression

is a coping mechanism. In these follow-up trials, oysters were gradually brought down to 25ºC after reaching $RMR_{peak\ temp}$, CTM, or PPD and allowed to recover for two weeks. Diploids and triploids all exhibited 100% survival after recovery from $RMR_{peak\ temp}$, and CTM. However, they exhibited 0% survival after "recovery" from PPD (Boyd, unpublished data). These results support the validity of CTM as a functional death endpoint from which recovery is possible, whereas PPD represented true physiological death.

A critique of acute thermal ramp assays for aquatic invertebrates is that temperatures where CTM is observed in the laboratory are rarely observed in natural systems (Lutterschmidt & Hutchison, 1997). However, desiccation practices used in oyster aquaculture can create situations where oyster cages experience temperatures approaching CTM. In 2021, surface water at Grand Bay Oyster Park, AL experienced seasonal fluctuations with surface water temperatures in late summer exceeding the thresholds beyond which oysters exhibit metabolic depression (~34°C) and increased closure frequency. Field data from HOBO temperature loggers on oyster cages lifted out of the water during desiccation treatments revealed that desiccating oysters experienced temperatures at a minimum 4°C higher than air temperatures (Boyd, unpublished data). Most gear used in oyster aquaculture is black to reduce equipment degradation caused by UV-exposure during the desiccation phase. While this practice improves the life of the gear, it may inadvertently increase the temperatures oysters are exposed to. Overnight desiccation also results in the cages experiencing wide temperature swings, in one instance going from an overnight temperature of 23.5°C to a mid-afternoon temperature of 41.5°C within the span of 12 hours at a rate of approximately 3°C/h (Boyd, unpublished data). This demonstrates that oysters are experiencing these intense temperature swings multiple times a month depending on the frequency and time of desiccation periods at each farm. The chronic impacts of these frequent

extreme temperature changes on closures and metabolic activity may be a contributing factor to overall oyster mortality during normal farming practices seen in field studies (Bodenstein et al., 2021; Vajedsamiei et al., 2021).

Given that the temperatures at which oysters experienced RMR_{peak}, CTM, or PPD did not significantly different between diploid and triploid oysters, acute thermal stress alone is likely not driving differential mortality between ploidies. However, increased triploid closures post-$RMR_{peak\ temp}$ may cause chronic effects during extended periods of high temperature that were not tested in this study. Studies testing for differential effects of chronic thermal stress between diploids and triploids would be the next logical step in assessing the importance of temperature in explaining higher triploid mortalities compared to their diploid counterparts.

4.5 Tables

Table 3. Smoothing spline predicted values for diploid and triploid oysters.

Endpoint	**Diploid**		**Triploid**		
	Mean	**95% CI**	**Mean**	**95% CI**	Sig.
$RMR_{peak\ activity}$ (mgO_2/kgDTW/h)	1880.5	1754.5-2006.5	1599.8	1486.4-1713.2	*
$RMR_{peak\ temp}$ (°C)	33.2	32.1-34.25	34.4	31.4-37.4	
T_{lower} (°C)	30.2	27.6-32.7	29.3	27.0-31.6	
T_{upper} (°C)	35.2	34.6-35.9	359	35.2-36.6	
$T_{breadth}$ (°C)	5.1	2.3-7.9	6.6	4.1-9.1	

Table 4. Multiple metabolic and behavioral endpoints derived from raw data, and functional (CTM) and physiological (PPD) endpoints derived from Kaplan-Meier survival analysis. No significant differences were found between diploid and triploid oysters for any endpoint.

Endpoint	**Diploid**		**Triploid**		
	Mean	**95% CI**	**Mean**	**95% CI**	Sig.
RMR at 25°C	1157.5	824.7-1490.2	1294.9	1101.0-1488.7	
Q_{10} before $RMR_{peak\ temp}$	1.57	0.15	1.44	0.16	
% Closures before $RMR_{peak\ temp}$	20.0%	4.8-35.2%	29.4%	8.7-50.1%	
% Closures after $RMR_{peak\ temp}$	38.3%	21.7-55.0%	69.7%	51.3-88.1%	*
CTM (°C)	43.5	42.8-44.2	42.8	42.0-43.6	
PPD (°C)	44.4	44.0-45.0	44.3	44.0-45.0	

Table 5. Results of Tukey's post-hoc test pairwise comparisons of a two-way ANOVA on proportion closure measurements between ploidy classes (diploid, triploid) and temperature classes (29-33°C; 34-38°C). Temperature classes were defined as a 5°C interval before or after $RMR_{peak\ rate}$. Significant differences are indicated by an asterisk and the ploidy with the higher proportion of closures is bolded.

Pairwise Comparison	**Diff of Means**	**p**	**q**	**P**	**sig.**
Triploid vs Diploid	0.204	2	3.168	.030	*
34-38°C vs 29-33°C	0.293	2	4.454	.003	*

4.6 Figures

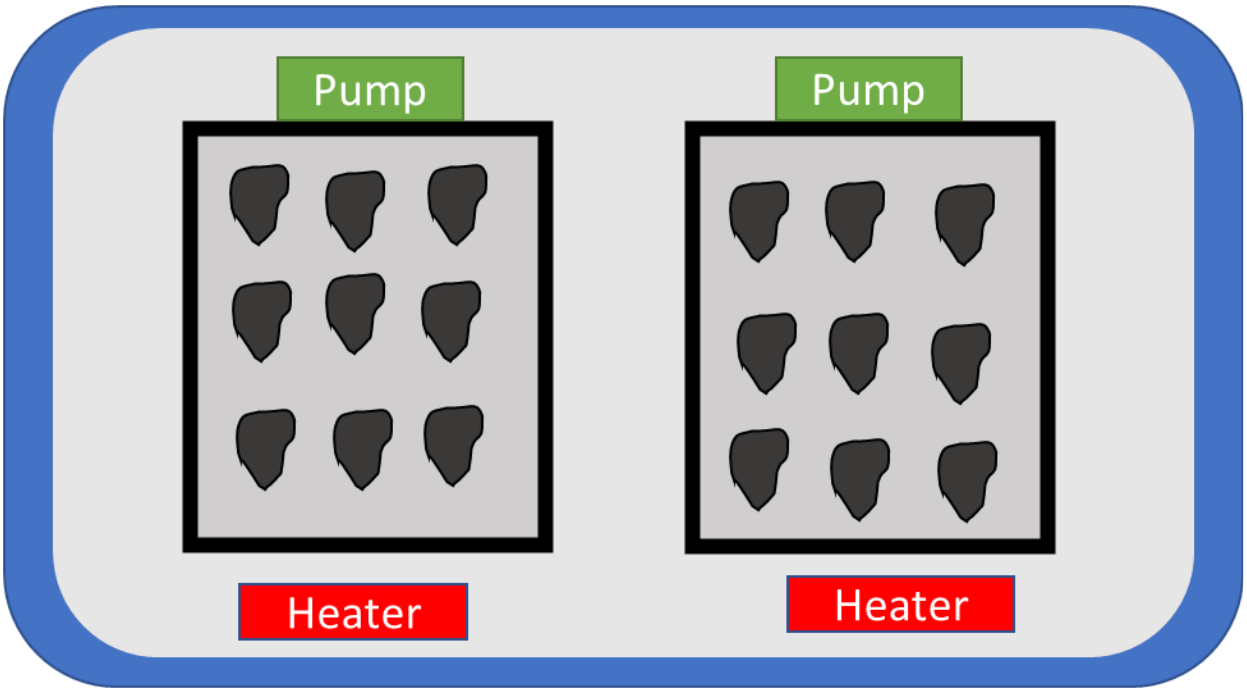

Figure 16. Schematic of oyster acclimation upwellers.

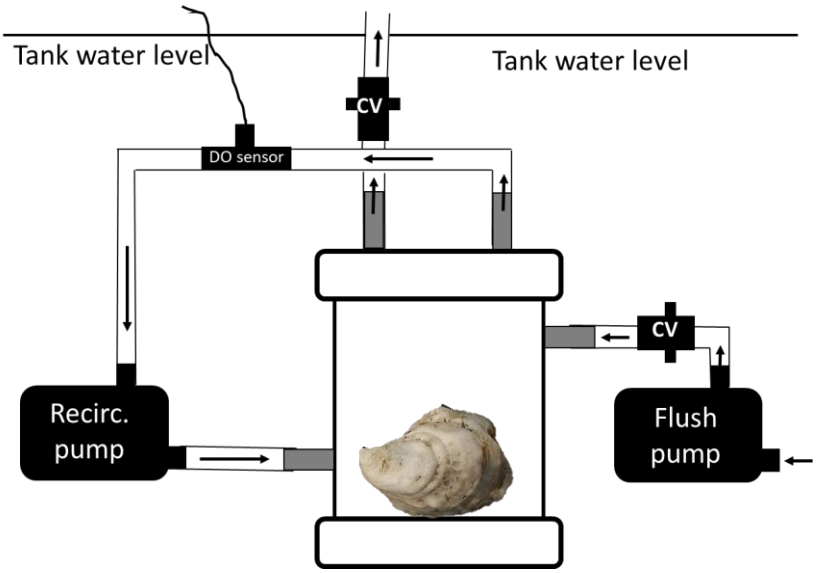

Figure 17. A schematic of the respirometry system components associated with each respirometry chamber. Modified from Haney et al. 2020.

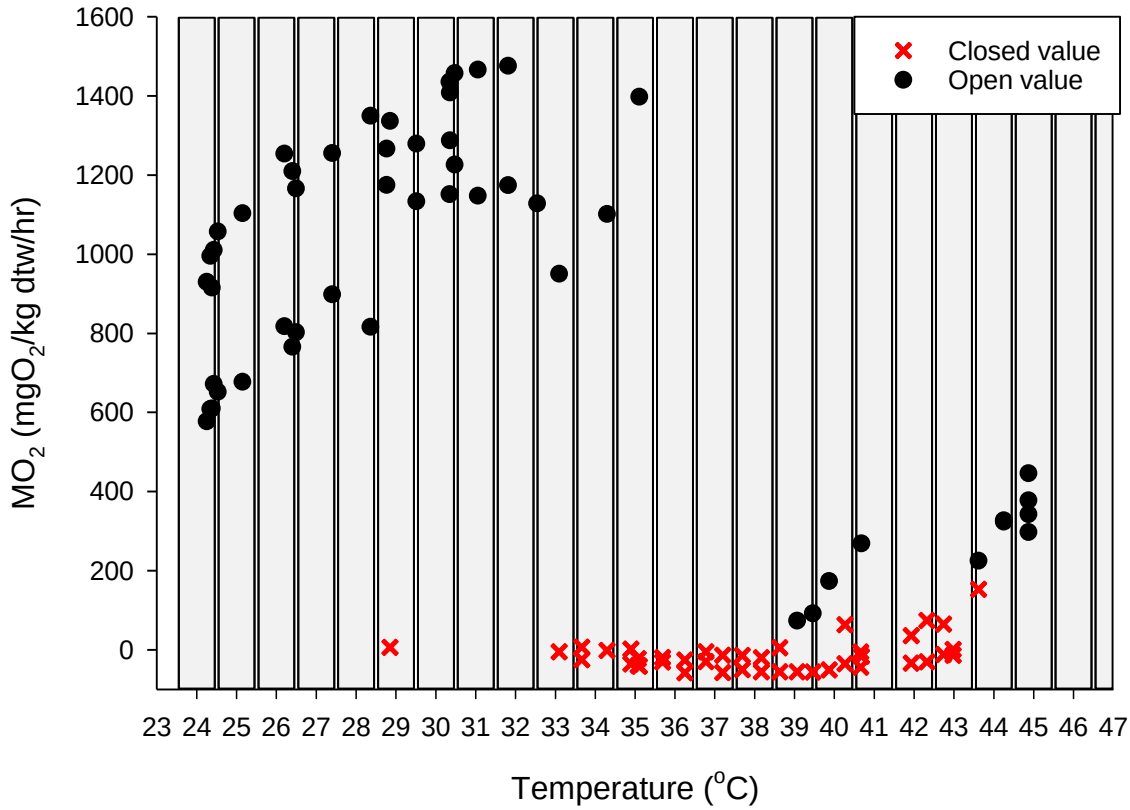

Figure 18. Example of evaluation of closures for an individual oyster. Black dots indicate respiration estimates indicating the oyster was open whereas red dots indicate an estimate as a closure. Grey bars denote integer temperature bins that were assigned to each measurement value for closure analysis.

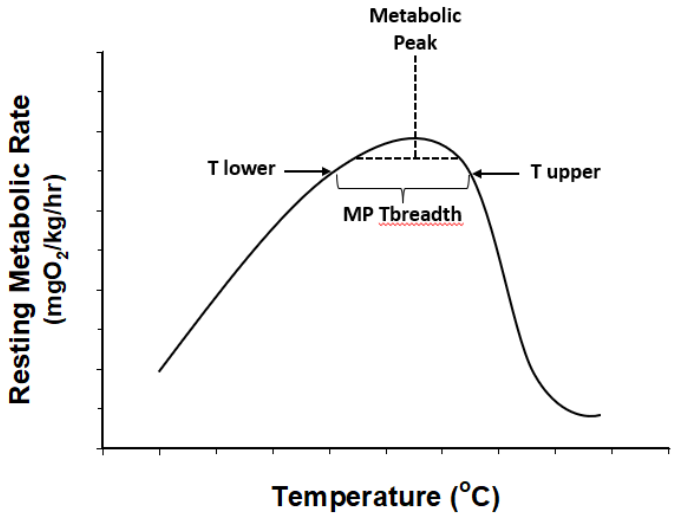

Figure 19. Visualization of thermal endpoints as estimated from the smoothing spline model, where $RMR_{peak\ rate}$ represents the maximum observed metabolic rate, $RMR_{peak\ temp}$ represents the temperature at which $RMR_{peak\ rate}$ is observed, T_{lower} and T_{upper} represent the lower and upper temperature bounds within which RMR is within 90% of the $RMR_{peak\ rate}$, respectively, and RMR $T_{breadth}$ represents the difference between T_{lower} and T_{upper}.

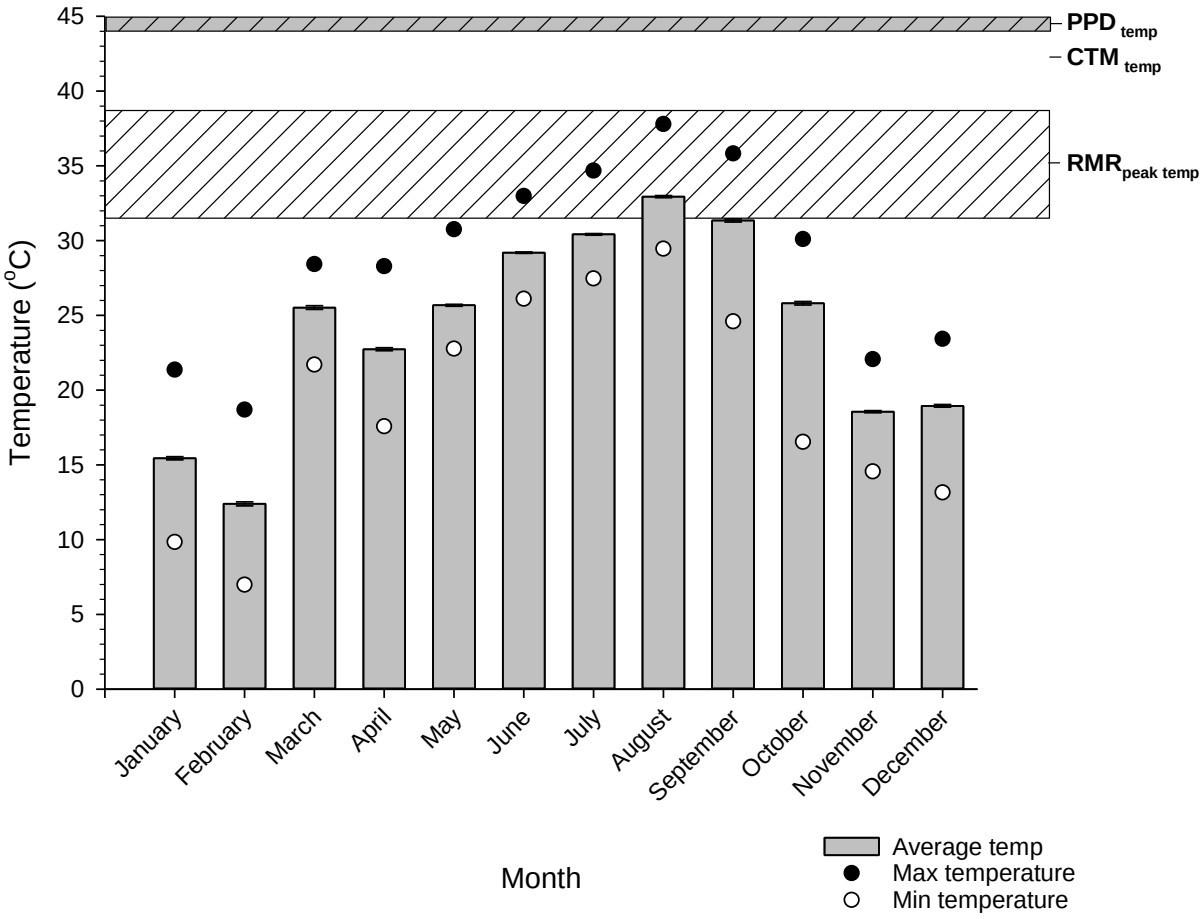

Figure 20. Average, maximum, and minimum water temperatures recorded each month in 2021 by HOBO loggers deployed ~20 cm below the surface at the Grand Bay Oyster Park in Bayou La Batre, AL. Black dots denote maximum recorded temperatures and white dots denote minimum temperatures for that month. The white striped box denotes $RMR_{peak\ temp}$ range (32.1-37.4°C), the medium grey striped box shows CTM temp range (42.0-44.2°C), and the dark grey striped box shows PPD_{temp} range (44.0-45.0°C) as identified by lower and upper 95% C.I. for diploid and triploids.

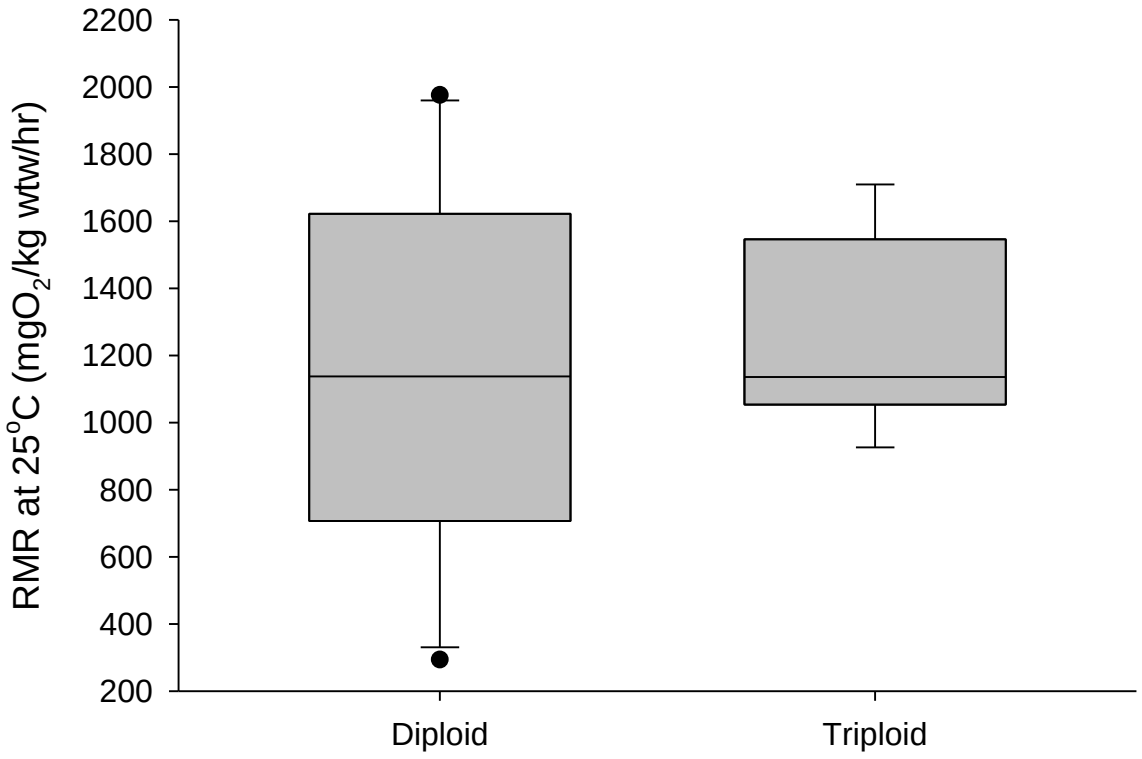

Figure 21. Boxplots of resting metabolic rate (RMR) of diploid and triploid oysters measured at the initial temperature of 25°C, just prior to initiating a thermal ramp. The solid horizontal line depicts the median, the grey box represents the interquartile range of Q1-Q3, the whiskers depict Q4 and the upper and lower dots depict the outliers. Diploid n = 10 and triploid n = 8

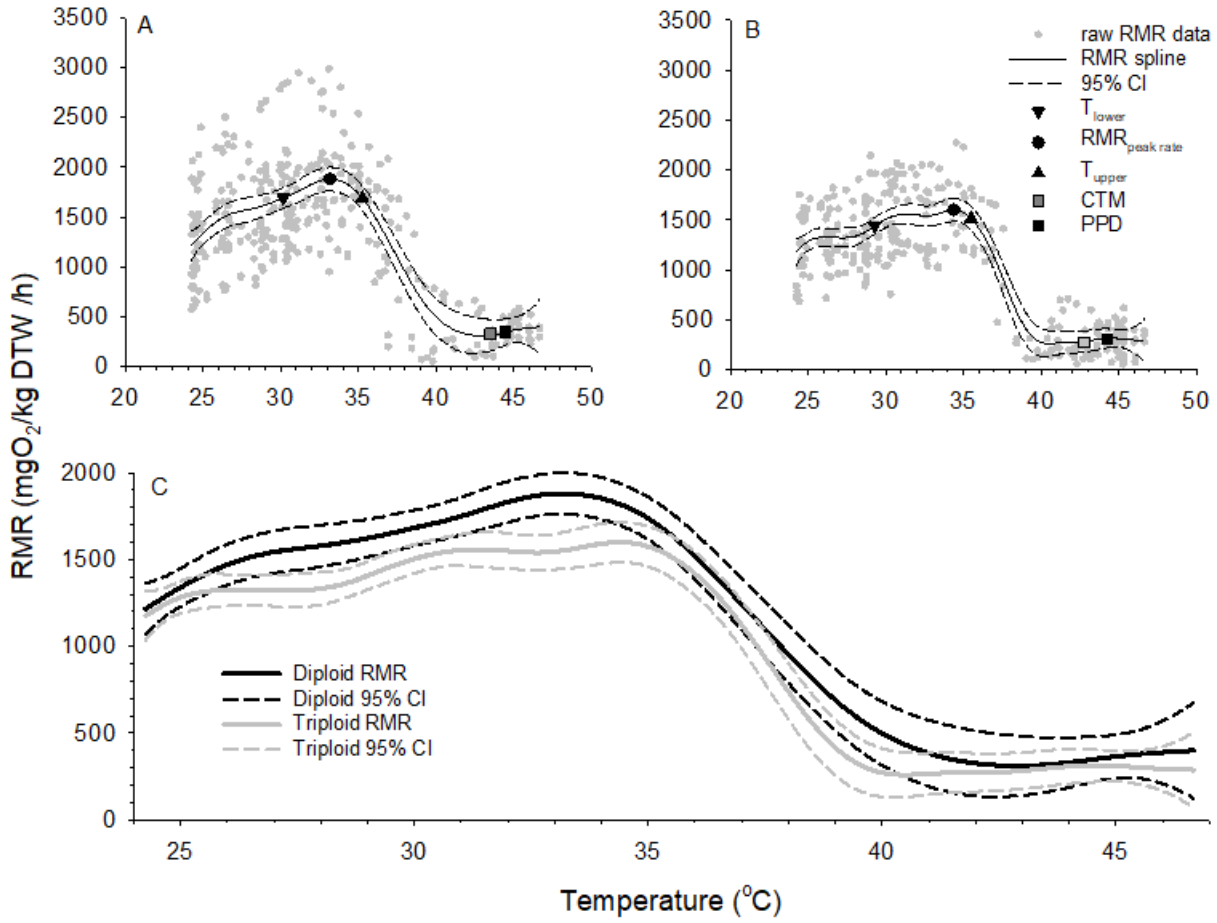

Figure 22. Effect of temperatures on resting metabolic rate (RMR) of A) diploid and B) triploid oysters where the grey dots represent the raw RMR data from individual oysters and the solid and dotted lines represent the smoothing spline and 95% CI respectively. Symbols show the temperatures at which multiple endpoints fall in relation to respiration. C) Overlay of diploid and triploid RMR splines shows a consistently higher diploid RMR spline, but frequent overlap of 95% CI intervals between diploids and triploids.

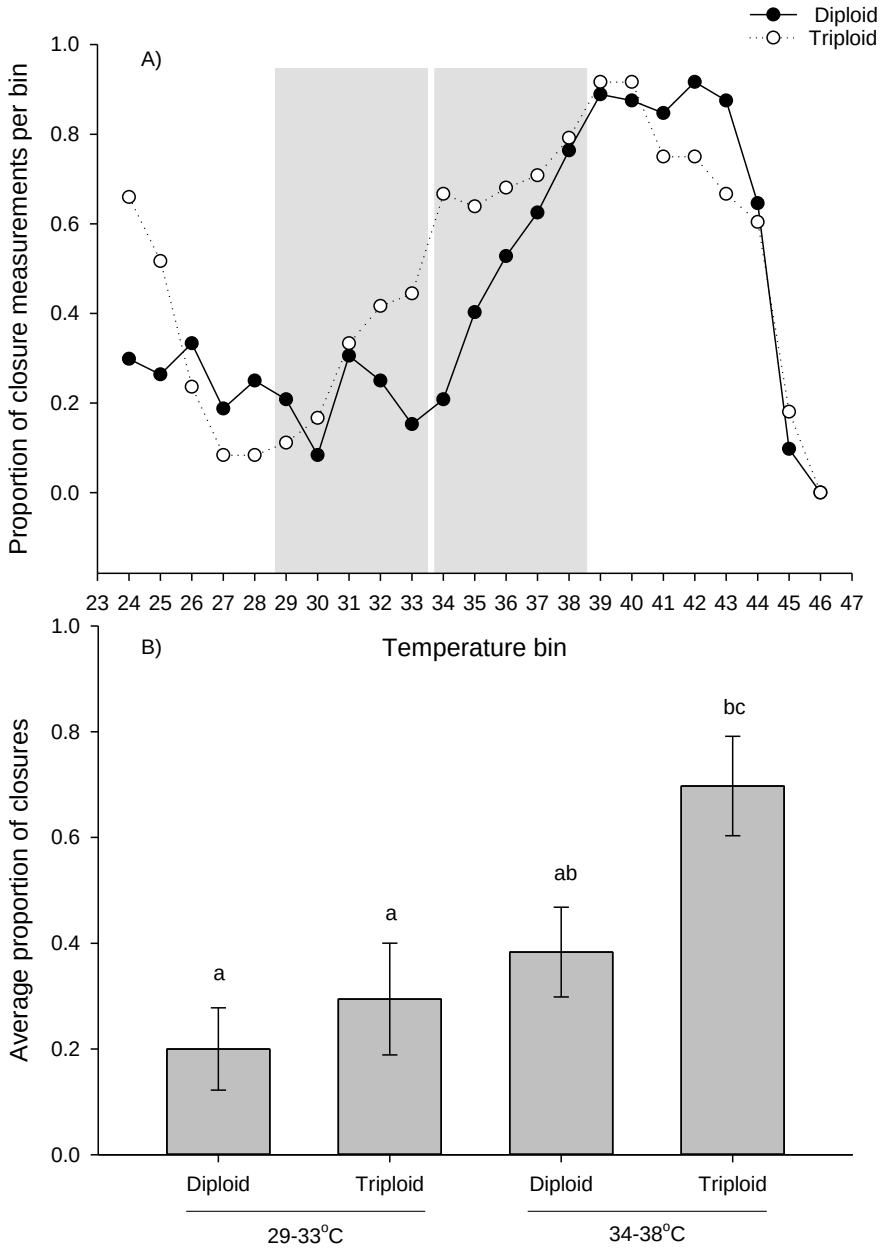

Figure 23. Proportion of measurements identified as closures in each binned temperature. (A) Average proportion of diploid and triploid measurements closed and (B) average proportion of closures of binned temperatures marked in grey before $RMR_{peak\ temp}$ (29-33°C) and after $RMR_{peak\ temp}$ (34-38°C). Significant differences in closures are denoted by letters.

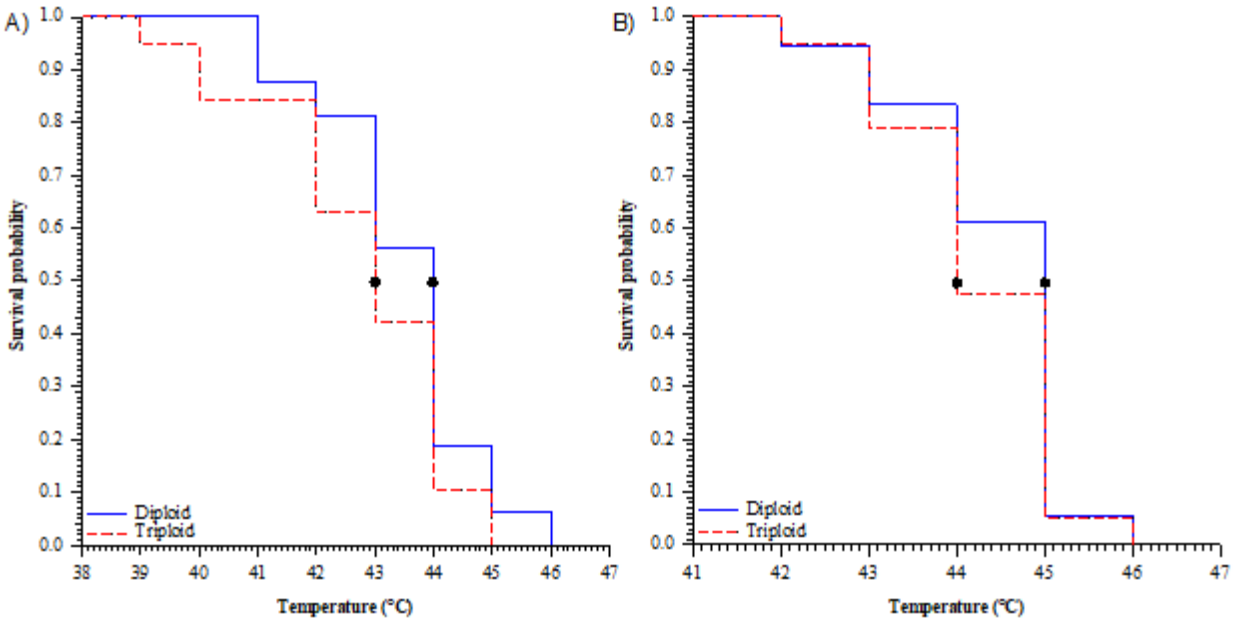

Figure 24. Kaplan Meier survival curves showing the A) probability of exhibiting CTM by temperature (Log-rank test: $\chi^2_{(1)} = 14.34$, $p = .2311$) and B) probability of exhibiting PPD by temperature (Log-rank test: $\chi^2_{(1)} = 0.45$, $p = .5033$). Median values of CTM and PPD where survival probability is 50% are marked with a black circle on each line.

4.7 References

Abbe, G. R., & Albright, B. W. (2003). An improvement to the determination of meat condition index for the eastern oyster Crassostrea virginica (Gmelin 1791). *Journal of Shellfish Research*, *22*(3), 747–752.

Anestis, A., Lazou, A., Pörtner, H. O., & Michaelidis, B. (2007). Behavioral, metabolic, and molecular stress responses of marine bivalve Mytilus galloprovincialis during long-term acclimation at increasing ambient temperature. *American Journal of Physiology. Regulatory, Integrative and Comparative Physiology*, *293*(2), R911-921. https://doi.org/10.1152/ajpregu.00124.2007

ARCOS. (2023, March 7). *Data Range Checking Criteria*. Dauphin Island Sea Lab. https://www.disl.edu/arcos/datarange/

Atkins, M. E., & Benfey, T. J. (2008). Effect of acclimation temperature on routine metabolic rate in triploid salmonids. *Comparative Biochemistry and Physiology Part A: Molecular & Integrative Physiology*, *149*(2), 157–161. https://doi.org/10.1016/j.cbpa.2007.11.004

Berry, L. N., & Helwig, N. E. (2021). Cross-Validation, Information Theory, or Maximum Likelihood? A Comparison of Tuning Methods for Penalized Splines. *Stats*, *4*(3), Article 3. https://doi.org/10.3390/stats4030042

Bible, J. M., & Sanford, E. (2016). Local adaptation in an estuarine foundation species: Implications for restoration. *Biological Conservation*, *193*, 95–102. https://doi.org/10.1016/j.biocon.2015.11.015

Bodenstein, S., Casas, S. M., Tiersch, T. R., & La Peyre, J. F. (2023). Energetic budget of diploid and triploid eastern oysters during a summer die-off. *Frontiers in Marine Science*, *10*. https://www.frontiersin.org/articles/10.3389/fmars.2023.1194296

Bodenstein, S., Walton, W., & Steury, T. (2021). Effect of farming practices on growth and mortality rates in triploid and diploid eastern oysters Crassostrea virginica. *Aquaculture Environment Interactions*, *13*, 33–40. https://doi.org/10.3354/aei00387

Boutilier, R. G., & St-Pierre, J. (2000). Surviving hypoxia without really dying. *Comparative Biochemistry and Physiology. Part A, Molecular & Integrative Physiology*, *126*(4), 481–490. https://doi.org/10.1016/s1095-6433(00)00234-8

Burford, M. O., Scarpa, J., Cook, B. J., & Hare, M. P. (2014). Local adaptation of a marine invertebrate with a high dispersal potential: Evidence from a reciprocal transplant experiment of the eastern oyster Crassostrea virginica. *Marine Ecology Progress Series*, *505*, 161–175. https://doi.org/10.3354/meps10796

Burge, C. A., Judah, L. R., Conquest, L. L., Griffin, F. J., Cheney, D. P., Suhrbier, A., Vadopalas, B., Olin, P. G., Renault, T., & Friedman, C. S. (2007). Summer seed mortality of the pacific oyster, *Crassostrea gigas* Thunberg grown in Tomales bay, California,

USA: the influence of oyster stock, planting time, pathogens, and environmental stressors. *Journal of Shellfish Research*, *26*(1), 163–172. https://doi.org/10.2983/0730-8000(2007)26[163:SSMOTP]2.0.CO;2

Burton, T., Killen, S. S., Armstrong, J. D., & Metcalfe, N. B. (2011). What causes intraspecific variation in resting metabolic rate and what are its ecological consequences? *Proceedings of the Royal Society B: Biological Sciences*, *278*(1724), 3465–3473. https://doi.org/10.1098/rspb.2011.1778

Callam, B. R., Allen, S. K., & Frank-Lawale, A. (2016). Genetic and environmental influence on triploid Crassostrea virginica grown in Chesapeake Bay: Growth. *Aquaculture*, *452*, 97–106. https://doi.org/10.1016/j.aquaculture.2015.10.027

Canty, A., & Ripley, B. (2021). *Boot: Bootstrap R (S-Plus) Functions. R package, version 1.3–28. 2021*.

Chabot, D., Zhang, Y., & Farrell, A. P. (2021). Valid oxygen uptake measurements: Using high r2 values with good intentions can bias upward the determination of standard metabolic rate. *Journal of Fish Biology*, *98*(5), 1206–1216. https://doi.org/10.1111/jfb.14650

Clements, J. C., Comeau, L. A., Carver, C. E., Mayrand, É., Plante, S., & Mallet, A. L. (2018). Short-term exposure to elevated pCO2 does not affect the valve gaping response of adult eastern oysters, Crassostrea virginica, to acute heat shock under an ad libitum feeding regime. *Journal of Experimental Marine Biology and Ecology*, *506*, 9–17. https://doi.org/10.1016/j.jembe.2018.05.005

de Zwaan, A., & Wijsman, T. C. M. (1976). Anaerobic metabolism in bivalvia (Mollusca) Characteristics of anaerobic metabolism. *Comparative Biochemistry and Physiology Part B: Comparative Biochemistry*, *54*(3), 313–323. https://doi.org/10.1016/0305-0491(76)90247-9

Efron, B., & Tibshirani, R. (1993). *An introduction to the bootstrap*. Chapman & Hall.

Feige, U., Morimoto, R. I., Yahara, I., & Polla, B. S. (Eds.). (1996). *Stress-Inducible Cellular Responses*. Birkhauser.

Galbraith, H. S., Blakeslee, C. J., & Lellis, W. A. (2012). Recent thermal history influences thermal tolerance in freshwater mussel species (Bivalvia:Unionoida). *Freshwater Science*, *31*(1), 83–92. https://doi.org/10.1899/11-025.1

Gérard, A., Ledu, C., Phelipot, P., & Naciri-Graven, Y. (1999). *The induction of MI and MII triploids in the Pacific oyster Crassostrea gigas with 6-DMAP or CB.* https://doi.org/10.1016/S0044-8486(99)00032-0

Grabowski, J. H., Brumbaugh, R. D., Conrad, R. F., Keeler, A. G., Opaluch, J. J., Peterson, C. H., Piehler, M. F., Powers, S. P., & Smyth, A. R. (2012). Economic Valuation of Ecosystem Services Provided by Oyster Reefs. *BioScience*, *62*(10), 900–909. https://doi.org/10.1525/bio.2012.62.10.10

Guevelou, E., Carnegie, R., Moss, J. A., Hudson, K., Reece, K., Rybovich, M., & Allen, S. (2019). Tracking Triploid Mortalities Of Eastern Oysters Crassostrea virginica In The Virginia Portion Of The Chesapeake Bay. *Journal of Shellfish Research*, *38*(1), 101–113. https://doi.org/ 10.2983/035.038.0110

Hui, T. Y., Dong, Y., Han, G., Lau, S. L. Y., Cheng, M. C. F., Meepoka, C., Ganmanee, M., & Williams, G. A. (2020). Timing Metabolic Depression: Predicting Thermal Stress in Extreme Intertidal Environments. *The American Naturalist*, *196*(4), 501–511. https://doi.org/10.1086/710339

Lampert, W. 1984. The measurement of respiration. In A Manual on methods for the assessment of secondary productivity in fresh waters. Edited by J. Downing and F. Rigler. Blackwell Scientific Pubs, Oxford. pp. 413–468.

Lampert, W. (1989). The Adaptive Significance of Diel Vertical Migration of Zooplankton. *Functional Ecology*, *3*(1), 21–27. https://doi.org/10.2307/2389671

Lutterschmidt, W. I., & Hutchison, V. H. (1997). The critical thermal maximum: Data to support the onset of spasms as the definitive end point. *Canadian Journal of Zoology*, *75*(10), 1553–1560. https://doi.org/10.1139/z97-782

Marshall, D. A., Casas, S. M., Walton, W. C., Rikard, F. S., Palmer, T. A., Breaux, N., La Peyre, M. K., Beseres Pollack, J., Kelly, M., & La Peyre, J. F. (2021). Divergence in salinity tolerance of northern Gulf of Mexico eastern oysters under field and laboratory exposure. *Conservation Physiology*, *9*(1), coab065. https://doi.org/10.1093/conphys/coab065

Matt, J. L., & Allen, S. K. (2021). A classification system for gonad development in triploid Crassostrea virginica. *Aquaculture*, *532*, 735994. https://doi.org/10.1016/j.aquaculture.2020.735994

Meng, J., Wang, T., Li, L., & Zhang, G. (2018). Inducible variation in anaerobic energy metabolism reflects hypoxia tolerance across the intertidal and subtidal distribution of the Pacific oyster (Crassostrea gigas). *Marine Environmental Research*, *138*, 135–143. https://doi.org/10.1016/j.marenvres.2018.04.002

Miller, N. A., & Stillman, J. H. (2012). Physiological Optima and Critical Limits. *The Nature Education*. https://www.nature.com/scitable/knowledge/library/physiological-optima-and-critical-limits-45749376/

NOAA. (2020). *NOAA Fisheries Landings Database*. Retrieved January 25, 2022, from https://www.fisheries.noaa.gov/foss/f?p=215:200:3510234029521::NO:RP::

Petrolia, D. R., Walton, W. C., & Cebrian, J. (2022). Oyster Economics: Simulated Costs, Market Returns, and Nonmarket Ecosystem Benefits of Harvested and Nonharvested Reefs, Off-Bottom Aquaculture, and Living Shorelines. *Marine Resource Economics*, *37*(3), 325–347. https://doi.org/10.1086/719969

Philipp, E. E. R., & Abele, D. (2010). Masters of longevity: Lessons from long-lived bivalves--a mini-review. *Gerontology*, *56*(1), 55–65. https://doi.org/10.1159/000221004

Pörtner, H.-O. (2012). Integrating climate-related stressor effects on marine organisms: Unifying principles linking molecule to ecosystem-level changes. *Marine Ecology Progress Series*, *470*, 273–290. https://doi.org/10.3354/meps10123

R Core team. (2021). *R: A language and environment for statistical computing. R Foundation for Statistical Computing, Vienna, Austria. URL https://www.R-project.org/.* https://www.R-project.org/.

Rikard, S. (2023). [Personal communication].

Ritchie, M. E. (2018). Reaction and diffusion thermodynamics explain optimal temperatures of biochemical reactions. *Scientific Reports*, *8*(1), Article 1. https://doi.org/10.1038/s41598-018-28833-9

SAS (9.4). (2013). [The SAS system for Windows]. SAS Institute Inc.

Sokolova, I. M., Bock, C., & Pörtner, H.-O. (2000). Resistance to freshwater exposure in White Sea Littorina spp. I: Anaerobic metabolism and energetics. *Journal of Comparative Physiology B*, *170*(2), 91–103. https://doi.org/10.1007/s003600050264

Sokolova, I. M., Frederich, M., Bagwe, R., Lannig, G., & Sukhotin, A. A. (2012). Energy homeostasis as an integrative tool for assessing limits of environmental stress tolerance in aquatic invertebrates. *Marine Environmental Research*, *79*, 1–15. https://doi.org/10.1016/j.marenvres.2012.04.003

Supan, J. (2002). *Extensive Culture of Crassostrea virginica in the Gulf of Mexico Region*.

Supan, J. (2014). *High-Density Rearing of Oyster Larvae in Flow-Through Systems*. 6.

Vajedsamiei, J., Melzner, F., Raatz, M., Morón Lugo, S. C., & Pansch, C. (2021). Cyclic thermal fluctuations can be burden or relief for an ectotherm depending on fluctuations' average and amplitude. *Functional Ecology*, *35*(11), 2483–2496. https://doi.org/10.1111/1365-2435.13889

Verberk, W. C. E. P., Bartolini, F., Marshall, D. J., Pörtner, H.-O., Terblanche, J. S., White, C. R., & Giomi, F. (2016). Can respiratory physiology predict thermal niches? *Annals of the New York Academy of Sciences*, *1365*(1), 73–88. https://doi.org/10.1111/nyas.12876

Wadsworth, P., Casas, S., La Peyre, J., & Walton, W. (2019). Elevated mortalities of triploid eastern oysters cultured off-bottom in northern Gulf of Mexico. *Aquaculture*, *505*, 363–373. https://doi.org/10.1016/j.aquaculture.2019.02.068

Wadsworth, P., Wilson, A. E., & Walton, W. C. (2019). A meta-analysis of growth rate in diploid and triploid oysters. *Aquaculture*, *499*, 9–16. https://doi.org/10.1016/j.aquaculture.2018.09.018

Walton, W. C., Davis, J. E., & Supan, J. E. (2013). *Off-Bottom Culture of Oysters in the Gulf of Mexico*. 6.

CHAPTER 5
DIFFERENCES IN TOLERANCE AND RESPONSES TO THERMAL STRESS IN DIPLOID AND TRIPLOID EASTERN OYSTERS (*Crassostrea virginica*) FROM THE NORTHERN GULF OF MEXICO IN HYPOSALINE CONDITIONS

5.1 Introduction

Eastern oysters have important cultural, ecological, and economic significance for coastal communities from the north Atlantic to the Gulf of Mexico. Recent collapses of wild oyster populations have driven a need for increased production of farmed oysters to meet market demand (Camp et al., 2015; Walton et al., 2013). As a result, oyster aquaculture has been expanding in the northern Gulf of Mexico (nGOM), especially in coastal Alabama (Walton et al., 2013). Intensive aquaculture of oysters, particularly for the half-shell market, has increased the demand for hatchery-raised triploids (Walton et al., 2012, 2013). Triploid oysters are commercially produced by hatcheries in two ways: 1) chemical induction by treating fertilized diploid oyster eggs with 6-dimethyl-aminopurine (6-DMAP) or cytochalasin B (CB) to retain either the first or second polar body and 2) by fertilizing diploid eggs with tetraploid sperm (Allen & Downing, 1986). Chemical induction is less effective at creating triploids than the fertilization method because of its higher rate of aneuploidy, reversion to diploids, and low survival rate (Gérard et al., 1999). Chemical induction also poses a health risk to hatchery workers (Guo, 1994). Because of this, chemical induction has been largely phased out in favor of the fertilization method.

Availability of tetraploids is one of the main limitations of the fertilization method for triploid production. Creation of tetraploids requires first identifying a previously produced triploid female that has generated viable eggs (Allen & Downing, 1986). Although most triploid females have malformed gonads, a small number (generally less than <15%) will produce viable

eggs (Matt & Allen, 2021). Tetraploids are created by fertilizing these triploid eggs with diploid sperm and then using chemical induction to retain either the first or second polar body (Guo, 1994). After line establishment, tetraploid lines are kept within reproductive age by breeding individuals within the line to maintain genetic lineage. However, this method of continuing tetraploid lines results in a high risk of risk of inbreeding due to the difficulty in injecting new genetics within the lines.

The use of hatchery-produced triploid oysters in aquaculture has been widely accepted by oyster farmers and restaurants because of their fast growth and seasonal quality consistency resulting from their low investment in reproduction. However, they may also have some disadvantages. Soon after introduction into nGOM aquaculture, triploid oysters were anecdotally reported to have higher mortality rates than diploids in one growing season with little indication of a primary cause in some cases (Wadsworth et al., 2019). Recent studies on polyploid oysters have conflicting conclusions on whether diploid or triploid oysters are more tolerant to environmental stressors including temperature and salinity (Bodenstein et al., 2021; Bodenstein, Callam, et al., 2023; Bodenstein, Casas, et al., 2023; Callam et al., 2016; Casas et al., 2024; Coxe et al., 2023; Dégremont et al., 2012; Wadsworth et al., 2019), although it has been observed that triploids are more susceptible to prolonged periods of desiccation compared to diploids (48 hrs) (Bodenstein et al., 2021). Triploid *C. virginica* lost their growth advantage in low salinity environments, moderate salinity resulted in equal growth between diploid and triploids, and high salinity gave triploids the greatest advantage over diploid oysters (Callam et al., 2016). However, in laboratory trials, diploid oysters were shown to be more susceptible to prolonged low salinity at high temperatures, with significantly higher mortalities starting as early as day 5 when at 33.3°C and 4ppt simultaneously (Marshall, Coxe, et al., 2021), but how that compares to triploid

performance has not yet been published. At elevated temperatures (37.8°C) mortalities in diploids occurred almost immediately after the target salinity (4ppt) was reached (Marshall, Coxe, et al., 2021).

Estuaries are well known for rapid salinity shifts due to tides and freshwater inflows, as well as for long-term shifts in salinity over the course of the year (Wadsworth et al., 2019). In Mobile Bay, AL located in the nGOM, water temperature can exceed 30°C and salinities can shift from 28ppt to <1ppt (Wadsworth et al., 2019). Individual sites along the nGOM coast can vary greatly from each other in terms of normal salinity regimes. Salinity-regime categories are subjective across the coastal United States but, for Louisiana, Mississippi, Alabama, and Florida, historical regimes are typically classified as follows: low: 0-10ppt; moderate:15-20ppt; high: >20ppt (King, unpublished data). The Mississippi Sound is typically classified as moderate salinity with lower salinities in the winter (typically 0-10ppt) and higher salinities in the summer (15-30ppt) (HOBO logger data). This area is also prone to rapidly changing salinities based on tidal fluctuations and input from Mobile Bay (Eleuterius, 1976). Oysters can tolerate salinities from 5 to 40ppt but their optimal salinity range is between 14-28ppt (Galtsoff, 1965) and local adaptations can shift an oyster population's salinity preference (Bible & Sanford, 2016).

Salinity affects many physiological processes in bivalves, particularly in the gill tissue. Marine bivalves acclimated to low and high salinities had their gill tissues excised and placed in different salinities from acclimation. Gills exhibited an initial inhibition of ciliary activity followed by recovery (Winkle, 1972). Ciliary activity in general was lower at low salinities compared to high salinities and the greater the difference between acclimation salinity and test salinity, the less likely the gill tissue was going to recover, possibly due to a reduction in activity caused by reduced levels of calcium and magnesium in the water. While the oxygen

consumption of the excised gill tissue was recorded, this method is now considered outdated and does not reflect the energetic demand for whole oysters (Lavaud et al., 2021). The whole shucked eastern oysters exhibited the same relationship: the greater the difference between acclimation salinity and test salinity, the less ciliary activity recovery there was. Calcium and magnesium ions have been hypothesized to drive this response and likely also affect the oyster's branchial nerve (Paparo & Dean, 1984). Some tissues such as the ventricle had protein-assisted regulation responses to reduce cell volume when moved to hyposaline conditions. However, the gill, mantle, and hemolymph cells did not exhibit a short-term cell volume regulatory response. The lack of a regulatory response is hypothesized to avoid large energetic expenditures from the short-term changes in salinity that are characteristic of estuaries (Neufeld & Wright, 1996).

Low salinity plays a major role in cellular response and function, and, in combination with cellular response to high temperature, there may be a compounding effect on oyster energy expenditure. Metabolic assays, such as respirometry, could provide some insights on the energetic cost required to maintain homeostasis during thermal and low salinity stress and may provide more insight into why triploids in low salinity conditions lose their growth advantage and are more susceptible to high temperatures compared to diploids.

The main objectives of this study were to 1) determine if low salinity affects the metabolic patterns, behavioral responses, and functional and physiological death endpoints differently in diploid compared to triploid eastern oysters during acute thermal stress, and 2) determine whether observed responses to the combined stress of temperature and acute salinity might explain reported differences in mortality between farmed diploid and triploid oysters during the summer months.

5.2 Methods

5.2.1 Oyster farm conditions

An Onset HOBO temperature and salinity logger (Onset, Bourne, MA, USA) was deployed at the Auburn University Shellfish Lab farm in Grand Bay Oyster Park, Bayou La Batre, Alabama from January 2021 to December 2021. The logger was submerged approximately 20cm below the water surface and recorded measurements every hour. The logger was periodically retrieved from the farm and replaced with a clean logger to reduce background interference by biofouling.

5.2.2 Oyster lineage

Oysters are known to have a high degree of local adaptation (Bible & Sanford, 2016; Burford et al., 2014) and environmental tolerance can be directly influenced by genetics passed from broodstock (Callam et al., 2016). To minimize differences based on parentage, we created half-sibling lines that used the same maternal diploid broodstock crossed with diploid males to produce diploid offspring and crossed with tetraploid males to produce triploid offspring. Female broodstock used in this experiment were from a commercially available lines produced at the Auburn University Shellfish Laboratory with parentage derived from Louisiana, Alabama, Florida, and Texas (LAFT) wild oysters. Diploids were produced using LAFT males resulting in a 2MLAFT21 (LAFT X LAFT) cohort. Triploids were produced by fertilizing LAFT females using Louisiana (GNL) tetraploid male sperm resulting in a 3MLAFTLA21 (LAFT X GNL) cohort. Diploid and triploid fertilization occurred at the same time using the same egg pool. Resulting half-sibling oyster cohorts were set on microcultch and raised at Grand Bay Oyster

Park, AL until they reached experimental size. Research animals were not desiccated during the growth period, which is a standard method to control biofouling. To control growth and to remove epibionts and mortalities from the population, oysters were periodically tumbled according to Auburn University Shellfish Lab (AUSL) standard management practices.

5.2.3 Oyster collection and transport

Research oysters mentioned above (65-75mm shell height) were collected from Grand Bay Oyster Park (30° 22’ 30” N, 88° 18’ 53” W) in November 2022. Oysters were transported back to by boat. Oysters were scrubbed of all biofouling organisms such as barnacles and algae and then placed in a freshwater dip for 20 minutes with gentle agitation and then transferred to a hypersaline salt dip for 8 minutes with gentle agitation. They were then placed on a flat surface cup-side down and allowed to dry overnight. After drying, oysters were assigned an ID number printed on an 8 X 4 mm external Hallprint shellfish tag (Hallprint, Hindmarsh Valley, South Australia) secured with superglue and then randomly assigned upwellers as detailed below.

5.2.4 Holding conditions

Oysters were evenly distributed between four self-contained upwellers (Fig. 25) filled with filtered (1 µm) seawater pumped from the GOM and adjusted to 18ppt salinity using Crystal Sea MarineMix (Baltimore, Maryland, USA) or deionized water as needed. Water temperature was held constant at 25℃ using a 300 watt Finnex heater bar and a Inkbird Controller. Oysters were batch fed 10-15mL of LPB algae diet (Reed Mariculture, Campbell, CA) three times a week to maintain health but not promote growth. Water changes were performed if ammonia rose above .5mg/L and salinity was adjusted to 18ppt as described previously. The room was

under a 12L:12D light cycle. Oysters were acclimated to these conditions >2 weeks prior to experiments. Diploid and triploid oysters both experienced ~5% mortality within the acclimation period.

5.2.5 Experimental salinities

Before each run, 10 diploid and 10 triploid oysters were randomly assigned to a salinity regime (18ppt or 5ppt) and assay (oxygen consumption or behavioral response). Regardless of the assigned salinity regime, on Day 0 at 09:00, experimental oysters were placed in a separate acclimation upweller at 25°C and 18ppt for 1 hour. Oysters assigned to the 18ppt salinity regime were kept at 18ppt for 48 hours pre-temperature increase. Oysters assigned to the 5ppt salinity regime experienced a hyposaline event beginning at 10:00 on Day 0 where salinity was dropped from 18ppt to 5ppt by 2ppt/h and held at 5ppt overnight. At 09:00 on Day 1, oysters were placed in either the respirometry system or the behavioral chamber.

Oxygen consumption trials were conducted in a 152cm x 76cm x 45cm (LxWxH) fiberglass trough filled with 200L seawater from the same source as for the acclimation upwellers and held under a 12h L: 12h D photoperiod. All water was filtered through a 1µm sieve to minimize availability of food particles in the respirometry trough. No additional food was added to the trough during trials. Salinity was adjusted to either 25ppt or 8ppt, depending on the salinity treatment, with Crystal Sea MarineMix or deionized water. Salinity treatments were alternated between each trial, with 3 trials per salinity (6 trials total), such that consecutive trials did not test the same salinity. To prepare for a trial, oysters were placed in holding chambers without food added at 09:00 to begin facilitating a fasting period on Day 0. Oysters were placed in each of 6 respirometry chambers before 21:00 on Day 0, and oriented with the flat valve

facing upwards. Oysters were allowed to acclimate to the chambers overnight, with the thermal ramp beginning at ~09:00 the following morning. Thus, oysters were fasted for ~24 hrs prior to each thermal ramp and 12 hours to acclimate post-handling stress.

Resting metabolic rate (RMR) of oysters was measured using an 8-chamber fiber-optic respirometry system with AutoResp™ 2.3.0 software (Loligo® Systems, Viborg, Denmark). Each oyster was placed in a separate acrylic chamber fitted with two Eheim® submersible 300 L/h pumps (Eheim GmbH & Co., Deizisau, Germany). The flush pump brought fresh, oxygenated water into the chamber to replace oxygen-depleted water and flush out waste metabolites. The closed pump recirculated water through a closed loop that included the chamber and a flow-through oxygen cell with a fiber-optic dissolved oxygen (DO) sensor (See Chapter 4). Probes were calibrated using a two-point calibration (0% and 100%) prior to each experimental run. The closed pump was left on during the entire experiment, while the flush pump was only turned on in between measurement periods.

Following placement in the chambers, oysters were allowed to draw down the oxygen for ~7 min during each measurement period which was followed by a 5 min flushing period. This open-closed cycle was repeated for the entire trial (including the overnight acclimation). Data collection for analysis began at 09:00 (2 hours after lights turned on) the morning after placement in the chamber. At 10:00, the water temperature was increased at a rate of 2°C/hr. Measurement period time was adjusted as needed to prevent the DO from reaching less than 80% of the ambient oxygen at a given temperature. Data collection ended after temperatures reached 45°C at which time oysters were shucked, and wet tissue mass was recorded. All tissues were frozen at -20°C and subsequently oven dried at 80°C for 48 hours and dry tissue weight was recorded.

Respiration rate (mL O_2/kgWWW/h) was calculated for each oyster during each measurement cycle by AutoResp^{TM} software using the formula:

$$\text{RMR (mg } O_2\text{/kgWWW/h)} = \frac{V([O_2]_{t0} - [O_2]_{t1})}{t \times WWW} \text{ where}$$

$[O_2]_{t0}$ = DO at time t0 (mg O_2/L)

$[O_2]_{t1}$ = DO at time t1 (mg O_2/L)

V = respirometer volume (L) – volume of oyster (L)

t = time t1 (h) – time t0 (h)

WWW = whole oyster wet weight (g)

5.2.7 Correcting for background oxygen consumption by bacteria and shells

Two control chambers were included in each trial. One control chamber was kept empty and was used to estimate background oxygen consumption of bacteria. To estimate oxygen consumption of bacteria and invertebrate communities associated with oyster shells, two valves from a freshly shucked diploid and two valves from a freshly shucked triploid oyster were placed in the second control chamber (4 valves total). Because the shell background chamber contained two sets of shells (4 valves), the mean respiration per set of two valves was estimated by dividing the respiration rate (mgO_2/chamber/h) by two and then subtracting the respiration rate of the bacterial control chamber (no valves). The bacterial respiration was then added to the mean shell (2 valves) respiration to estimate the total background associated with shell (2 valves) and bacteria. Oyster respiration rates were then corrected by subtracting the total background respiration rate from the respiration rates measured in each oyster chamber during each measurement cycle.

5.2.8 Valve closures and unreliable measurements

Closures were defined as any respiration rate that was negative or <50% of the neighboring positive value. Measurements during periods when the linear relationship between DO and time yielded an R^2 of <.9 were automatically excluded from the data set as being unreliable (Chabot et al., 2021) unless it was identified as a closure. Closure frequency of each individual oyster was then estimated by first identifying the number of closed measurements that were recorded within each integer ± 5°C temperature bin (i.e., 28 ± 5°C, 29 ± 5°C, etc.). The number of "closed" measurements was then divided by the number of total measurements within each bin to calculate the proportion of closed measurements at each integer temperature for each individual.

5.2.9 Respiratory thermal performance curves of open oysters

Closure measurements were removed from each dataset and, for each oyster ploidy class, a thermal performance curve (TPC) was created by fitting a smoothing spline (SS) model to a plot of RMR (y-axis) vs temperature (x-axis). The selection of the smoothing parameter (λ) was based on the restricted maximum likelihood (REML) method to ensure the compromise between the smoothness of the function and the lack of fit (Berry & Helwig, 2021). Each spline was fitted to a temperature range that started when the first open measurement was recorded and ended at the temperature at which all oysters exhibited mantle tissue retraction. As a result, fitted SS models were used to predict RMR across slightly different temperature ranges for each salinity × ploidy group: 25.55 – 45.35ºC (5ppt_Triploid), 25.54-45.81ºC (18ppt_Triploid), 26.16-45.35ºC (5ppt_Diploid), 24.53-45.81ºC (18ppt_Diploid) with an interval of .001ºC. For each

oyster ploidy class, 95% confidence intervals (95% CI) of predicted RMR curves were created via bootstrapping (Efron & Tibshirani, 1993) implemented in the boot package (version 1.3-28; Canty and Ripley, 2021). Data were resampled with replacement 1,000 times, with the SS model re-fitted to these data each time, and the 95% CIs were determined from the 2.5^{th} and 97.5^{th} percentiles.

5.2.10 Behavior, functional death, and physical death

An insulated test chamber was filled with 75L of natural seawater filtered through 1µm filter bag and heated to 25°C. For each trial, salinity was adjusted to either 18ppt or 5ppt salinity. An air stone and pump were used to keep water circulating and oxygenated throughout the assay. An 800W Finnex titanium heater bar (Chicago, IL, USA) was affixed to the center of the chamber via suction cups. Diploid and triploid oysters were evenly placed on both sides of the heater bar (see chapter 4). The water temperature was increased 2°C every hour until 46°C or 100% of oysters showed mantle tissue retraction. Oysters were checked every half hour for changes in behavior. Functional death (CTM) was recorded as the temperature when they began gaping and ceased responding to physical stimulus (pinching valves). Presumed physical death (PPD) was recorded as the temperature where the individual gaped, failed to respond to physical stimulation and exhibited mantle tissue that was retracted and detached from the shell. At the end of each trial, oysters were removed from the test chamber and shucked. Their wet weight was recorded, and tissues were stored frozen at -20°C.

5.2.11 Condition index

Condition index was calculated for all individuals. After shucking, shells were airdried for >1 week before being weighed on a AL204 Mettler Toledo analytical balance (Columbus, OH, USA). Frozen oyster tissues were thawed and dried in a Fisher Scientific Isotemp Oven (Waltham, MA, USA) at 80°C for 48 hours before being weighed. Condition index was calculated using the following equation (Abbe & Albright, 2003):

$$CI=[\text{dry tissue weight(g)}/(\text{whole oyster wet weight (g)}-\text{dry shell weight(g)})]*100$$

5.2.12 Statistical analysis

All respirometry, closure, and behavioral temperature data was checked for normality using Shapiro-Wilk's test. Differences in RMR between all temperature bins were compared using two-way repeated measures analysis of covariates (ANCOVA) between salinity × ploidy groups (5ppt_Diploid, 5ppt_Triploid, 18ppt_Diploid, 18ppt_Triploid). Salinity × ploidy groups were compared using the Johnson-Neyman technique at each integer temperature and differences between groups were determined by a Tukey-Kramer test. Proportion closed data across temperatures was converted into percentage and log transformed to meet normality assumptions and differences between the salinity × ploidy groups were analyzed using the Johnson-Neyman technique and Tukey-Kramer test as mentioned above for RMR. Likelihood of exhibiting CTM and PPD were analyzed using the survival analysis methods. Kaplan-Meier survival analyses were used to determine the median CTM and PPD for each oyster ploidy class and salinity treatment. Log-rank tests were used to compare probabilities of CTM and PPD between ploidy groups and salinity trials. A Cox proportional hazard regression model was used to determine the effect of shell height on the estimate of the onset of CTM and PPD. Statistical significance was

set at $p < .05$, and data were presented as the mean ± *SD*. Survival analyses were performed in SAS® version 9.4 (*SAS*, 2013).

5.3 Results

5.3.1 Site specific environmental parameters

Temperature and salinity monitored at an off-bottom oyster farm on the Alabama coast showed wide fluctuations in temperature and salinity throughout the year. Temperature ranged from <10°C in Spring to >35°C in late Summer. Salinity ranged from highs of 20-30ppt in winter months to sporadic lows approaching 0ppt throughout Spring, Summer, and Fall. During this time salinity fluctuated rapidly often going from >20ppt to <5ppt within a matter of days. In the summer months, periods of low (<10ppt) salinity sometimes lasted for >1 week and coincided with water temperatures exceeding a threshold (30°C) above which is considered stressful to oysters (Fig. 27) (Marshall, Coxe, et al., 2021).

5.3.2 Closures

There was no significant difference ($p < .05$) in proportion closures between diploids and triploids at 18ppt as temperatures increased from 24-44°C (Fig. 28 A,B). However, at a salinity of 5ppt, the proportion of closures for triploid oysters was consistently higher ($p < .05$) than diploids as temperatures rose from 26-34°C, with >60% of measurements designated as closures (Fig. 28 C,D).

Proportion closures for diploids were significantly higher ($p < .05$) at 5ppt than at 18ppt as temperatures increased from 24-28°C but did not differ as temperature increased further from

28 to 44ºC (Fig. 28 A,C). Proportion closures for triploids were significantly higher ($p < .05$) at 5ppt than 18ppt across all temperatures (Fig. 28 B,D).

5.3.3 Metabolic rate

Regardless of temperature, there were significant differences in RMR among the four salinity × ploidy groups (18ppt_Triploid, 18ppt_Diploid, 5ppt_Triploid, 5ppt_Diploid) ($F_{3,332} = 8.2$, $p < .001$). Regardless of ploidy, there was a significant effect of temperature on RMR ($F_{1,332} = 165.32$, $p < .001$) with a reduction in RMR observed at the higher temperatures. Resting metabolic rates of diploids were not significantly different ($p > .05$) between 5ppt and 18ppt as temperatures increased from 24-45ºC (Fig. 29 A,C). Similarly, resting metabolic rates of triploids were not significantly different ($p > .05$) between 5ppt and18ppt as temperatures increased from 24-45ºC (Fig. 29 B,D). There was a significant interaction between salinity-ploidy group and temperature ($F_{3,332} = 10.44$, $p < .001$), indicating that the relationship between RMR and temperature differed among salinity-ploidy groups.

Further analysis revealed no significant difference ($p < .05$) in RMR between diploids and triploids at 18ppt as temperatures increased (Fig. 29 A,B). However, at a salinity of 5ppt, the RMR of triploid oysters was consistently lower ($p < .05$) than diploids as temperatures rose from 24-31ºC, but there was no difference as temperatures increased further from 32 to 45ºC (Fig. 5 C,D).

Based on confidence intervals around the smoothing splines, $RMR_{peak\ activity}$ of diploids did not differ significantly between salinities, but $RMR_{peak\ activity}$ of triploids was significantly higher at 18ppt compared to 5ppt. Triploid $RMR_{peak\ activity}$ was significantly lower than diploid $RMR_{peak\ activity}$ at both salinities tested (Table 6, Fig. 30).

$RMR_{peak\ temp}$ was significantly lower at 5ppt compared to 18ppt for diploids. Triploid $RMR_{peak\ temp}$ had relatively wide CI intervals at each salinity and thus did not differ significantly between salinities for triploids even though difference between the estimated $RMR_{peak\ temp}$ at 18ppt and 5ppt was similar to that for diploids. Triploid $RMR_{peak\ temp}$ did not differ significantly from diploids at either salinity (Table 6, Fig. 30).

5.3.4 Functional and presumed physiological death

CTM for each group manifested approximately 7°C after $RMR_{peak\ temp}$ in both ploidies at 18ppt. At 5ppt, both ploidies did not reach CTM until ~13°C post-$RMR_{peak\ temp}$ (Table 6).

Regardless of ploidy, salinity had a significant effect on CTM, with CTM significantly lower at 5ppt compared to 18ppt (Log-rank test: $\chi^2_{(1)} = 6.32$, $p = .0120$). Regardless of salinity, there was no significant effect of ploidy on CTM (Log-rank test: $\chi^2_{(1)} = .10$, $p = .7580$). There was no significant interaction between salinity and ploidy (Log-rank test: $\chi^2_{(3)} = 6.60$, $p = .0860$) (Fig. 31).

We also tested for effects of different physical metrics on CTM using a Cox proportional hazards regression model. There was no significant effect of dry shell weight, dry tissue weight, whole wet weight, condition index, or shell height on CTM ($p > .05$).

The temperature at which PPD was observed occurred approximately 1°C after CTM (Table 6). There was no significant effect of ploidy on PPD (Log-rank test: $\chi^2_{(1)} = .05$, $p = .8260$) regardless of salinity, but there was a significant effect of salinity on PPD regardless of ploidy (Log-rank test: $\chi^2_{(1)} = 4.05$, $p = .0440$). There was no significant interaction between salinity and ploidy (Log-rank test: $\chi^2_{(3)} = 4.79$, $p = .1880$) (Fig. 32). A Cox proportional hazards regression model identified that shell height had a statistically significant effect on PPD hazard rate (Cox

regression: $\chi^2_{(1)} = 5.68$, $p = .0172$) where every 1mm increase in SH decreases the hazard risk of expressing PPD by 3.3% (95% Wald's S.H.: .941 – .994). This relationship was driven by triploids at 5ppt (95% Wald's S.H.: .862-.997), but not by diploids at 18ppt (95% Wald's S.H.: .923-1.114), triploids at 18ppt (95% Wald's S.H.: .899-1.085), or diploids at 5ppt (95% Wald's S.H.: .9936-1.004) (Fig. 33).

5.4 Discussion

Oyster aquaculture is an important industry in the Gulf of Mexico and typically takes place in the nearshore coastal waters around estuaries. Estuaries can be hostile areas for many organisms and require significant adaptations to tolerate the rapid salinity and temperature swings characteristic of this habitat (Bible & Sanford, 2016; Somero, 2002). Environmental stressors can have major impacts on oyster physiology, each stressor demanding the oyster to adjust to new conditions. With farmed oysters around the Gulf of Mexico occasionally experiencing sudden mortalities during times of high temperature and low salinity, differences in metabolic stress at low and high salinities between ploidies may help explain the disproportionately high mortality rates in triploids compared to diploids reported from field studies (Callam et al., 2016; Guevelou et al., 2019; Wadsworth et al., 2019).

5.4.1 Low salinity and thermal stress prior to metabolic depression

Thermal stress in aquatic ectotherms is accompanied by a higher metabolism up to Mpeak, a byproduct of which is an overabundance of reactive oxygen species (ROS) (Slimen et al., 2014). Molecular chaperones such as *HSP70* and other proteins in the heat shock family help to repair or degrade abnormal proteins resulting from oxidative stress (Sies, 1991) and thermal

damage. These chaperones require ATP to be produced (Goldberg, 1992; Hochachka & Somero, 2002). As long as the ATP produced during thermal stress is enough to fuel production of sufficient molecular chaperones to repair proteins and other damage resulting from thermal stress and ROS production, the organism can still function properly (Verberk et al., 2016).

Low salinity stress results in changes in closure behavior in an attempt to allow oyster tissue cells time to osmoconform without causing major cellular damage from hypotonic stress (Casas et al., 2018, 2024). Higher energetic requirements for osmoconformation is evidenced by the trend of higher (though not significantly higher) respiration rates of diploid oysters at 5ppt compared to both ploidies at 18ppt between 24 and 31^{o}C. This may signal a decrease in the upper threshold for thermal stress for oysters at lower salinities. Triploid oysters take a longer time to osmoconform than diploid oysters at low salinity at moderate temperatures (Casas et al., 2024), which may explain why the interaction between low salinity and acute thermal stress further increased triploid closures significantly more than diploid closures at low salinity. Triploid cells are larger, resulting in lower surface area to volume ratio compared to diploids and is likely why triploid oysters generally had lower RMR values compared to diploids at 24-31°C regardless of salinity, a trend that was also previously seen in Chapter 4. There was no increase or decrease in energetic cost associated with osmoregulation during low salinity prior to metabolic depression compared to moderate salinity in diploids or triploids.

5.4.2 Metabolic and behavioral patterns after metabolic depression

Valve closure increased significantly as temperatures increased regardless of salinity, a characteristic bivalve response to thermal stress (Anestis et al., 2007; Philipp & Abele, 2010; Sokolova et al., 2012). Closures are often employed by bivalves to reduce their metabolism

(metabolic depression) during times of thermal stress by temporarily switching to anaerobic respiration (Boutilier & St-Pierre, 2000; Pörtner, 2012; Ritchie, 2018; Vajedsamiei et al., 2021).

Metabolic depression is an adaptation by bivalves used to reduce damage from ROS production and is initiated via valve closures (Anestis et al., 2007; Philipp & Abele, 2010; Sokolova et al., 2012). However, by initiating metabolic depression, ATP turnover is heavily reduced and, as a result, creation of new molecular chaperones to assist in protein repair is limited (Kültz, 2005). When temperatures continue to increase and the available proteins are not sufficient for the resulting damage, the cell exceeds its tolerance limits and results in cellular apoptosis (Kültz, 2005). If apoptosis is widespread enough across tissues, organismal death occurs (Lutterschmidt & Hutchison, 1997).

Metabolic peak temperature occurred around 34°C in both diploid and triploid oysters at 18ppt. Given that it is very common that surface water temperatures at farm sites in the Gulf of Mexico reach these temperatures in the peak of summer, it would be reasonable to assume that some mortality events in farmed oysters is due to reaching and exceeding these temperatures for extended periods of time. However, behaviors indicative of functional death (i.e. gaping and unresponsiveness to probing) did not occur until ~7°C beyond which signs of metabolic stress appear (i.e. RMR peak followed by decline). Additional studies not included in this dissertation showed that signs of functional death were not necessarily indicative of actual physical death. Oysters exhibited 100% recovery from “functional death” for both ploidies if oysters were cooled to 25°C at a rate of 3°C/h (pers. obs.). The temperature which demarcates the breakpoint between increasing and decreasing metabolic rate did not appear to be a sign of lethal thermal stress and imminent death. This and the fact that the breakpoint temperature did not significantly

differ between ploidies show that metabolic peak temperature was not a driver of differential morality between triploid and diploid oysters.

While neither CTM nor PPD differed between diploid and triploid oysters, salinity did have a significant influence on the temperature at which both ploidies showed behavioral signs of stress indicative of functional death (i.e. gaping and unresponsiveness to probing, but not mantle retraction). While subtidal oysters would not typically reach CTM and PPD temperatures, farmed oysters would experience temperatures close to CTM during periodic desiccation in the summer in Alabama. The frequency of these events would be dictated by each farm's management practices, although anecdotally desiccation regimes increase in frequency as biofouling increases throughout the summer. This suggests that if acute low salinity events occur in the summer, oysters of both ploidies may be more susceptible to acute thermal stress during routine summer desiccation.

The threat of low salinity events in the warm summer months in the Mississippi Sound is readily apparent and confirmed by environmental parameters recorded in this study. Low salinity decreases the temperature at which diploids and triploids initiate metabolic depression compared to moderate salinity indicating an increased susceptibility to thermal stress in hyposaline conditions. Between both ploidies at low salinities, triploids had a lower metabolic rate and increased closures compared to diploids. In chronic trials, the combined effect of low salinity and temperatures at and above the onset of metabolic depression in diploids resulted in increased mortalities compared to diploids at moderate salinity (Marshall, Casas, et al., 2021). Whether or not triploids are more susceptible compared to diploids in these conditions (5ppt; >33°C) due to their increased closure rate has not been studied.

The negative impact of low salinity on oyster survival has been extensively studied and is well known in the oyster farming community (Bodenstein, Callam, et al., 2023; Casas et al., 2018; Gledhill et al., 2020; Marshall, Casas, et al., 2021; Marshall, Coxe, et al., 2021). Development of genetic lines of oysters that are able to survive at lower salinities is currently being undertaken at hatcheries across the Gulf of Mexico and east coast in an attempt to improve survival rates (Bodenstein, Callam, et al., 2023; McCarty et al., 2020, 2023). Oyster management practices involving tumbling and desiccation increase cumulative mortality in both diploid and triploid oysters (Bodenstein et al., 2021). Thermal and low salinity stress on top of management practices may incur greater mortalities seen in the spring and summer months. If so, reducing handling stress by reducing or delaying tumbling and desiccation during unfavorable conditions (<5ppt; >30°C) until salinity improves may reduce overall farm mortality.

5.5 Tables

Table 6. Metabolic, behavioral, and lethal endpoints for diploid and triploid oysters estimated at two different salinities. Subscripts indicate significant differences between ploidies and salinities indicated by non-overlapping confidence intervals.

Endpoint	**Diploid**				**Triploid**			
	18ppt		**5ppt**		**18ppt**		**5ppt**	
	Spline estimate	**95% CI**	**Spline estimate**	**95% CI**	**Spline estimate**	**95% CI**	**Spline estimate**	**95% CI**
$RMR_{peak\ activity}$ (mgO_2/kgDTW/h)	1903.23^{a}	1771.37-2035.09	1823.59^{a}	1683.52-1963.66	1517.27^{b}	1415.75-1618.79	1125.91^{c}	997.82-1253.98
$RMR_{peak\ temp}$ (°C)	36.41^{a}	33.81-39.01	30.55^{b}	27.59-33.51	35.31^{ab}	30.06-40.56	28.19^{b}	24.02-32.36
	Mean	**95% CI**	**Mean**	**95% CI**	**Mean**	**95% CI**	**Mean**	**95% CI**
CTM_{temp} (°C)	43.92	43.16-44.68	43.17	42.57-43.76	43.80	43.28-44.32	43.20	42.89-43.51
PPD_{temp} (°C)	44.69	44.31-45.07	44.00	43.45-44.55	44.60	44.25-44.95	44.32	43.67-44.79

5.6 Figures

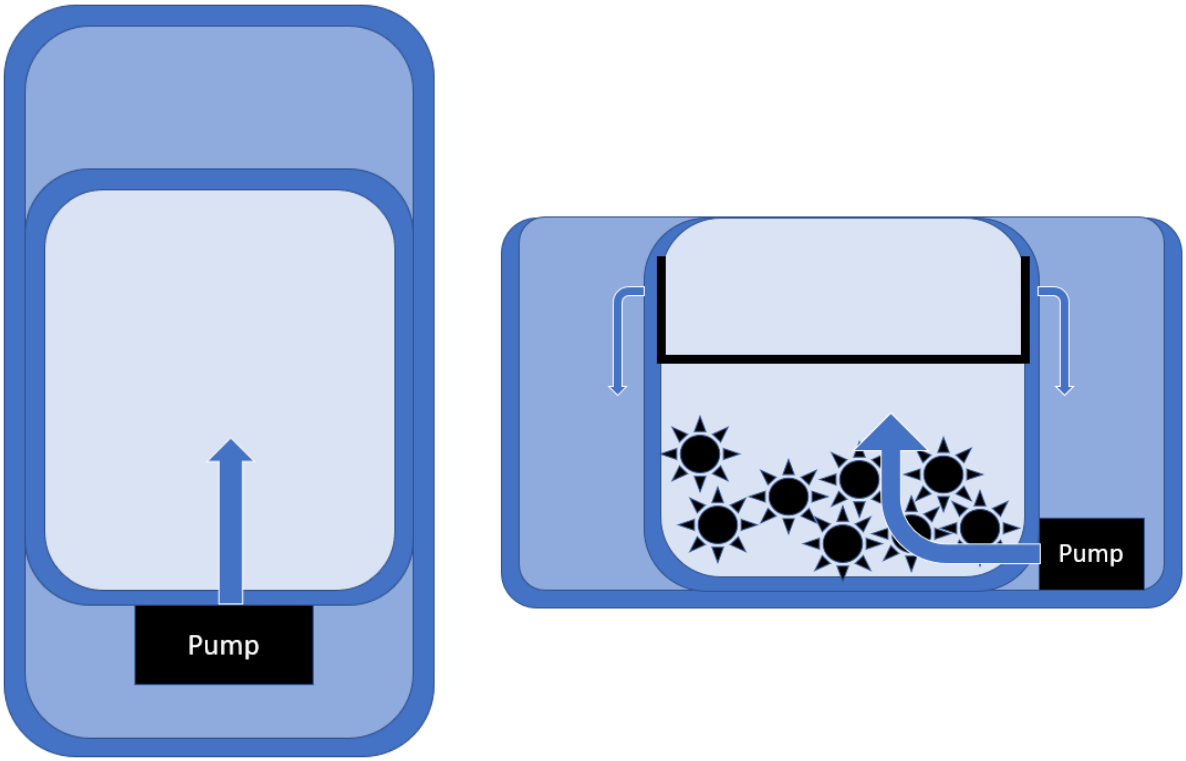

Figure 25. Upweller Schematics top-down view (left) and side view (right). Water movement direction is indicated by arrows.

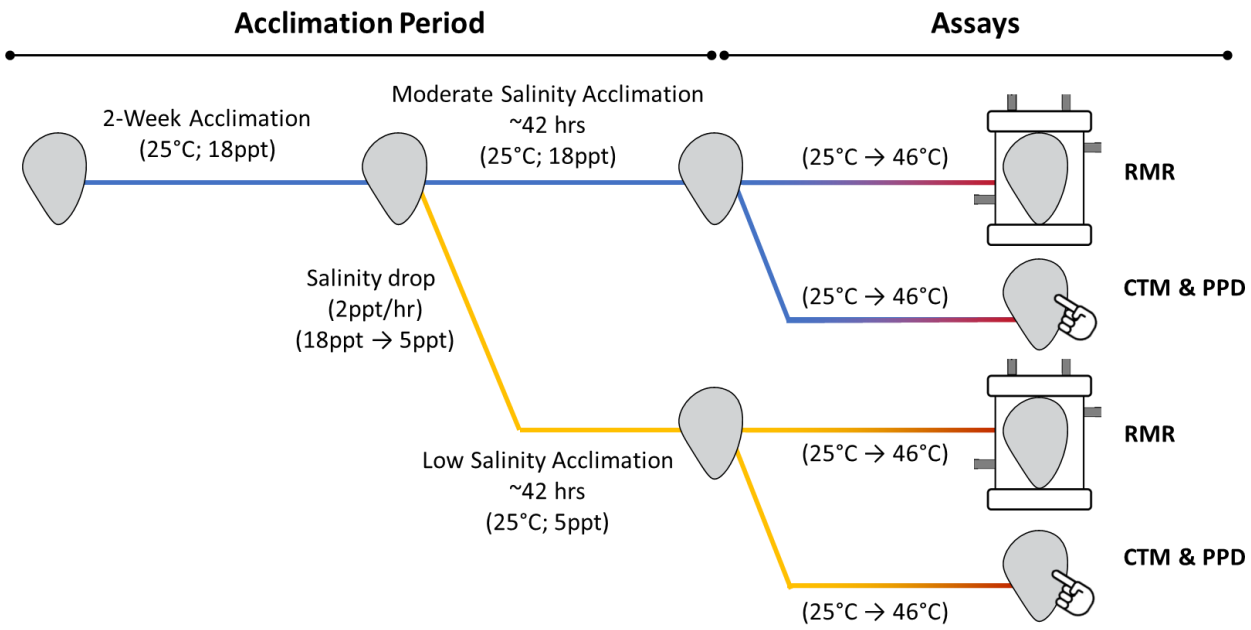

Figure 26. Visual representation of experimental timeline of acclimation, simulated hyposaline event, and experimental assays.

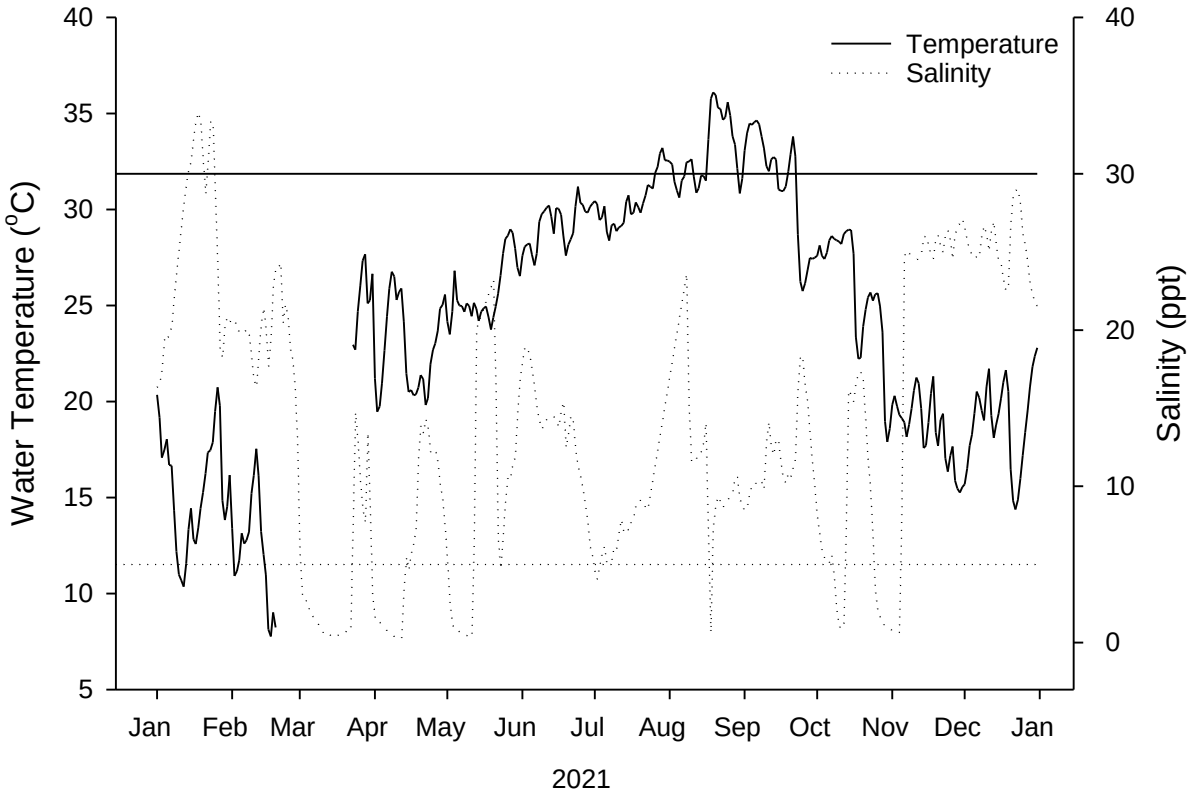

Figure 27. Daily water temperature (°C, solid line) and salinity (ppt, dashed line) at Grand Bay Oyster Park from January 2021 to January 2022. Horizontal lines mark environmental thresholds for salinity and temperature, beyond which conditions are considered stressful to oysters (<5ppt; >30°C).

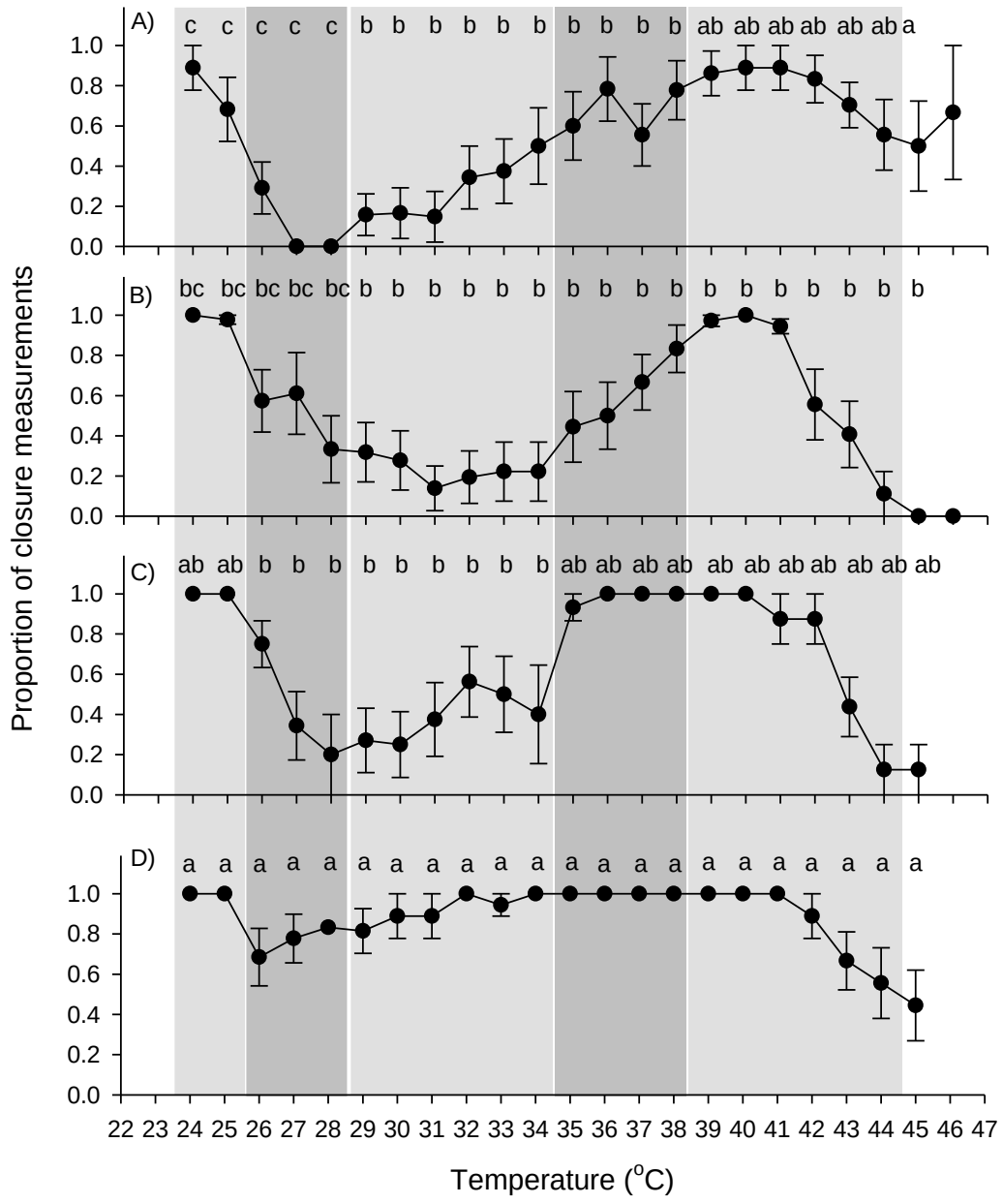

Figure 28. Relationship between mean proportion of closure measurements and temperature for the salinity × ploidy categories tested: A) 18ppt_Diploid, B) 18ppt_Triploid, C) 5ppt_Diploid, and D) 5ppt_Triploid. Letters indicate differences in proportion closure among salinity × ploidy categories at each integer temperature. Grey rectangles indicate temperature ranges within which the relationships among salinity × ploidy categories were consistent. Error bars represent ± 1 SE.

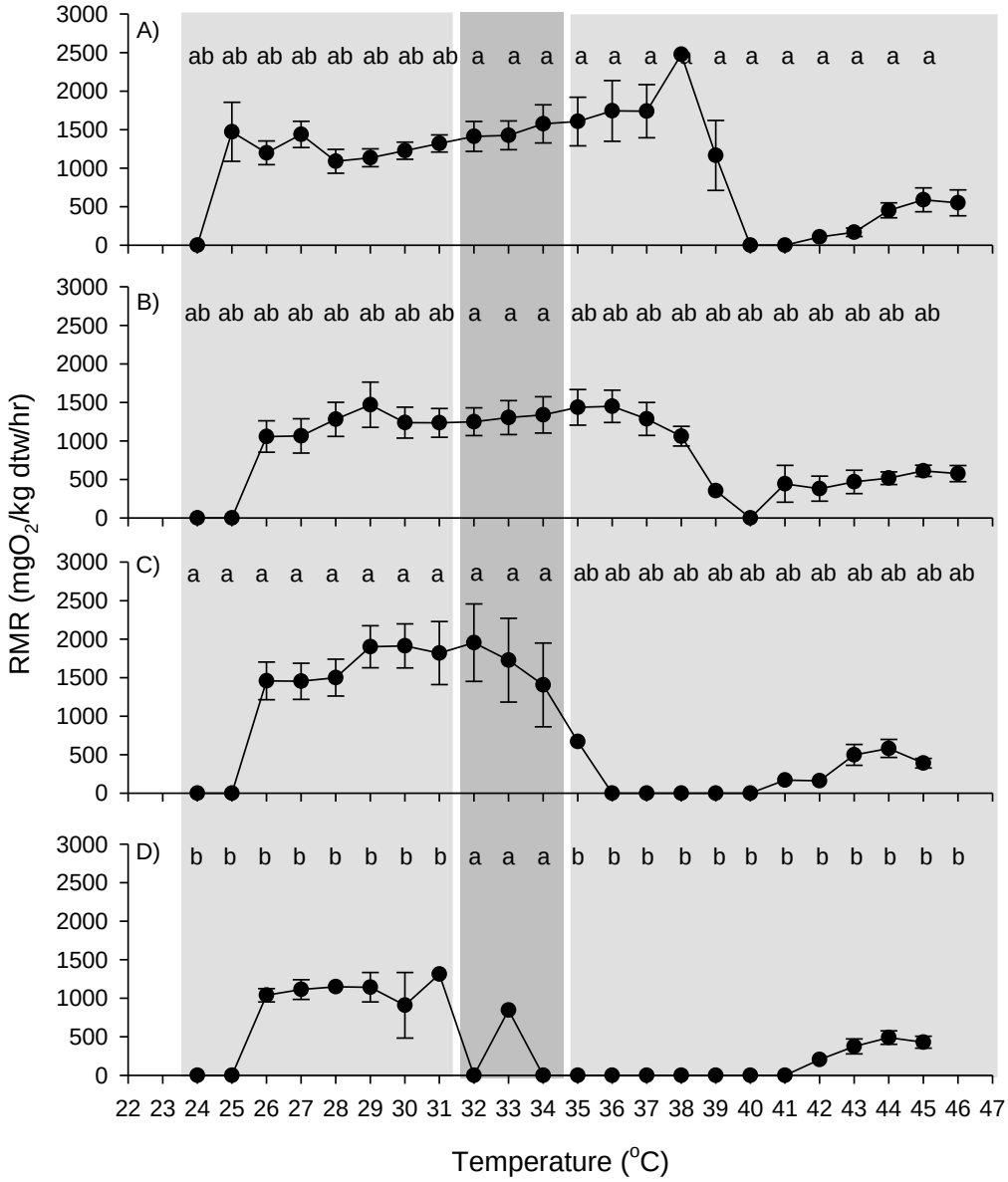

Figure 29. Relationship between resting metabolic rate (RMR) and temperature for the salinity × ploidy categories tested: A) 18ppt_Diploid, B) 18ppt_Triploid, C) 5ppt_Diploid, and D) 5ppt_Triploid. Letters indicate differences in proportion closure among salinity × ploidy categories at each integer temperature. Grey rectangles indicate temperature ranges within which the relationships among salinity × ploidy categories were consistent. Error bars represent ± 1 SE.

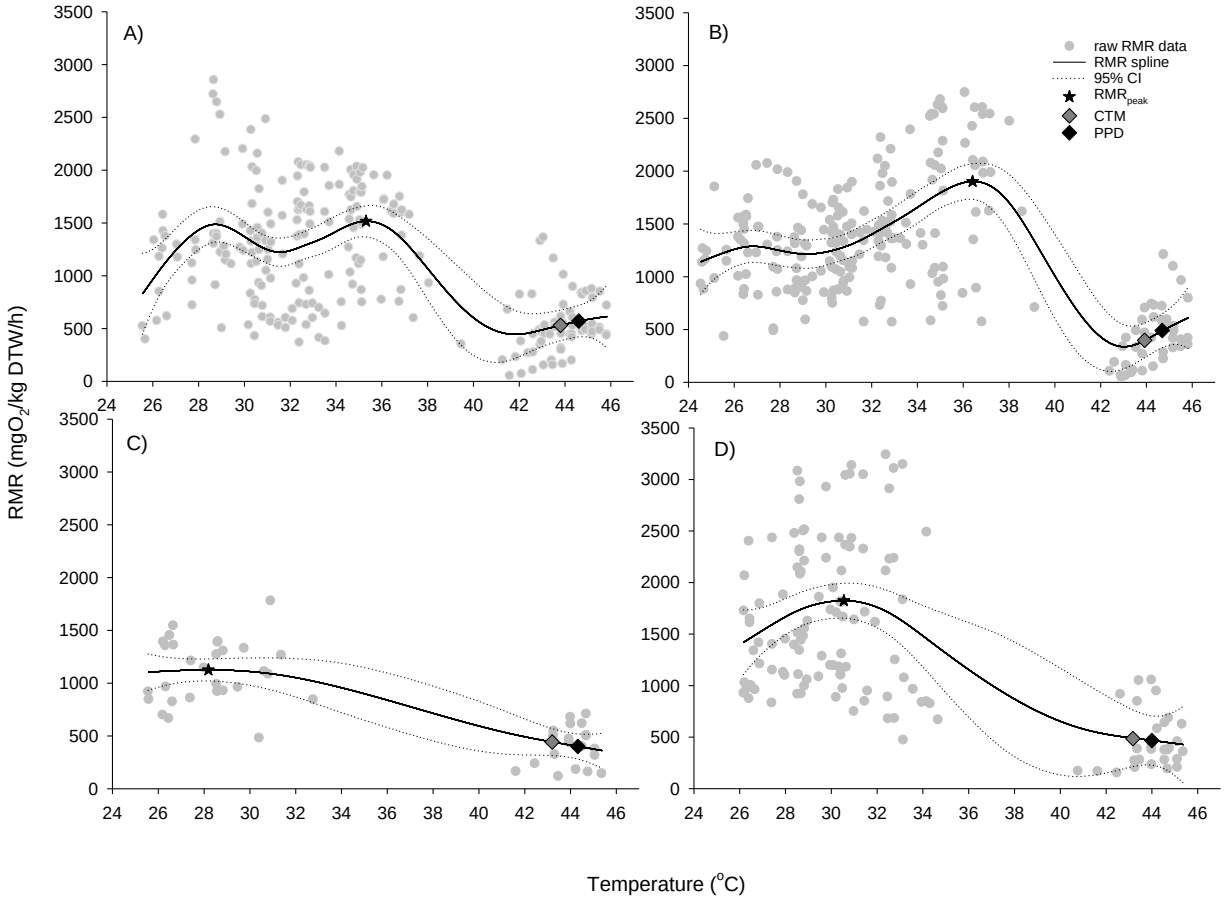

Figure 30. Relationships between RMR and temperature for A) 18ppt_Triploid, B) 18ppt_Diploid, C) 5ppt_Triploid, D) 5ppt_Diploid where the grey dots represent the raw RMR data from individual oysters and the solid and dotted lines represent the smoothing spline and 95% CI respectively. Locations of RMR_{peak} and functional and physiological death on each curve are indicated by symbols.

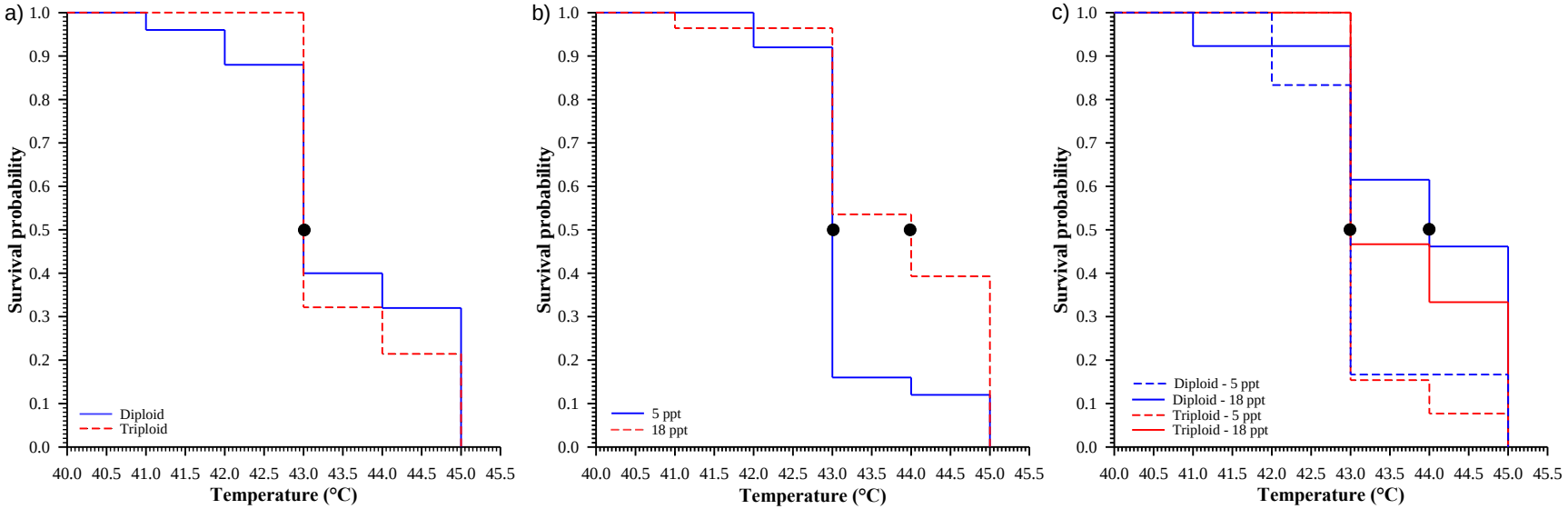

Figure 31. Comparison of CTM survival curves among a) ploidy regardless of salinity, b) salinity regardless of ploidy, and c) the interaction between ploidy and salinity. Survival probability show the proportion of oysters that had not yet reached CTM. Median CTM occurs where survival probability is 50% and is marked with black circles on each line. There was a significant effect of salinity on CTM survival curves (b).

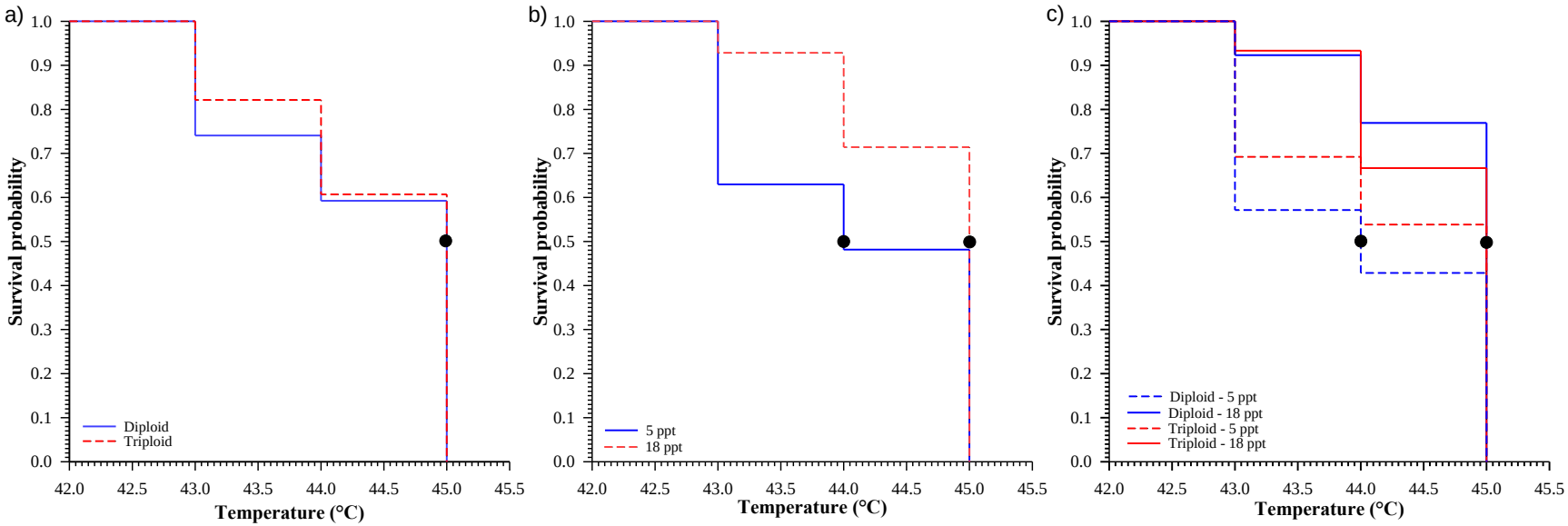

Figure 32. Comparison of PPD survival curves among a) ploidy regardless of salinity, b) salinity regardless of ploidy, and c) the interaction between ploidy and salinity. Survival probability show the proportion of oysters that had not yet reached PPD. There was a significant effect of salinity on PPD survival curves (b). Median PPD occurs where survival probability is 50% and is marked with black circles on each line.

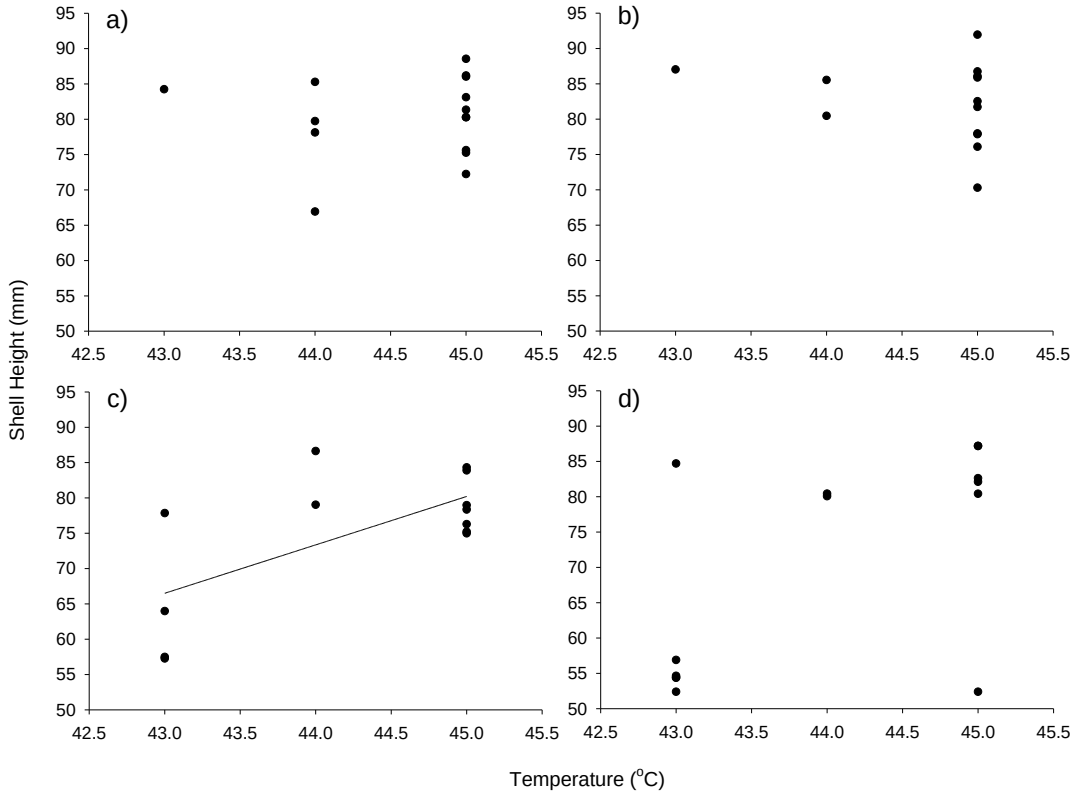

Figure 33. Scatterplots showing the relationship between oyster shell height and PPD in a) 18ppt_Triploid, b) 18ppt_Diploid, c) 5ppt_Triploid, and d) 5ppt_Diploid. The line in plot c identifies the positive correlation between shell height and PPD.

5.7 References

Abbe, G. R., & Albright, B. W. (2003). An improvement to the determination of meat condition index for the eastern oyster Crassostrea virginica (Gmelin 1791). *Journal of Shellfish Research*, *22*(3), 747–752.

Allen, S. K., & Downing, S. L. (1986). Performance of triploid Pacific oysters, Crassostrea gigas (Thunberg). I. Survival, growth, glycogen content, and sexual maturation in yearlings. *Journal of Experimental Marine Biology and Ecology*, *102*(2), 197–208. https://doi.org/10.1016/0022-0981(86)90176-0

Anestis, A., Lazou, A., Pörtner, H. O., & Michaelidis, B. (2007). Behavioral, metabolic, and molecular stress responses of marine bivalve Mytilus galloprovincialis during long-term acclimation at increasing ambient temperature. *American Journal of Physiology. Regulatory, Integrative and Comparative Physiology*, *293*(2), R911-921. https://doi.org/10.1152/ajpregu.00124.2007

Berry, L. N., & Helwig, N. E. (2021). Cross-Validation, Information Theory, or Maximum Likelihood? A Comparison of Tuning Methods for Penalized Splines. *Stats*, *4*(3), Article 3. https://doi.org/10.3390/stats4030042

Bible, J. M., & Sanford, E. (2016). Local adaptation in an estuarine foundation species: Implications for restoration. *Biological Conservation*, *193*, 95–102. https://doi.org/10.1016/j.biocon.2015.11.015

Bodenstein, S., Callam, B. R., Walton, W. C., Rikard, F. S., Tiersch, T. R., & La Peyre, J. F. (2023). Survival and growth of triploid eastern oysters, Crassostrea virginica, produced from wild diploids collected from low-salinity areas. *Aquaculture (Amsterdam, Netherlands)*, *564*, 739032. https://doi.org/10.1016/j.aquaculture.2022.739032

Bodenstein, S., Casas, S. M., Tiersch, T. R., & La Peyre, J. F. (2023). Energetic budget of diploid and triploid eastern oysters during a summer die-off. *Frontiers in Marine Science*, *10*. https://www.frontiersin.org/articles/10.3389/fmars.2023.1194296

Bodenstein, S., Walton, W., & Steury, T. (2021). Effect of farming practices on growth and mortality rates in triploid and diploid eastern oysters Crassostrea virginica. *Aquaculture Environment Interactions*, *13*, 33–40. https://doi.org/10.3354/aei00387

Boutilier, R. G., & St-Pierre, J. (2000). Surviving hypoxia without really dying. *Comparative Biochemistry and Physiology. Part A, Molecular & Integrative Physiology*, *126*(4), 481–490. https://doi.org/10.1016/s1095-6433(00)00234-8

Callam, B. R., Allen, S. K., & Frank-Lawale, A. (2016). Genetic and environmental influence on triploid Crassostrea virginica grown in Chesapeake Bay: Growth. *Aquaculture*, *452*, 97–106. https://doi.org/10.1016/j.aquaculture.2015.10.027

Camp, E. V., Pine, W. E., Havens, K., Kane, A. S., Walters, C. J., Irani, T., Lindsey, A. B., & Morris, J. G. (2015). Collapse of a historic oyster fishery: Diagnosing causes and identifying paths toward increased resilience. *Ecology and Society, 20*(3). https://www.jstor.org/stable/26270266

Canty, A., & Ripley, B. (2021). *Boot: Bootstrap R (S-Plus) Functions. R package, version 1.3–28. 2021*.

Casas, S. M., Comba, D., La Peyre, M. K., Rikard, S., & La Peyre, J. F. (2024). Rates of osmoconformation in triploid eastern oysters, and comparison to their diploid half-siblings. *Aquaculture, 580*, 740326. https://doi.org/10.1016/j.aquaculture.2023.740326

Casas, S. M., Filgueira, R., Lavaud, R., Comeau, L. A., La Peyre, M. K., & La Peyre, J. F. (2018). Combined effects of temperature and salinity on the physiology of two geographically-distant eastern oyster populations. *Journal of Experimental Marine Biology and Ecology, 506*, 82–90. https://doi.org/10.1016/j.jembe.2018.06.001

Chabot, D., Zhang, Y., & Farrell, A. P. (2021). Valid oxygen uptake measurements: Using high r2 values with good intentions can bias upward the determination of standard metabolic rate. *Journal of Fish Biology*, *98*(5), 1206–1216. https://doi.org/10.1111/jfb.14650

Collier, R. J., Baumgard, L. H., Zimbelman, R. B., & Xiao, Y. (2019). Heat stress: Physiology of acclimation and adaptation. *Animal Frontiers, 9*(1), 12–19. https://doi.org/10.1093/af/vfy031

Coxe, N., Mize, G., Casas, S., Peyre, M. K. L., Lavaud, R., Callam, B., Rikard, S., & Peyre, J. L. (2023). Hypoxia and Anoxia Tolerance in Diploid and Triploid Eastern Oysters at High Temperature. *Journal of Shellfish Research, 42*(1), 29–43. https://doi.org/10.2983/035.042.0104

Dégremont, L., Garcia, C., Frank-Lawale, A., & Allen, S. K. (2012). Triploid Oysters in the Chesapeake Bay: Comparison of Diploid and Triploid Crassostrea virginica. *Journal of Shellfish Research, 31*(1), 21–31. https://doi.org/10.2983/035.031.0103

Efron, B., & Tibshirani, R. (1993). *An introduction to the bootstrap*. Chapman & Hall.

Eleuterius, C. (1976). *Mississippi Sound: Salinity distribution and indicated flow patterns* (MASGP-76-023). Mississippi-Alabama Sea Grant Consertium. https://repository.library.noaa.gov/view/noaa/13145

Galtsoff, P. S. (1965). *The American Oyster Crassostrea Virginica Gmelin* (Vol. 64). U.S. Fish and Wildlife Service. https://www.cambridge.org/core/journals/journal-of-the-marine-biological-association-of-the-united-kingdom/article/american-oyster-crassostrea-virginica-gmelin-by-paul-s-galtsoff-fishery-bull-fish-wild-serv-us-vol-64-480-pp-1964/1E911EB4AC9E6EFBAD57F18D6FE9BEC0

Gérard, A., Ledu, C., Phélipot, P., & Naciri-Graven, Y. (1999). The induction of MI and MII triploids in the pacific oyster Crassostrea gigas with 6-DMAP or CB. *Aquaculture*, *174*(3–4), 229–242. Scopus. https://doi.org/10.1016/S0044-8486(99)00032-0

Gledhill, J. H., Barnett, A. F., Slattery, M., Willett, K. L., Easson, G. L., Otts, S. S., & Gochfeld, D. J. (2020). Mass Mortality of the Eastern Oyster Crassostrea virginica in the Western Mississippi Sound Following Unprecedented Mississippi River Flooding in 2019. *Journal of Shellfish Research*, *39*(2), 235–244. https://doi.org/10.2983/035.039.0205

Goldberg, A. L. (1992). The mechanism and functions of ATP-dependent proteases in bacterial and animal cells. *European Journal of Biochemistry*, *203*(1–2), 9–23. https://doi.org/10.1111/j.1432-1033.1992.tb19822.x

Guevelou, E., Carnegie, R., Moss, J. A., Hudson, K., Reece, K., Rybovich, M., & Allen, S. (2019). Tracking Triploid Mortalities Of Eastern Oysters Crassostrea virginica In The Virginia Portion Of The Chesapeake Bay. *Journal of Shellfish Research*, *38*(1), 101–113. https://doi.org/ 10.2983/035.038.0110

Guo, X. (1994). Tetraploid induction with mitosis inhibition and cell fusion in the pacific oyster Crassostrea gigas (Thunberg). *J Shellfish Res*, *13*, 193–198.

Hochachka, P., & Somero, G. N. (2002). *Biochemical adaptation: Mechanism and Process in Physiological Evolution* (1st ed.). Oxford University Press.

Kültz, D. (2005). Molecular and Evolutionary Basis of the Cellular Stress Response. *Annual Review of Physiology*, *67*(1), 225–257. https://doi.org/10.1146/annurev.physiol.67.040403.103635

Lavaud, R., La Peyre, M. K., Justic, D., & La Peyre, J. F. (2021). Dynamic Energy Budget modelling to predict eastern oyster growth, reproduction, and mortality under river management and climate change scenarios. *Estuarine, Coastal and Shelf Science*, *251*, 107188. https://doi.org/10.1016/j.ecss.2021.107188

Lutterschmidt, W. I., & Hutchison, V. H. (1997). The critical thermal maximum: Data to support the onset of spasms as the definitive end point. *Canadian Journal of Zoology*, *75*(10), 1553–1560. https://doi.org/10.1139/z97-782

Marshall, D. A., Casas, S. M., Walton, W. C., Rikard, F. S., Palmer, T. A., Breaux, N., La Peyre, M. K., Beseres Pollack, J., Kelly, M., & La Peyre, J. F. (2021). Divergence in salinity tolerance of northern Gulf of Mexico eastern oysters under field and laboratory exposure. *Conservation Physiology*, *9*(1), coab065. https://doi.org/10.1093/conphys/coab065

Marshall, D. A., Coxe, N. C., La Peyre, M. K., Walton, W. C., Rikard, F. S., Pollack, J. B., Kelly, M. W., & La Peyre, J. F. (2021). Tolerance of northern Gulf of Mexico eastern oysters to chronic warming at extreme salinities. *Journal of Thermal Biology*, *100*, 103072. https://doi.org/10.1016/j.jtherbio.2021.103072

Matt, J. L., & Allen, S. K. (2021). A classification system for gonad development in triploid Crassostrea virginica. *Aquaculture*, *532*, 735994. https://doi.org/10.1016/j.aquaculture.2020.735994

McCarty, A. J., Hood, S., Huebert, K., Cram, J., McFarland, K., & Plough, L. V. (2023). Evaluating a short vs. Long-term progeny test and investigating physiology associated with survival in extreme low salinity for the eastern oyster Crassostrea virginica. *Aquaculture*, *574*, 739688. https://doi.org/10.1016/j.aquaculture.2023.739688

McCarty, A. J., McFarland, K., Small, J., Allen, S. K., & Plough, L. V. (2020). Heritability of acute low salinity survival in the Eastern oyster (Crassostrea virginica). *Aquaculture*, *529*, 735649. https://doi.org/10.1016/j.aquaculture.2020.735649

Neufeld, D. S., & Wright, S. H. (1996). Salinity change and cell volume: The response of tissues from the estuarine mussel Geukensia demissa. *Journal of Experimental Biology*, *199*(7), 1619–1630. https://doi.org/10.1242/jeb.199.7.1619

Paparo, A. A., & Dean, R. C. (1984). Activity of the lateral cilia of the oyster Crassostrea virginica gmelin: Response to changes in salinity and to changes in potassium and magnesium concentrationt. *Marine Behaviour and Physiology*, *11*(2), 111–130. https://doi.org/10.1080/10236248409387039

Philipp, E. E. R., & Abele, D. (2010). Masters of longevity: Lessons from long-lived bivalves--a mini-review. *Gerontology*, *56*(1), 55–65. https://doi.org/10.1159/000221004

Pörtner, H.-O. (2012). Integrating climate-related stressor effects on marine organisms: Unifying principles linking molecule to ecosystem-level changes. *Marine Ecology Progress Series*, *470*, 273–290. https://doi.org/10.3354/meps10123

Ritchie, M. E. (2018). Reaction and diffusion thermodynamics explain optimal temperatures of biochemical reactions. *Scientific Reports*, *8*(1), Article 1. https://doi.org/10.1038/s41598-018-28833-9

SAS (9.4). (2013). [The SAS system for Windows]. SAS Institute Inc.

Sies, H. (1991). Oxidative stress: From basic research to clinical application. *The American Journal of Medicine*, *91*(3, Supplement 3), S31–S38. https://doi.org/10.1016/0002-9343(91)90281-2

Slimen, I. B., Najar, T., Ghram, A., Dabbebi, H., Ben Mrad, M., & Abdrabbah, M. (2014). Reactive oxygen species, heat stress and oxidative-induced mitochondrial damage. A review. *International Journal of Hyperthermia: The Official Journal of European Society for Hyperthermic Oncology, North American Hyperthermia Group*, *30*(7), 513–523. https://doi.org/10.3109/02656736.2014.971446

Sokolova, I. M., Frederich, M., Bagwe, R., Lannig, G., & Sukhotin, A. A. (2012). Energy homeostasis as an integrative tool for assessing limits of environmental stress tolerance in

aquatic invertebrates. *Marine Environmental Research*, *79*, 1–15. https://doi.org/10.1016/j.marenvres.2012.04.003

Somero, G. N. (2002). Thermal Physiology and Vertical Zonation of Intertidal Animals: Optima, Limits, and Costs of Living1. *Integrative and Comparative Biology*, *42*(4), 780–789. https://doi.org/10.1093/icb/42.4.780

Vajedsamiei, J., Melzner, F., Raatz, M., Morón Lugo, S. C., & Pansch, C. (2021). Cyclic thermal fluctuations can be burden or relief for an ectotherm depending on fluctuations' average and amplitude. *Functional Ecology*, *35*(11), 2483–2496. https://doi.org/10.1111/1365-2435.13889

Verberk, W. C. E. P., Bartolini, F., Marshall, D. J., Pörtner, H.-O., Terblanche, J. S., White, C. R., & Giomi, F. (2016). Can respiratory physiology predict thermal niches? *Annals of the New York Academy of Sciences*, *1365*(1), 73–88. https://doi.org/10.1111/nyas.12876

Wadsworth, P., Casas, S., La Peyre, J., & Walton, W. (2019). Elevated mortalities of triploid eastern oysters cultured off-bottom in northern Gulf of Mexico. *Aquaculture*, *505*, 363–373. https://doi.org/10.1016/j.aquaculture.2019.02.068

Walton, W. C., Davis, J. E., Chaplin, G. I., Rikard, F. S., Hanson, T. R., Waters, P. J., & Swann, D. L. (2012). *OFF-BOTTOM OYSTER FARMING*. 8.

Walton, W. C., Davis, J. E., & Supan, J. E. (2013). *Off-Bottom Culture of Oysters in the Gulf of Mexico*. 6.

Winkle, W. V. (1972). Ciliary activity and oxygen consumption of excised bivalve gill tissue∗∗Contribution No. 406 from the Virginia Institute of Marine Science. *Comparative Biochemistry and Physiology Part A: Physiology*, *42*(2), 473–485. https://doi.org/10.1016/0300-9629(72)90126-0

CHAPTER 6
SUMMARY AND CONCLUSIONS

6.1 Summary of dissertation

In this dissertation, select environmental stressors (PFAS exposure, acute temperature stress, low salinity) were tested individually and combined to study the impact of common environmental conditions on oyster metabolism and behaviors. At a non-stressful temperature, diploid oysters did not incur an energetic cost associated with PFAS depuration demonstrating that the MXR pathway is likely efficient at detoxifying and removing these compounds at low concentrations. At temperatures above what is considered the optimum for oysters, the effect of PFAS exposure did not further increase oyster respiration compared to control oysters. However, the effect of temperature did result in an increase in metabolic rates compared to oysters at optimal temperatures. The results from chapter 2 and 3 suggest that PFAS exposure at concentrations an order of magnitude higher than what is seen in the tributaries of Mobile Bay are not energetically impacting oysters significantly enough to be a concern. However, there is a risk of PFAS bioaccumulation within oyster tissues and studying the concentrations of a variety of PFAS in wild and farmed oyster tissue should be undertaken to address possible human health concerns related to seafood contamination.

During acute thermal stress, there was no significant difference in temperatures that diploids and triploids reached metabolic stress, sublethal behaviors, and their lethal endpoints, suggesting that thermal stress alone may not be accounting for the disproportionately higher triploid mortalities during unexpected mortality events seen in the summer months. The decreased resting metabolic rate shown in triploids during acute thermal stress does warrant further investigation as to whether this is a benefit for growth or if it is a result of inefficient gas exchange across the cell membrane due to their increased cell size. Under hyposaline conditions,

a temperature ramp revealed that metabolic peak was significantly lower and closure frequency, and the risk of death was significantly higher than oysters at a moderate salinity regardless of ploidy. Low salinity had a significantly negative effect on closures and metabolism on oysters regardless of ploidy, indicating that salinity stress compounds with thermal stress. The results of chapters 4 and 5 suggest that, while major mortality events are occurring regardless of ploidy, triploids may be disproportionately more susceptible to some types of environmental stress compared to diploids.

6.2 Utility of metabolic assays

While examining the acute influence of biocontaminants, temperature, and salinity on metabolism does not immediately answer the cause of sudden mortality events in farmed oysters, I do believe that using metabolic and behavioral assays can provide thresholds for environmental stress in oysters across lines and ploidies. The greatest advantage of these metabolic assays is their ecological relevancy and relatively quick turn-around time. Chronic exposures can take months and a lot of space while these metabolic assays take a month, and these assays can provide explanations for mortalities from an energetic cost viewpoint. Identifying metabolic peak temperature via intermittent respirometry in oysters has been shown to be ecologically relevant and is also the temperature where major mortalities appear during chronic studies.

6.3 Spring/Summer Sudden Unexplained Mortality Syndrome

Sudden and unexplained mortalities of oysters are a major detriment to oyster aquaculture and current theories are pointing to a complex interplay between genetics, internal biological processes, environmental conditions, and husbandry practices. Environmental stress, when

independent from each other, has a major impact on oyster physiology, each stressor demanding the oyster to adjust to new conditions. When examined in tandem, the metabolic and behavioral impacts seen in this dissertation lend evidence that combined stressors are likely impacting oyster mortality by overdrawing their energetic budget. While this dissertation only addressed a select number of stressors, it's important that we continue to keep in mind that many stressors occur simultaneously, both biotically and abiotically, throughout the year. Gametogenesis in diploid and triploids begins in the spring during times which can include extended periods of low salinity, increasing water temperature, and shifts in nutritional availability in water column. It has been reported that GOM oyster farmers sometimes see a secondary mortality event around mid to late summer. Summer in Mobile Bay is commonly accompanied by higher salinities compared to the spring and is when temperatures are at their highest. In the Gulf of Mexico specifically, oysters tend to have a secondary spawning season in late summer/early fall, unlike colder growing areas which usually only have one spawning season.

External environmental conditions are important to note but stressful conditions caused by routine farming practices such as biofouling, desiccation, and tumbling also likely play a role in compounding stress. Oyster seed shortages and lack of oyster hatcheries in the GOM have resulted in farmers acquiring juvenile oysters with broodstock origins different than the ones that they are moved to (with juvenile oysters sometimes shipped from east coast to GOM and vice versa) which may be resulting in a mismatch between genetics of the broodstock and environmental thermal and salinity regimes resulting in increased mortalities. As we continue to move into a rapidly changing ecosystem driven by climate change, I believe investigating the effects of environment and farming practices on oyster energetic budgets and survival rates will be crucial to help address and reduce future mortality events.